DOT/FAA/AR-11/7

Air Traffic Organization
NextGen & Operations Planning
Office of Research and
Technology Development
Washington, DC 20591

Usage and Maneuver Loads Monitoring of Heavy Air Tankers

March 2011

Final Report

This document is available to the U.S. public through the National Technical Information Services (NTIS), Springfield, Virginia 22161.

This document is also available from the Federal Aviation Administration William J. Hughes Technical Center at actlibrary.tc.faa.gov.

U.S. Department of Transportation
Federal Aviation Administration

NOTICE

This document is disseminated under the sponsorship of the U.S. Department of Transportation in the interest of information exchange. The United States Government assumes no liability for the contents or use thereof. The United States Government does not endorse products or manufacturers. Trade or manufacturer's names appear herein solely because they are considered essential to the objective of this report. The findings and conclusions in this report are those of the author(s) and do not necessarily represent the views of the funding agency. This document does not constitute FAA certification policy. Consult your local FAA aircraft certification office as to its use.

This report is available at the Federal Aviation Administration William J. Hughes Technical Center's Full-Text Technical Reports page: actlibrary.tc.faa.gov in Adobe Acrobat portable document format (PDF).

Technical Report Documentation Page

1. Report No. DOT/FAA/AR-11/7	2. Government Accession No.	3. Recipient's Catalog No.
4. Title and Subtitle USAGE AND MANEUVER LOADS MONITORING OF HEAVY AIR TANKERS		5. Report Date March 2011
		6. Performing Organization Code
7. Author(s) Kamran Rokhsaz, Linda K. Kliment, and Richard B. Bramlette		8. Performing Organization Report No.
9. Performing Organization Name and Address Wichita State University 1840 Fairmount Wichita, KS 67260-0044		10. Work Unit No. (TRAIS)
		11. Contract or Grant No. Grant No. 08-G-016
12. Sponsoring Agency Name and Address U.S. Department of Transportation Federal Aviation Administration Air Traffic Organization NextGen & Operations Planning Office of Research and Technology Development Washington, DC 20591		13. Type of Report and Period Covered Final Report
		14. Sponsoring Agency Code ANM-210L

15. Supplementary Notes

The Federal Aviation Administration Airport and Aircraft Safety R&D Division Technical Monitor was James Newcomb.

16. Abstract

Wichita State University, in conjunction with the Federal Aviation Administration (FAA) and the United States Forest Service (USFS), conducted research in the area of structural integrity requirements for aircraft flying in firefighting missions. The primary goal of this research was to conduct a comprehensive operational loads analysis of the heavy air tanker fleet. The objectives of this program were to evaluate typical operational in-service data and compare the results with the data used in the design and qualification of such aircraft and to provide a basis to improve the structural criteria and methods of operation and maintenance of these airplanes. The scope of this program included (1) defining the service-related factors that affect the operational life of heavy air tankers and (2) reducing, analyzing, and providing processed data in statistical formats, which will enable the FAA, the USFS, and the operators to better understand and control the factors that influence the structural integrity of these aircraft.

For this research, data were collected from various P2V and P3A air tankers in actual operation over several fire seasons; 5316 flight files were collected during the 2008 and 2009 fire seasons, using an Appareo Systems recording system, and 3958 flight files were collected from the 2007 and 2008 fire seasons, using an older recording system from Systems and Electronics, Inc.

Basic flight parameters, such as airspeed, altitude, flight duration, distance, and bank and pitch angles, are shown in statistical form. Flights were divided into multiple phases, separating the segments in which the retardant is dropped from other phases of flight. Maneuver loads were determined for various phases and are presented graphically as cumulative occurrences. The aircraft usage results and loads shown in this report appear to match the expected outcomes. The altitudes, the normal accelerations, and the airspeeds did not reveal any operation outside of the established boundaries. Relatively large dive and roll angles are prominently present during all but the drop phases of flight, but they and their associated load factors remain within the stated limits. The statistical data formats used in this report allowed thorough examination of various parameters related to the life cycle of these air tankers.

Cumulative occurrences of maneuver load factor did not show any significant altitude dependence, and varied by flight phase, with the largest values associated with the drop and exit phases of flight. These were also the shortest phases of flight. Maneuver loads were also shown to occur at lower frequencies than those stated in MIL 8866.

The report concludes with some recommendations for improved data acquisition for future similar efforts.

17. Key Words Flight profiles, Flight loads spectrum, Statistical loads data		18. Distribution Statement This document is available to the U.S. public through the National Technical Information Service (NTIS), Springfield, Virginia 22161. This document is also available from the Federal Aviation Administration William J. Hughes Technical Center at actlibrary.tc.faa.gov.	
19. Security Classif. (of this report) Unclassified	20. Security Classif. (of this page) Unclassified	21. No. of Pages 88	22. Price

Form DOT F 1700.7 (8-72) Reproduction of completed page authorized

ACKNOWLEDGEMENTS

The work reported in this document was performed by the Flight Loads Group within the Department of Aerospace Engineering of the College of Engineering at Wichita State University (WSU). This effort was funded by the Federal Aviation Administration (FAA) through an Interagency Agreement with the United States Forest Service. At WSU, the principal investigators were Dr. Kamran Rokhsaz and Dr. Linda K. Kliment of the Department of Aerospace Engineering. Mr. Richard B. Bramlette developed some of the earlier data reduction algorithms and software and established the data reduction criteria for data collected using instrumentation developed by Systems and Electronics, Inc. The format used for presentation of the statistical data was adopted from the work previously performed by the principal investigators and the University of Dayton Research Institute. The Program Manager for the FAA was Mr. James Newcomb of the FAA William J. Hughes Technical Center.

TABLE OF CONTENTS

		Page
EXECUTIVE SUMMARY		xi
1.	INTRODUCTION	1
2.	AIRCRAFT DESCRIPTION	3
3.	AVAILABLE DATA	3
3.1	Flight Data	3
3.2	Recorded Data	5
3.2.1	The SEI System	5
3.2.2	The Appareo System	6
3.2.3	Data Quality	8
4.	WICHITA STATE UNIVERSITY DATA PROCESSING	9
4.1	Filtering and Normalizing	9
4.2	Derived and Extracted Parameters	9
4.2.1	Weight Estimation	9
4.2.2	Flight Distance	9
4.2.3	Flight Duration	10
4.2.4	Corrections for Sensor Location	10
4.3	Data Management	12
4.4	Data Reduction Criteria	12
4.4.1	Phases of Flight	12
4.4.2	Computer Programs	14
4.4.3	Sign Convention	15
4.4.4	Peak and Valley Selection	15
4.4.5	Separation of Maneuver and Gust Load Factors	16
4.4.6	Altitude Bands	16
5.	DATA PRESENTATION	17
5.1	Aircraft Usage Data	20
5.1.1	Flight Distance and Duration Data, all Phases	20
5.1.2	Altitude and Airspeed Data, all Phases	21
5.1.3	Number and Duration of Drops	21
5.1.4	Maneuvering Flight, all Phases	22

5.1.5 Bay Door Opening, all Phases, P2V, SEI System 22
5.1.6 Comparison of Flight Phases, Appareo System 23

5.2 Flight Loads Data 24

5.2.1 Vertical Loads—Appareo System 24
5.2.2 Vertical Loads—Comparison With Other Sources 25
5.2.3 Effect of Weight on Vertical Loads 26

6. CONCLUSIONS AND RECOMMENDATIONS 27

7. REFERENCES 28

APPENDIX A—STATISTICAL FORMATS AND AIRCRAFT USAGE DATA

LIST OF FIGURES

Figure		Page
1	Sensor Location Relative to the CG	11
2	Flight Phases	13
3	A Typical Flight Time History Showing two Drops	13
4	Sign Convention for Airplane Accelerations	15
5	Peak-Between-Means Classification of Loads	16

LIST OF TABLES

Table		Page
1	Medium and Heavy Air Tankers Analyzed in Reference 4	2
2	P2V and P3A Aircraft Characteristics	3
3	Summary of the Aircraft, Data Type, and Number of Flight Files	4
4	Parameters Recorded by the SEI System	5
5	Parameters Recorded by the Appareo System	7
6	Flight Phase Separation Criteria for P2V Data From the SEI System	14
7	Flight Phase Separation Criteria for all Aircraft Data From the Appareo System	14
8	Altitude Bands	16
9	Single-Flight, Single-Drop Files From P2V Aircraft and the SEI System	17
10	Flight Files From P2V Aircraft and the Appareo System	17
11	Flight Files From P3A Aircraft and the Appareo System	18
12	Statistical Formats	19

LIST OF ACRONYMS

AGL	Above ground level
CG	Center of gravity
DFDR	Digital flight data recorder
FAA	Federal Aviation Administration
GPS	Global positioning system
MSL	Mean sea level
NTSB	National Transportation Safety Board
SEI	Systems and Electronics, Inc.
UDRI	University of Dayton Research Institute
USFS	United States Forest Service
WSU	Wichita State University

EXECUTIVE SUMMARY

The United States Forest Service, through the Federal Aviation Administration William J. Hughes Technical Center, funded Wichita State University to conduct a survey of the operational loads experienced by a fleet of heavy air tankers. The program involved using data collected by various P2V and P3A air tankers in actual operation over several seasons. The majority of the data used for this study was collected during the 2008 and 2009 fire seasons, using the recording devices developed and supported by Appareo Systems. This data set consisted of 5316 flight files, although not all were useful due to a variety of reasons. Some results are also included here from the data collected prior to 2008 using different hardware developed and supported by Systems and Electronics, Incorporated. This data set consisted of 3958 flight files from the 2007 and 2008 fire seasons.

Basic flight parameters, such as airspeed, altitude, flight duration, distance, and bank and pitch angles, were shown in statistical form. Flights were divided into multiple phases, separating the segments when the retardant is dropped from other phases of flight. Maneuver loads were determined for various phases and are presented graphically as frequencies of occurrence. In addition, V-n diagrams and several coincident flight events are shown and compared with operational limits when available.

The statistical formats used in this study are those developed previously by the principal investigators and by the University of Dayton Research Institute. The data presented in this form allowed easy comparison of the design criteria with actual usage data, thereby providing the aircraft operators with a better understanding of those factors that influence the structural integrity of these aircraft. This data could also be used by both original equipment manufacturers and designated engineering representatives for design, repair, and/or alterations.

1. INTRODUCTION.

Under contract to United States Forest Service (USFS), air tankers perform public aircraft operations and, therefore, are not subject to the same regulatory requirements as other certified aircraft. However, it has been a known fact that these aircraft are operated differently from their intended design. In 1974, Jewel, et al. [1], published the results of an examination of the flight loads measured on two DC-6B aircraft flying in firefighting mode. The data used in the current study consisted of 337 flight hours in firefighting mode and 1919 flight hours in commercial transport service. The results clearly showed that the aircraft flying in firefighting mode were repeatedly subjected to flight loads exceeding, in frequency and magnitude, those experienced by their counterparts in commercial operation.

In 2004, following their investigation of the catastrophic in-flight structural failures of two heavy air tankers in 2002, the National Transportation Safety Board (NTSB) issued Recommendation A-04-29 recommending that the USFS should "Develop maintenance and inspection programs for aircraft that are used in firefighting operations that take into account and are based on… the magnitude of maneuver loading and the level of turbulence in the firefighting environment and the effect of these factors on remaining operational life" [2]. Since then, the USFS has made a concerted effort to have maintenance and inspections programs driven by the operational loads that aerial firefighting aircraft experience in this usage. This has been done through detailed damage tolerance and fatigue evaluations to Federal Aviation Administration (FAA) standards for the P2V and P3A aircraft that produced instructions for continued airworthiness for usage as air tankers. Another aspect of this effort has been the methodical collection of operational loads via digital flight data recorders (DFDR). Presently, this database contains information from thousands of flights for a variety of aircraft, collected over 4 years. Some of the work surrounding this effort is presented in reference 3.

In October 2005, Hall [4] published the results of a preliminary analysis of loads spectra for large air tankers. The fleet used for in the reference 4 study consisted of a P3A, C-130A, DC-4/6/7, and P2V. The data for reference 4, pertaining to medium and heavy air tankers, is shown in table 1. Based on this limited data, Hall showed that air tankers, due to their missions and the environment in which they fly, experienced significantly more severe load spectra than in their original design role. Hall also suggested establishing a central repository for data collection related to aerial firefighting. Similar endeavors were also undertaken by Avenger Aircraft Services [5-11], although from the perspective of structural analysis.

Table 1. Medium and Heavy Air Tankers Analyzed in Reference 4

Aircraft	MTOW (lb)	No. of Flights	No. of Hours
Medium Tanker 1	64,000	61	29
Medium Tanker 2	80,000	304	305
Heavy Tanker 1 & 2	106,000	343 & 391	285 & 328
Heavy Tanker 3 & 4	126,000	163 & 28	14 & 324
Totals		1290	1114

MTOW = Maximum takeoff weight

In 2007, the FAA entered into an Interagency Agreement with the USFS to conduct a comprehensive operational loads analysis of the heavy air tanker fleet. Wichita State University (WSU) was awarded a grant to process and perform a statistical evaluation of the flight loads data collected by various aircraft operators. The objectives of this program were to evaluate typical operational in-service data to

- compare with the data used in the design and qualification of aircraft employed as heavy air tankers.

- provide a basis to improve the structural criteria and methods of design, evaluation, and operation of such airplanes.

The scope of the project was defined as follows:

- By agreement with the USFS, all the firefighting data would be sent to HBM nCode for preprocessing, instantaneous weight estimation, and storage, and would be made available to WSU for postprocessing.

- WSU would extract usage information and perform statistical analysis of the data for the heavy air tankers, consisting of P2V and P3A aircraft, from data acquisition systems manufactured by Appareo Systems.

- The statistical analysis would focus on low-level atmospheric turbulence and maneuvers, as measured from recorded vertical accelerations.

- Derived gust velocities (U_{de}) would be determined to describe the atmospheric properties of the airspace traversed by the firefighters.

During the course of this project, it was determined that the placement of the sensors on these aircraft prevented accurate measurement of the gust load factors, and thus, extraction of the associated derived gust velocities. Therefore, the results presented here include basic statistical

information on a variety of parameters in formats that can be easily compared to the manufacturer's existing design criteria. Vertical accelerations are used to determine maneuver loads, which are then grouped in various mean sea level (MSL) altitude bands. Frequencies of occurrence are provided for different flight phases. Aircraft usage data includes flight duration, distance, maximum load factors, maximum and minimum bank and pitch angles, and a variety of coincident parameters.

The statistical formats used here are those developed earlier by the University of Dayton Research Institute (UDRI). The data presented in this form should allow an objective examination of these parameters, thereby affording the operators a better understanding and control of those factors that influence the structural integrity of these aircraft.

2. AIRCRAFT DESCRIPTION.

The analysis presented in this report pertains to fleets of P2V and P3A aircraft flying as heavy air tankers. Table 2 shows some of the characteristics of these aircraft. In this table, the weights were determined from the average of what was recorded in pilot supplemental data and were used only in extracting normalized vertical accelerations. The fuel burn rates and the dimensions can be found in references 12 and 13.

Table 2. P2V and P3A Aircraft Characteristics

Parameter	P2V	P3A
Average gross weight at takeoff (lb)	71,750	95,000
Average retardant weight at takeoff (lb)	18,700	23,000
Average fuel weight at takeoff (lb)	9,000	18,000
Average fuel burn rate (lb/hr)	1,500	4,880
Wing span (ft)	103.8	99
Wing reference area (ft^2)	1,000	1,312
Wing reference chord length (ft)	9.4	14.1

3. AVAILABLE DATA.

3.1 FLIGHT DATA.

Operational data was collected from DFDR installed on a fleet of P2V and P3A aircraft operating as heavy air tankers. Starting in 2005, data was collected with recording devices developed by Systems and Electronics, Inc. (SEI). Later, USFS switched to a different recording device developed by Appareo Systems. By 2008, a large amount of the flight data was recorded using the Appareo system. The bulk of the results shown in this report were extracted from the data collected using this system.

The data were organized initially by the USFS and placed in a library managed by the company HBM nCode. WSU downloaded these files from the library and translated them from the

company's proprietary .s3t format into .csv format, readable by codes developed for processing and analysis for this final report. The resulting aircraft usage data and statistical maneuver loads are presented here in formats that were developed previously by UDRI.

Operational data was available from multiple seasons. However, for the current study, the data was used from 18 heavy air tankers: 12 P2V aircraft and 6 P3A aircraft during the 2008 and 2009 fire seasons. A summary of the type of data and the number of flight files for these aircraft is shown in table 3. In this table, the names of the operators and the tanker designations were omitted, and the aircraft were simply numbered sequentially.

Table 3. Summary of the Aircraft, Data Type, and Number of Flight Files

No.	Aircraft	2007	No. of Files	2008	No. of Files	2009	No. of Files
1	P-2E	-	-	SEI/Appareo	166/399	Appareo	209
2	P-2E	-	-	SEI/Appareo	68/63	Appareo	412
3	P-2E	-	-	SEI/Appareo	179/142	Appareo	522
4	P-2H	SEI	106	-	-	-	-
5	P-2H	-	-	Appareo	360	Appareo	591
6	P-2H	-	-	Appareo	2	Appareo	196
7	P-2H	-	-	Appareo	335	-	-
8	P-2H	SEI	103	SEI	128	-	-
9	P-2E	SEI	185	SEI	66	-	-
10	P-2H	-	-	SEI/Appareo	94/8	Appareo	244
11	SP2-H	SEI	268	SEI	334	-	-
12	P-2V	SEI	205	SEI	235	-	-
13	P-3A	-	-	SEI/Appareo	206/78	Appareo	269
14	P-3A	-	-	SEI/Appareo	875/63	Appareo	54
15	P-3A	SEI	313	SEI	336	-	-
16	P-3A	-	-	SEI/Appareo	502/137	Appareo	220
17	P-3A	-	-	SEI/Appareo	147/1	Appareo	155
18	P-3A	SEI	486	SEI	520	-	-
P2V from SEI		867		1270		0	
P2V from Appareo		0		1309		2174	
P3A from SEI		799		2586		0	
P3A from Appareo		0		279		698	

3.2 RECORDED DATA.

Data were recorded over time using the SEI and the Appareo systems. Although the scope of this project called for analysis of the data from the latter system, attempts were made to use some of the SEI system data as well. The two systems differed fundamentally in that the SEI system recorded the data using a triggering logic, but the Appareo system recorded the information at a constant rate of 8 Hz. The type of information recorded by the two systems also differed.

3.2.1 The SEI System.

The SEI system, employed uniformly before 2008, was primarily designed to record information related to structural integrity of the aircraft. This was done to support the USFS sponsored Damage Tolerance and Fatigue assessments of the P2V and P3A aircraft. As a result, depending on the year and the model, the system recorded up to 12 channels of data from various strain gauges. Additionally, the number of channels recorded by this system varied over time. For example, the data recorded from aircraft 11 of table 3 lacked flap and varicam data prior to March 2007. Furthermore, the type of information varied, depending on the type of aircraft. Table 4 shows the format of the recorded data for P2V and P3A after March 2007.

Table 4. Parameters Recorded by the SEI System

P2V Data			P3A Data		
Channel	Parameter	Units	Channel	Parameter	Units
1	Strain gauge 1	Microstrain	1	Strain gauge 1	Microstrain
2	Strain gauge 2	Microstrain	2	Strain gauge 2	Microstrain
3	Strain gauge 3	Microstrain	3	Strain gauge 3	Microstrain
4	Strain gauge 4	Microstrain	4	Strain gauge 4	Microstrain
5	Strain gauge 5	Microstrain	5	Strain gauge 5	Microstrain
6	Strain gauge 6	Microstrain	6	Strain gauge 6	Microstrain
7	Strain gauge 7	Microstrain	7	Strain gauge 7	Microstrain
8	Strain gauge 8	Microstrain	8	Strain gauge 8	Microstrain
9	Strain gauge 9a	Microstrain	9	Strain gauge 9	Microstrain
10	Strain gauge 9b	Microstrain	10	Strain gauge 10	Microstrain
11	Strain gauge 9c	Microstrain	11	Strain gauge 11	Microstrain
12	Strain gauge 12	Microstrain	12	Strain gauge 12	Microstrain
13	Roll acceleration	Deg/sec/sec	13	Roll acceleration	Deg/sec/sec
14	Vertical acceleration	g's	14	Vertical acceleration	g's
15	Flap position	Degrees	15	Fuel 1	Pound
16	Varicam	Degrees	16	Fuel 2	Pound
17	Airspeed	Knots	17	Fuel 3	Pound
18	Pressure altitude	Feet	18	Fuel 4	Pound
19	Jet tachometer	rpm	19	Airspeed	Knots
20	Left aileron position	Degrees	20	Pressure altitude	Feet

Table 4. Parameters Recorded by the SEI System (Continued)

P2V Data			P3A Data		
Channel	Parameter	Units	Channel	Parameter	Units
21	Elevator position	Degrees	21	Flap position	Degrees
22	GPS altitude	Feet	22	Left aileron position	Degrees
23	GPS track	Degrees	23	Elevator position	Degrees
24	GPS latitude	Decimal degree	24	Float position	Gallons
25	GPS longitude	Decimal degree	25	GPS altitude	Feet
26	Spoiler deployed	Boolean	26	GPS track	Degrees
27	Avionics bus	Boolean	27	GPS latitude	Decimal degree
28	Door number 6	Boolean	28	GPS longitude	Decimal degree
29	Door number 5	Boolean	29	Weight off wheels	Boolean
30	Door number 4	Boolean	30	Engine #2 ON	Boolean
31	Door number 3	Boolean	31	Time	Seconds
32	Door number 2	Boolean	32	Trigger channel	Trigger channel
33	Door number 1	Boolean	33	Peak valley	Peak valley
34	Right wing tank	Pound	34	Days	Days
35	Right center tank	Pound	35	Seconds	Seconds
36	Gear up and locked	Boolean	36	Microseconds	Microseconds
37	Time	Seconds			
38	Trigger channel	Trigger channel			
39	Peak valley	Peak valley			
40	Days	Days			
41	Seconds	Seconds			
42	Microseconds	Microseconds			

rpm = revolutions per minute
GPS = Global positioning system

Another fundamental characteristic of the SEI system was that it would generate a line of recording every time one of the parameters in the first 14 channels triggered an output. Consequently, its data was recorded at variable time increments. The details of the triggered data output logic are described in references 14 through 16.

3.2.2 The Appareo System.

The data collected by the Appareo system, shown in table 5, had different parameters than the SEI system. Furthermore, this data was recorded at a fixed rate of 8 Hz, which required entirely different programming logic for information extraction and its statistical analysis. For example, the absence of information on flap deflection, propulsion information, and a reliable squat switch caused significant challenges in separation of flight phases. Also, the same information was collected for both P2V and P3A aircraft, even though the two have vastly different systems. The USFS transitioned to this system as a result of the many issues encountered when instrumenting

older aircraft. The system is mostly self-contained and did not rely as heavily on signals from the older airframe systems, resulting in higher-quality data.

Table 5. Parameters Recorded by the Appareo System

Channel	Parameter	Units
1	Bay door	Discrete
2	Discrete	Discrete bitmask
3	Latitude	Degrees
4	Elevation	Feet
5	Longitude	Degrees
6	Pitch	Degrees
7	Roll	Degrees
8	Speed	Knots
9	Vertical speed	Knots
10	Heading	Degrees
11	Pitch rate	Degrees per second
12	Roll rate	Degrees per second
13	Yaw rate	Degrees per second
14	Longitudinal acceleration	g force
15	Lateral acceleration	g force
16	Normal acceleration	g force
17	True airspeed	Knots
18	Equivalent airspeed	Knots
19	Indicated airspeed	Knots
20	Course direction	Degrees
21	Pitot pressure	InHg
22	Static pressure	InHg
23	Outside air temperature	Degrees Celsius
24	Horizontal accuracy	mm
25	Vertical accuracy	mm
26	Weight on wheels	Discrete

InHg = Inches of mercury

Unlike the SEI data, the Appareo data appeared to be geared toward easier ways of reproducing the flights in a simulation environment. In this case, more information was collected related to navigation and guidance than those related to structural loads. Nonetheless, this data contained airframe accelerations along all three axes, as well as all three rotation rates. The Appareo system was chosen for multiple purposes: operational loads monitoring, flight operations quality

assurance, and accident investigation. This system has crash-hardened memory that was used by the NTSB to investigate two fatal large air tanker fatal accidents.

3.2.3 Data Quality.

In general, the quality of the Appareo system data was better than the SEI system data, although both systems exhibited anomalies. Some of the anomalies detected were as follows.

- In SEI data:
  - There was significant noise in the recorded airspeed just before takeoff and immediately after landing, making it impossible to use the airspeed as an indicator for these events.
  - In most cases, the pressure altitude was incorrect, so the global positioning system (GPS) altitude was used.
  - Some of the data was intermittent, which is typical of electrical connections subjected to vibration.
  - Aircraft 11 in table 3 had reversed signals on two of the bay doors.
  - A significant number of files contained zero airspeed throughout.
  - On aircraft 9, the flap indication was clearly erroneous, reaching as high as 60°.
- In Appareo data:
  - In many cases, the squat switch indication did not change. Furthermore, the indication was not consistent from one aircraft to the next. In most P2V data, the indicator was set at 0, whereas in most P3A cases, it was uniformly set at 1. Therefore, the takeoff and landing points could not be pinpointed with any accuracy.
  - Recorded true airspeed was erroneous. Although this issue was resolved later, in all calculations, true airspeed was estimated by correcting the indicated airspeed. This method also produced values closer to those extracted from dynamic pressure.
  - On one tanker (aircraft 5 in table 3), the bay door signal never changed. Therefore, various flight phases could not be separated, although the data was used for extracting information on overall aircraft usage.
  - Recorded values of vertical velocity did not correlate with values estimated from changes in altitude. The two values were significantly different.
  - Lateral accelerations recorded on the P2V aircraft were erroneous due to a mounting problem.

4. WICHITA STATE UNIVERSITY DATA PROCESSING.

4.1 FILTERING AND NORMALIZING.

The noise in the recorded data prevented clear identification of various altitudes. Therefore, the recorded altitude was filtered, using a 2-second running average. In those cases where altitude above ground level (AGL) was of interest, takeoff field elevation was used as the reference.

4.2 DERIVED AND EXTRACTED PARAMETERS.

Some information, such as true airspeed, had to be extracted or derived from the time history of other parameters. In those cases when aircraft parameters had to be derived, for consistency, the values used were those that best represented the fleet across the board (table 2). Issues pertaining to specific calculations and the derivations of the required parameters are described in the following section.

4.2.1 Weight Estimation.

All aircraft were assumed to takeoff at gross takeoff weight, with a full load of retardant. It was assumed the retardant would be dropped completely over the course of the drop phases at a constant rate. The drop rate was established from the ratio of the total retardant weight and the total phase duration for either single or multiple drops.

When a file contained information from more than one flight, it was assumed that the retardant load was replenished in between flights, but not the fuel. In the absence of propulsion information in the Appareo data, fuel burn rates were assumed to be constant throughout the mission.

With the SEI data, the analysis was limited to single-drop cases. Therefore, a constant average weight was used over each phase. However, over the drop phase, the weight was assumed to vary linearly.

4.2.2 Flight Distance.

Flight distance from integration of the true airspeed was determined from

$$D = \sum_{t_{liftoff}}^{t_{touchdown}} V_T \left(\Delta t\right) \tag{1}$$

where

D	=	Distance
V_T	=	True airspeed
Δt	=	Time increment

Again, in the absence of additional information, the indicated airspeed was assumed to be the same as calibrated airspeed. Also, since the airspeeds were not large enough to require inclusion

of compressibility effects, true airspeed was derived from the indicated airspeed using the ratio of air densities, that is

$$V_T = V_C \sqrt{\frac{\rho_0}{\rho}} \approx V_i \sqrt{\frac{\rho_0}{\rho}} \tag{2}$$

where

V_C	=	Calibrated airspeed
V_i	=	Indicated airspeed
ρ_0	=	Sea level air density
ρ	=	Local air density

For the Appareo data, outside air temperature and static pressure were among the recorded parameters. Therefore, the corresponding air density could be calculated from

$$\rho = \frac{p}{\bar{R}T} \tag{3}$$

where

p	=	Local absolute pressure (lbf/ft^2)
$\bar{R}$	=	1716 ft-lbf/lbm-R, specific gas constant for air
T	=	Local absolute temperature (R)

For the SEI data, in the absence of pressure and temperature recordings, local air density was derived from the pressure altitude, assuming standard atmosphere. Therefore, local density was derived from

$$\rho = \rho_0 \left(1 - 6.876 \times 10^{-6} \times H_p\right)^{4.256} \tag{4}$$

where

ρ_0	=	0.0023769 slug/ft^3 is air density at sea level
H_p	=	Pressure altitude (ft)

4.2.3 Flight Duration.

The flight duration was defined as the time from aircraft liftoff to touchdown.

4.2.4 Corrections for Sensor Location.

The Appareo system sensors were located far away from the aircraft center of gravity (CG), as shown in figure 1. Therefore, the maneuver loads that they measured were affected by the

aircraft rotation rates and angular accelerations. It was necessary to correct for the sensor offset from the CG. In this analysis, the sensor and the CG were assumed to be in the same plane.

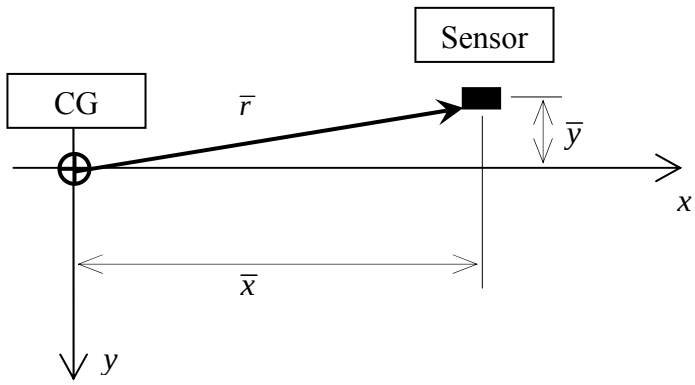

Figure 1. Sensor Location Relative to the CG

Accelerations measured by the sensor were assumed to be related to those of CG by

$$\vec{a}_{sensor} = \vec{a}_{CG} + \dot{\vec{\omega}} \times \vec{r} + \vec{\omega} \times \vec{\omega} \times \vec{r} + 2\vec{\omega} \times \dot{\vec{r}} + \ddot{\vec{r}} \tag{5}$$

where

$\vec{a}_{sensor}$ = Sensor acceleration
$\vec{a}_{CG}$ = CG acceleration
$\vec{\omega}$ = Rotational velocity of the body = $P\vec{i} + Q\vec{j} + R\vec{k}$
$\dot{\vec{\omega}}$ = Rotational acceleration of the body = $\dot{P}\vec{i} + \dot{Q}\vec{j} + \dot{R}\vec{k}$
$\vec{r}$ = Offset location of the sensor = $\bar{x}\vec{i} + \bar{y}\vec{j}$
$\dot{\vec{r}}$ = Velocity of the sensor relative to the fuselage, which was zero
$\ddot{\vec{r}}$ = Acceleration of the sensor relative to the fuselage, which was zero

Therefore, the difference between what was measured and the acceleration of the CG would be the error, given by

$$\vec{E} = \vec{a}_{sensor} - \vec{a}_{CG} = \dot{\vec{\omega}} \times \vec{r} + \vec{\omega} \times \vec{\omega} \times \vec{r} \tag{6}$$

where

$\vec{E}$ = Acceleration error

Carrying the cross products and considering only the vertical component resulted in

$$E_z = \left[\dot{Q}\bar{x} - \dot{P}\bar{y} - R\left(P\bar{x} + Q\bar{y}\right) \right] \tag{7}$$

where

E_z = Vertical component of acceleration error
$\dot{Q}$ = Pitch acceleration
$\dot{P}$ = Roll acceleration
R = Yaw rate
P = Roll rate
Q = Pitch rate

Also, since a right-handed coordinate system was used for this analysis, positive vertical accelerations in equations 5 through 7 would be pointed downward. To be consistent with the coordinate system used to measure normal accelerations, the error calculated in equation 7 had to be added to the recorded values.

4.3 DATA MANAGEMENT.

All data were stored by tanker number. For each tanker, the data were divided into two groups according to the recording device used. In each group, the data were also subdivided by year. The results for each type of tanker (i.e., P2V or P3A) and for each season were kept separate to allow a more detailed examination of the information.

Cases were only considered when the file contained information about complete flights, with or without a drop. Files containing drops were used for flight loads analysis. However, all files containing complete flights were used to assess aircraft usage information.

As the result of the data handling described above, not all results stemmed from the same number of flights or flight duration. Therefore, for clarity, detailed information is included in the legend of each figure that describes the number of flight phases, their total duration, and other pertinent information.

4.4 DATA REDUCTION CRITERIA.

4.4.1 Phases of Flight.

Each flight was divided into at least seven phases that consisted of:

- Taxi 1—Ground operation prior to liftoff, including takeoff roll
- Cruise 1—Climb to altitude and cruise to the drop zone
- Entry—Preparation for drop, including brief loiter and descent into the drop site
- Drop—The actual time the retardant leaves the aircraft
- Exit—Climbing out to cruise altitude immediately following the drop
- Cruise 2—Depart from the drop zone for the return trip and descent for landing
- Taxi 2—Ground operation after landing, including landing roll

The flight phases are shown in figure 2. Also, a typical flight time history, showing two drops, is presented in figure 3 for comparison.

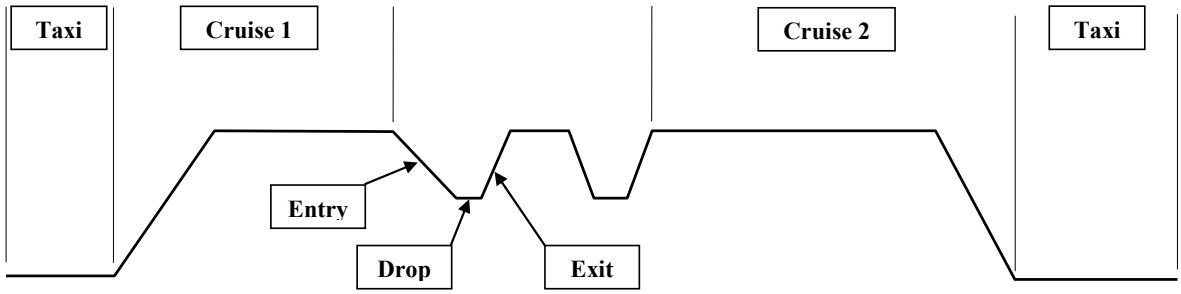

Figure 2. Flight Phases

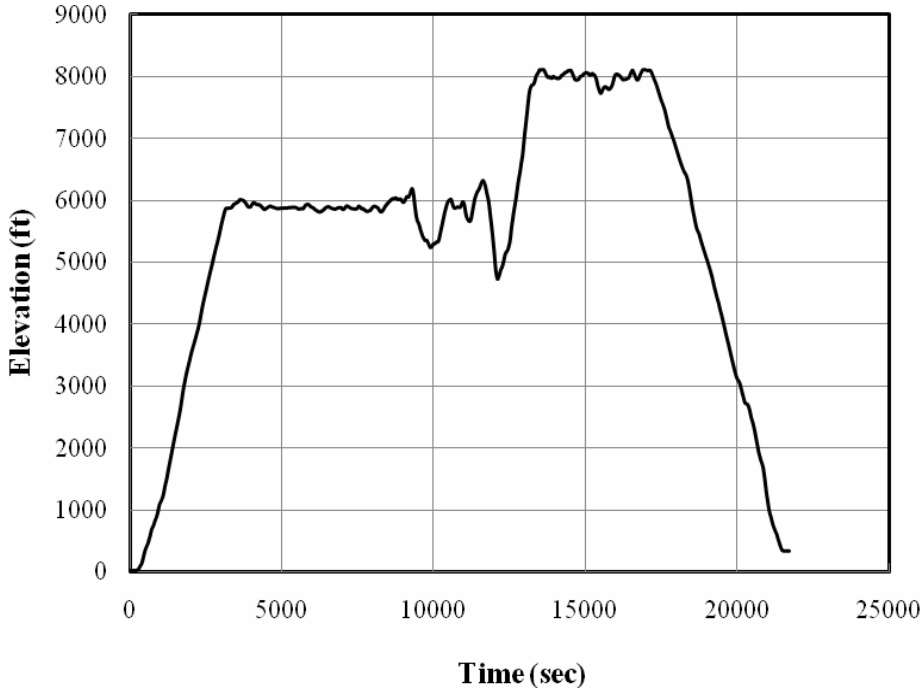

Figure 3. A Typical Flight Time History Showing two Drops

When a flight contained more than one drop, each entry, drop, and exit phase was considered. However, only one cruise 1 and one cruise 2 phase were associated with each flight. Also, no analysis was performed on the taxi phases.

Because each system recorded different parameters, the conditions used for flight phase separation depended on the recording device. Therefore, the same conditions could not be used in both cases. However, the priority was to avoid overlapping of various phases. For this reason, where such overlaps were possible, some parts of the data were omitted from the analysis. Tables 6 and 7 show the criteria used for flight phase separation for the two recording systems. Since the analysis was limited only to the airborne phases, these tables make no references to the ground phases.

Table 6. Flight Phase Separation Criteria for P2V Data From the SEI System

Flight Phase	Start Time (t_1) Identification	Stop Time (t_2) Identification
Cruise 1	Altitude above the departure runway for 30 seconds	Start of entry
Entry	Flaps down to the first position	Start of the drop
Drop	First bay door opening	2 seconds after sixth bay door opening
Exit	End of drop	Decrease in the jet tach >2000 rpm
Cruise 2	End of exit	Altitude less than 50 feet above the landing runway

Table 7. Flight Phase Separation Criteria for all Aircraft Data From the Appareo System

Flight Phase	Start Time (t_1) Identification	Stop Time (t_2) Identification
Cruise 1	Airspeed greater than 85 KIAS for 10 seconds or 60 seconds into the file if airborne	Three minutes before the start of the first entry phase
Entry	Three minutes before the opening of the first bay door	Opening of the first bay door
Drop	Opening of the first bay door	Closing of the last bay door plus 1 second
Exit	End of the drop phase	Ninety seconds past the end of the drop phase
Cruise 2	Three minutes past the end of the last exit phase	Airspeed below 85 KIAS for 10 seconds or 60 seconds before the end of the file if airborne

4.4.2 Computer Programs.

All analysis was performed using FORTRAN codes developed in-house at WSU. Primarily, two types of codes were used; one for determining the overall aircraft usages and a second for flight phase separation and flight loads analysis.

Overall usage information was determined independent of flight phases and the number of occurrences. This information was deemed most pertinent to determining the number of ground-air-ground (GAG) cycles. However, usage information was also extracted per flight phase to pinpoint the specific characteristics of each phase.

For the SEI data, three FORTRAN codes were developed. The first code translated the data from .csv format to .txt form with constant field lengths, readable by the subsequent codes. This was especially necessary because the data was not written in uniform time steps. The .txt files were then read by two other codes, one that determined the overall aircraft usage, and a second code that separated the flight phases and performed statistical analysis of the flight loads. Since the data formats for the P2V and the P3A aircraft were different and because the analysis of the

SEI data was outside the scope of this study, this study was limited to files with single flights and single drops for the P2V aircraft only.

For the Appareo data, all tasks were performed in a single FORTRAN code that could track up to 20 flights per file and up to 20 drops per flight, although these limits were never encountered. Also, since the same data format was used for both aircraft types, the program could process both. However, the physical dimensions and the inertial characteristics of each aircraft type had to be loaded in manually before the analysis.

4.4.3 Sign Convention.

For the Appareo data, accelerations were recorded in three directions: normal (z), longitudinal (x), and lateral (y). As shown in figure 4, the positive z direction was up and the positive x direction was forward. Since the longitudinal acceleration was too sensitive to the aircraft pitch attitude, not enough meaningful information could be extracted from it for the airborne phases. However, vertical and lateral accelerations could be analyzed. The SEI data contained only normal accelerations.

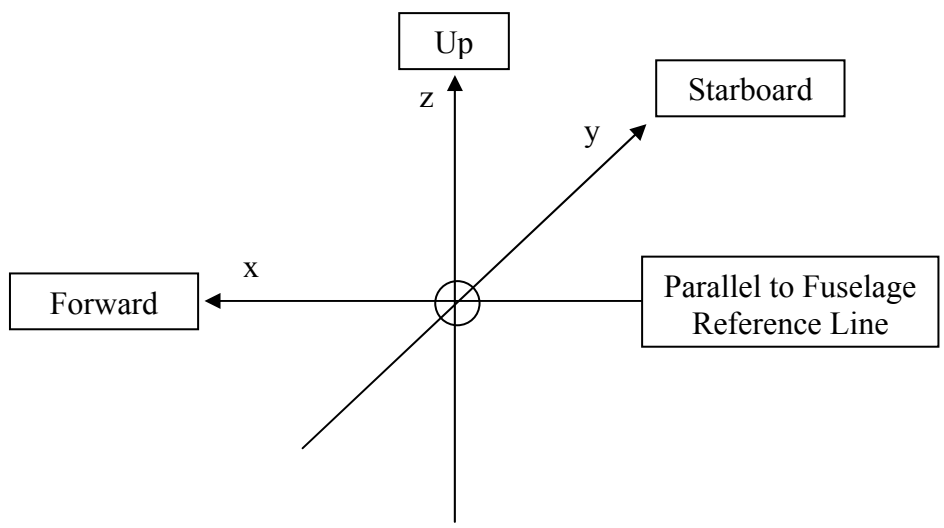

Figure 4. Sign Convention for Airplane Accelerations

4.4.4 Peak and Valley Selection.

The method of peaks-between-means, outlined in reference 17, was used for counting the peaks and valleys in the incremental vertical acceleration. This method is consistent with past practices and can be applied regardless of whether the accelerations resulted from gusts or maneuvers. In this method, only one peak or valley is counted between two successive crossings of the mean. A threshold zone (dead band) is used in the data reduction to filter out the noise around the mean, as shown in figure 5. For the vertical accelerations, the width of the dead band was ±0.05 g around the mean.

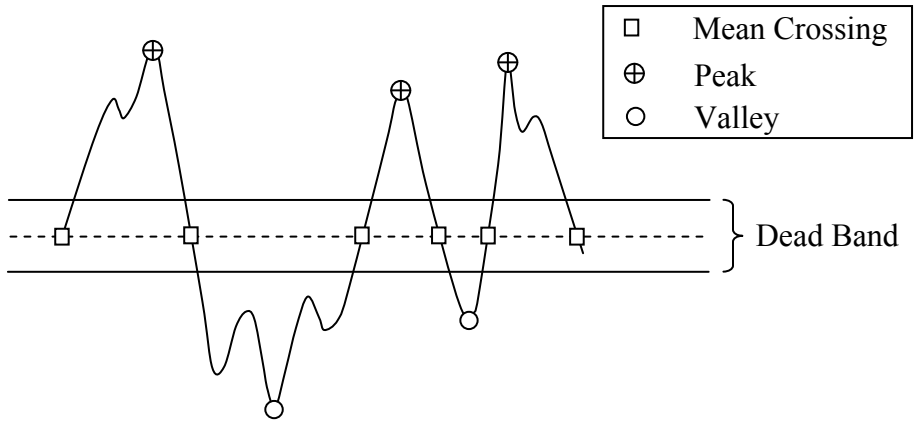

Figure 5. Peak-Between-Means Classification of Loads

4.4.5 Separation of Maneuver and Gust Load Factors.

The incremental vertical accelerations can be the result of gusts or maneuvers. MIL 8866 [18] focuses on the accelerations caused by maneuvers only. Therefore, it was necessary to separate the incremental vertical accelerations caused by gusts and by maneuvers. After studying the flight loads on B-737 and MD-82/83, Rustenburg, et al., [19], recommended a 2.0-second cycle duration be used for categorizing the incremental vertical accelerations. Therefore, accelerations lasting longer than 2.0 seconds were assumed to be due to maneuvers.

For each flight, the maximum and minimum maneuver load factors were determined from just after liftoff to just before touchdown. For the in-flight phases, the cumulative occurrences of incremental load factors were determined as cumulative counts per 1000 hours and cumulative counts per nautical mile.

4.4.6 Altitude Bands.

Recorded altitudes were acquired from GPS. The altitude bands used in the analysis are shown in table 8.

Table 8. Altitude Bands

Bands	MSL and AGL Altitudes (ft)
1	Less than 500
2	501-1,500
3	1,501-4,500
4	4,501-9,500
5	9,501-14,500
6	Greater than 14,501

5. DATA PRESENTATION.

This section contains the results of this investigation. Available results from the SEI system are given first, followed by the Appareo system for each aircraft type. The results for the P2V and the P3A aircraft are shown separately for the most part. The Appareo data used for these analyses were collected over the 2008 and 2009 fire seasons, but the results were not separated by the year. Furthermore, all analyses have been limited to the airborne phases of the operation. The SEI data used for this study was limited to single-flight and single-drop cases, which are summarized in table 9. Flight files from the Appareo recording system could contain as many as 20 flights and drops, although these limits were never reached. Tables 10 and 11 contain information about the Appareo flight files. Flights recorded by the SEI system were not divided into phases. Therefore, the associated results are presented only for the entire flight. However, detailed information was extracted for every flight phase from the Appareo data.

Table 9. Single-Flight, Single-Drop Files From P2V Aircraft and the SEI System

Flight File Characteristics	Aircraft						
	4	8	8	11	11	12	12
Year	2007	2007	2008	2007	2008	2007	2008
Total number of files with data	106	103	128	268	334	205	235
Number of flight for usage analysis	40	31	0	17	253	123	158
Flight time for usage analysis (hr)	44.0	1.2	0	14.0	183.6	90.4	137.0
Number of flights for loads analysis	3	0	0	0	191	16	77
Flight time for loads analysis (hr)	2.3	0	0	0	138.9	12.7	62.4

Table 10. Flight Files From P2V Aircraft and the Appareo System

Flight File Characteristics	Aircraft Number						
	1	2	3	5	6	7	10
Total number of files with data	608	475	664	951	198	335	252
Good files	608	475	664	845	198	0	252
Bad files*	0	0	0	106	0	335	0
Number of flights	308	180	165	436	90	0	43
Number of files without flights	385	376	501	434	136	0	216
Number of drops	341	161	187	0	24	0	54
Flight time (hr)	214	134	131	299	65	0	54
Number of flights without drops	21	45	21	436	72	0	10
Number of flights with one drop	246	115	112	0	14	0	17
Flights with multiple drops	41	20	32	0	4	0	16

*Files are missing pressure and outside air temperature information.

Table 11. Flight Files From P3A Aircraft and the Appareo System

Flight File Characteristics	Aircraft Number					
	13	14	15	16	17	18
Total number of files with data	347	117	0	357	156	0
Good files	347	117	0	357	156	0
Bad files	0	0	0	0	0	0
Number of flights	473	140	0	317	202	0
Number of files without flights	134	37	0	192	77	0
Number of drops	566	165	0	441	250	0
Flight time (hr)	322	122	0	231	114	0
Number of flights without drops	47	9	0	53	13	0
Number of flights with one drop	325	104	0	163	150	0
Flights with multiple drops	101	27	0	101	39	0

Statistical summaries of parameters pertaining to aircraft usage are presented and discussed in section 5.1. Quantities, such as number and frequency of flights and distances, airspeeds, altitudes, bank and pitch angles, maximum incremental vertical load factor, and a variety of others, are reduced and presented in formats that can be used easily by the FAA, the operators, and the manufacturers to better understand those factors that influence the structural integrity of these aircraft.

Section 5.2 presents a discussion of the flight loads. Cumulative frequencies of occurrence are discussed for various flight phases, as well as for the entire flight. Maneuver loads are separated using the 2-second rule and are shown separately for each phase. Comparisons are also made with the results of Jewel, et al. [1], Hall [4], and MIL 8866 [18]. In appendix A, each figure shows the number of phases, the number of flight hours, and the number of nautical miles traveled.

Table 12 lists the statistical data formats and the identification of the corresponding figure where the processed data plot or table can be found in appendix A. The figures have been grouped into categories as discussed above. Subcategories are used to further organize and group the figures and tables. Each figure and table is discussed in the following paragraphs.

Table 12. Statistical Formats

Aircraft Usage Data	Figure
FLIGHT DISTANCE AND DURATION DATA, ALL PHASES	
Correlation of Flight Distance and Flight Duration, all Phases	A-1
Distribution of the Flight Durations, all Phases	A-2
Cumulative Probability of Flight Distance, all Phases	A-3
Cumulative Probability of Flight Duration, all Phases	A-4
ALTITUDE AND AIRSPEED DATA, ALL PHASES	
Maximum AGL Altitude and Coincident Indicated Airspeed, all Phases	A-5
Correlation of Maximum Altitude and Flight Distance, all Phases	A-6
Maximum Airspeed and Coincident AGL Altitude, all Phases	A-7
NUMBER AND DURATION OF DROPS	
Number of Flights and Associated Drops	A-8
Distribution of Single-Drop Durations	A-9
MANEUVERING FLIGHTS, ALL PHASES	
Maximum Incremental Vertical Load Factor and Coincident Indicated Airspeed, all Phases	A-10
Cumulative Probability of the Maximum/Minimum Pitch Angle, all Phases	A-11
Cumulative Probability of the Maximum/Minimum Bank Angle, all Phases	A-12
Extreme Values of Pitch Angle Correlated With Flight Phase	A-13
Extreme Values of Roll Angle Correlated With Flight Phase	A-14
FLAP USAGE AND BAY DOOR OPENING, ALL PHASES, P2V, SEI SYSTEM	
Cumulative Probability of Maximum Airspeed With at Least One Bay Door Open, all Phases, P2V, SEI System	A-15
Cumulative Probability of Maximum Incremental Vertical Load Factor With at Least One Bay Door Open, all Phases, P2V, SEI System	A-16
Cumulative Probability of Any Flap Deflection With at Least One Bay Door Open, all Phases, P2V, SEI System	A-17
COMPARISON OF FLIGHT PHASES, APPAREO SYSTEM	
Maximum AGL Altitude and Coincident Indicated Airspeed, P2V Aircraft	A-18
Maximum AGL Altitude and Coincident Indicated Airspeed, P3A Aircraft	A-19
Maximum Indicated Airspeed and Coincident AGL Altitude, P2V Aircraft	A-20
Maximum Indicated Airspeed and Coincident AGL Altitude, P3A Aircraft	A-21
Maximum Incremental Vertical Load Factor and Coincident Indicated Airspeed, P2V Aircraft With P3A Limits	A-22
Maximum Incremental Vertical Load Factor and Coincident Indicated Airspeed, P3A Aircraft	A-23
Average Maximums, Average Minimums, and Standard Deviations of Pitch and Roll Angles, P2V Aircraft, Appareo System	A-24
Average Maximums, Average Minimums, and Standard Deviations of Pitch and Roll Angles, P3A Aircraft, Appareo System	A-25

Table 12. Statistical Formats (Continued)

Flight Loads Data	Figure
VERTICAL LOADS, APPAREO SYSTEM	
Sensor Locations	A-26
Cumulative Occurrences of Incremental Maneuver Vertical Load Factor, Cruise 1, P2V, Appareo Data for Various MSL Altitudes	A-27
Cumulative Occurrences of Incremental Maneuver Vertical Load Factor, Cruise 1, P3A, Appareo Data for Various MSL Altitudes	A-28
Cumulative Occurrences of Incremental Maneuver Vertical Load Factor, Entry, P2V, Appareo Data for Various MSL Altitudes	A-29
Cumulative Occurrences of Incremental Maneuver Vertical Load Factor, Entry, P3A, Appareo Data for Various MSL Altitudes	A-30
Cumulative Occurrences of Incremental Maneuver Vertical Load Factor, Drop, P2V, Appareo Data for Various MSL Altitudes	A-31
Cumulative Occurrences of Incremental Maneuver Vertical Load Factor, Drop, P3A, Appareo Data for Various MSL Altitudes	A-32
Cumulative Occurrences of Incremental Maneuver Vertical Load Factor, Exit, P2V, Appareo Data for Various MSL Altitudes	A-33
Cumulative Occurrences of Incremental Maneuver Vertical Load Factor, Exit, P3A, Appareo Data for Various MSL Altitudes	A-34
Cumulative Occurrences of Incremental Maneuver Vertical Load Factor, Cruise 2, P2V, Appareo Data for Various MSL Altitudes	A-35
Cumulative Occurrences of Incremental Maneuver Vertical Load Factor, Cruise 2, P3A, Appareo Data for Various MSL Altitudes	A-36
VERTICAL LOADS, COMPARISON WITH OTHER SOURCES	
Cumulative Occurrences of Incremental Vertical Maneuver Load Factor, SEI and Appareo Systems, Compared With Other Sources, P2V, all Phases	A-37
Cumulative Occurrences of Incremental Vertical Maneuver Load Factor, P2V From SEI and Appareo Systems Compared With P3A, all Phases	A-38
Effect of Weight on Cumulative Occurrences of Incremental Vertical Maneuver Load Factor, all Altitudes, all Phases	A-39

5.1 AIRCRAFT USAGE DATA.

The aircraft usage information shown in appendix A pertains to the airborne phases. Statistical information about total flight distance and duration, drop durations, number of drops per flight, altitude and speed data for all phases combined and separated by flight phase, and V-n diagrams is given in the following sections. This type of information can be used developing future design criteria, as well as for fine-tuning maintenance schedules and structural component life limits.

5.1.1 Flight Distance and Duration Data, all Phases.

The correlation of flight distance and flight duration is shown in figure A-1. It is important to note that the data from the SEI system pertains only to single flights with single drops, whereas

the Appareo data relates to all flights. Flight speed averages from figure A-1 (a-c) are 200.5, 196.8, and 213.7 KIAS, respectively. Also, this figure clearly shows that a significant percentage of the flights were under 1.5 hours. Generally, longer flights were due to ferrying the aircraft. This is also observable in the distribution of flight durations, shown in figure A-2. It is obvious from this figure that the majority of the flights were under 1 hour. In fact, the average flight durations for the two aircraft types were very close to 45 minutes. Cumulative probabilities of flight distance and duration are also shown in figures A-3 and A-4.

5.1.2 Altitude and Airspeed Data, all Phases.

Maximum AGL altitude and coincident indicated airspeeds are shown in figure A-5. In cases where maximum altitude occurred multiple times within a flight, the one with the highest associated airspeed was used. Also, the departure airport's field elevation was used as reference.

This figure clearly shows that the two systems correlated well in average maximum altitude and coincident airspeed. However, the data from the SEI system showed a larger range of values, both in airspeed and in maximum altitude. The P3A data showed a slightly larger spread of maximum altitudes than the P2V data. However, for the most part, maximum AGL altitudes remained below 12,000 feet.

Maximum AGL altitude and coincident flight distance are correlated in figure A-6. Again, the data from the two recording systems matched well for the P2V aircraft. There were significant similarities between the data for both types of aircraft.

Figure A-7 shows maximum airspeed and coincident AGL altitudes. The SEI showed maximum airspeeds approaching 300 knots. However, this was not supported with the data collected by the Appareo system. In fact, the data from the latter system showed both aircraft types were flown at maximum airspeeds below 250 knots. It is noteworthy that this is a limit imposed by the FAA Type Certificate Data Sheet for the P3A fleet, even though the U.S. Navy limit is 400 knots. The U.S. Navy limit for the P2V is 320-350 knots.

5.1.3 Number and Duration of Drops.

The analysis of the SEI-collected data was limited to single flights with single drops. However, in the data collected by the Appareo system, as many as 20 flights per file and 20 drops per flight could be tracked. Therefore, it was of interest to determine how many of the flights were associated with multiple drops.

Figure A-8 shows the number of flights and the number of drops in each. The bay door signal on one P2V tanker (aircraft 5) never changed, which placed all of its flights in the ferry category. However, examination of its flight profile showed that many of its flights were actually associated with carrying and dropping retardant. This explains the large number of ferry flights in figure A-8(a). Removing the data from this tanker resulted in figure A-8(b), which clearly shows that roughly 65% of the flights had a single drop. This trend is also consistent with the P3A tanker shown in figure A-8(c). In a number of cases, more than two drops were detected. Most of these cases could be attributed to the flight crew cycling the bay doors.

The durations of single-drop flights are shown in figure A-9. The average drop duration for the two aircraft was slightly different primarily due to (1) each carried a different amount of retardant and (2) a less significant contributor was the difference in the delivery mechanism of the two types of aircraft. On the P2V, drops were accomplished by opening and shutting the six bay doors. However, the P3A employed a constant flow mechanism that could regulate the retardant flow rate more closely.

5.1.4 Maneuvering Flight, all Phases.

Maximum incremental vertical load factor and coincident indicated airspeed are shown in figure A-10 for all phases. For the P3A, reference 13 showed very specific V-n diagrams. However, similar data was not readily available for P2V. Therefore, the limits for P3A are shown for comparison.

For the P2V, there was generally good agreement between the results obtained from the two recording systems. However, some airspeeds recorded by the SEI system seemed high. Also, it was interesting that the maximum/minimum incremental load factors were outside the P3A limits in 1 of the 622 flights with the SEI system and in 3 of the 1219 flights with the Appareo system. For the P3A, none of the flights exceeded the prescribed load limits.

Cumulative probability of the pitch angle is shown in figure A-11 for all phases. The average values of the pitch angle appeared reasonable and agreed between the two aircraft. However, negative pitch attitudes for the P3A had a slightly larger standard deviation than the other cases. Since the Appareo data lacked information about flap deflection, this parameter could not be correlated with the pitch angle. Likewise, figure A-12 shows the cumulative probability of the roll angle for all phases.

Considering that average values of the roll angle exceeded ±30° and that there was a larger spread in negative pitch angles of the P3A fleet, these parameters were examined more closely. It was of interest to determine if the extremes of these angles could be correlated with any of the flight phases. This information is shown in figures A-13 and A-14. In these figures, each pair of points (i.e., maximum and minimum values) represents one flight phase per flight. Therefore, there are five pairs of points for each flight in these figures. The data were organized to present the occurrences by flight phase and shows the differences in maneuvering associated with each.

As expected, relatively large dive angles could be associated with the entry and the drop phases. Likewise, roll angles as large as ±60° were prominent during all but the drop phases. For the roll angle, the manufacturer's limits are shown with the dashed lines on these figures. It is evident from the figures in appendix A that the drop phase was flown with the least amount of banking, relative to the other phases. These trends were quite consistent with the cumulative occurrences of the maneuver loads during the drop and exit phases discussed in section 5.2. It is interesting that despite such aggressive maneuvering, the load factors did not exceed the prescribed limits.

5.1.5 Bay Door Opening, all Phases, P2V, SEI System.

Figure A-15 shows the cumulative probability of maximum airspeed with at least one bay door open. Likewise, figure A-16 shows the cumulative probability of maximum load factor with at

least one bay door open. It is not clear if there are airspeed and load limitations associated with the operation of the bay doors. However, the average values of the maximum load factor and the maximum airspeed seem reasonable. Figure A-17 shows the cumulative probability of the maximum flap deflection with at least one bay door open. Data from aircraft 12 was omitted in this analysis because of its faulty flap recordings.

5.1.6 Comparison of Flight Phases, Appareo System.

In this section, aircraft usage per flight phase is discussed for better understanding of the influence of individual phases. This discussion is limited to the data collected from the Appareo system.

Figure A-18 shows the maximum AGL altitude and the coincident indicated airspeed for each flight phase for the P2V fleet. The same information is shown in figure A-19 for the P3A aircraft. Understandably, the lowest maximum AGL altitudes and the lowest coincident airspeeds were associated with the drop phase. The reader is reminded that the reference altitude for determining the AGL altitude was the takeoff field elevation. Therefore, the higher altitudes during the drop phase shown in figures A-18 and A-19 must be related to fires at higher elevations.

Maximum indicated airspeeds and coincident AGL altitudes are shown in figures A-20 and A-21 for the P2V and the P3A fleets, respectively. The same trends observed in figures A-18 and A-19 are also evident here. Again, the lowest maximum indicated airspeeds and AGL altitudes are associated with the drop phase.

Although the Appareo system did not record the flap position, it was assumed that most drops were performed with large flap deflections, perhaps in excess of 25°. Examining the maximum indicated airspeed shows that a number of flights were flown faster than the placard speed for these flap settings (145-200 KIAS for the P2V and 170-190 KIAS for the P3A). However, the cruise phases showed that the airspeeds remained well within the prescribed limits.

Maximum incremental vertical load factor and coincident indicated airspeed for the P2V aircraft with P3A limits are given in figure A-22. The same results for the P3A fleet are shown in figure A-23. It is clear from these figures that the highest indicated airspeeds and the lowest incremental vertical loads were associated with the cruise phases. Understandably, the drop and the exit phases exhibited the highest incremental vertical load factors.

Figures A-13 and A-14 show that drop phases were executed with minimal roll angle. The same is shown in figures A-24 and A-25, where the averages of the maximum and minimum pitch and roll angles are shown along with their standard deviation for the P2V and the P3A aircraft, respectively. It is clear from these figures that roll angles were invariably the lowest for the drop phases. Another observation is that left bank turns (negative roll angle) were executed at steeper angles than right bank turns (positive roll angle).

5.2 FLIGHT LOADS DATA.

This section discusses the frequencies of occurrence of flight loads. As previously discussed, the vertical loads were divided into gust and maneuver loads using the 2-second rule. However, there were several issues associated with the recorded accelerations.

For the SEI system, the sensors were located close to the wing leading edge, and therefore, close to the aircraft CG. However, the Appareo systems were located as far as 15 feet in front of the wing leading edge, as shown in figure A-26. Consequently, the recorded accelerations were contaminated by airframe vibration and the pitch accelerations of the fuselage. Although adjustments could be made for the latter effect, the influence of the airframe vibration could not be subtracted from the recorded values. However, it was understood that airframe vibration would occur at frequencies higher than the maneuver loads (0.5 Hz based on the 2-second rule) and would contaminate the gust loads more. Therefore, maneuver loads were corrected for fuselage rotational accelerations and are discussed below. However, gust loads could not be determined with enough certainty to be included in this report.

The SEI system did not record lateral load factors. On the other hand, the lateral accelerations recorded by the Appareo system on the P2V aircraft behaved unexpectedly. Upon further inspection of the installation, it was found that the bracket holding the accelerometers on the P2V aircraft needed to be redesigned.

For the reasons discussed here, the flight loads discussed in this report are limited to vertical maneuver load factors. Flight loads are shown per 1000 hours and per nautical mile. Once all the phases have been discussed, the results will be compared with those of other studies.

5.2.1 Vertical Loads—Appareo System.

Vertical maneuver load factors, separated from the gust loads using the 2-second rule, are presented in figures A-27 through A-39. The maneuver loads were divided into various MSL altitude bands. In these figures, where appropriate, the results from aircraft 21 of Hall's study [4] and MIL 8866 are also shown for comparison. Aircraft 21 of Hall's study [4] had a gross takeoff weight of 80,000 pounds, which placed it between P2V and P3A. The results from Hall [4] and MIL 8866, shown here for comparison only, are for maneuver loads but were not separated by flight phase. The data shown in these figures indicated that maneuvers with positive load factors occurred much more frequently that those with negative load factors.

Figures A-27 and A-28 show the cumulative occurrences of incremental vertical maneuver load factor for cruise 1, for P2V and P3A aircraft, respectively. It is clear from these figures that load factors greater than 0.5 g in magnitude occurred less frequently than reported by Hall [4] and MIL 8866. Furthermore, comparing the results from the two aircraft showed a remarkable resemblance, which justifies placing them in one category (i.e., heavy air tanker). It is noteworthy that the results included data for altitudes below 500 and above 14,500 ft MSL. However, the scarcity of recorded data in these altitude bands resulted in large scatter in the cumulative occurrences.

Entry was characterized with slightly higher load factors and more frequent occurrences, as shown in figures A-29 and A-30. For positive load factors, the results from the two aircraft matched almost perfectly. However, there were small differences for negative load factors in which the results from the P2A showed a slightly higher level of activity. In both cases, the present results crossed MIL 8866 at roughly 0.75 g. Below this value, the present results were more frequent, while for larger load factors, the frequency of occurrence was lower than MIL 8866.

Cumulative occurrences of incremental maneuver load factors for the drop phase are shown in figures A-31 and A-32. On the positive side, the load factors were much larger and much more frequent than MIL 8866 and reported by Hall [4]. However, the reader is cautioned that this phase lasted for only a few seconds in each mission and, therefore, did not have as large of an impact on the fatigue life of the structure as the cruise phases would. In fact, for the P2V aircraft, 834 drop phases led to only 0.9 cumulative hours of flight. For the P3A aircraft, 1422 drops represented only 1.9 cumulative hours of flight. Damage accumulation from this or any other flight phase can only be quantified by a detailed damage tolerance and fatigue evaluation for the entire mission. Again, the scarcity of the recorded negative values resulted in some scatter in the results, especially for the P2V fleet.

During the drop phase, some of the maneuver loads were caused by the significant weight loss due to release of the retardant. However, the vertical accelerations due to change in the weight would not exceed an incremental value of 0.25 g. Furthermore, the higher frequencies of vertical accelerations during entry, drop, and exit are consistent with the pitch and bank angles shown in earlier sections. Therefore, the higher load factors during drop and exit could only be attributed to maneuvering flight.

The exit phase, shown in figures A-33 and A-34, had many of the same features as the entry phase but with slightly elevated load factors. This could be attributed to the lower weight and wing loading in the exit phase, compared with entry. Again, the results of the two aircraft showed good agreement.

The results from cruise 2 are presented in figures A-35 and A-36. Cumulative occurrences of incremental maneuver vertical load factors agreed between the two aircraft and remained well below MIL 8866 and Hall's study [4]. Even though this phase was flown at slightly lower average airspeeds, the magnitude and the frequency of occurrence of its load factors resembled those of cruise 1 very closely.

5.2.2 Vertical Loads—Comparison With Other Sources.

The first set of comparisons made was with the results from the two recording systems. This is shown in figure A-37 for maneuver loads. Since the data from the SEI system was not divided into individual phases, the data from the Appareo system was combined for the entire flight for the purpose of comparison. This was also true for aircraft 21 of Hall's study [4]. The points shown in this figure are limited to those from the P2V fleet because no SEI data from the P3A aircraft was analyzed.

This figure also shows the results from Jewel [1] and Hall [4], as well as MIL 8866. As indicated in this figure, for load factors greater than 0.5 g, both Jewel and Hall showed a higher frequency of occurrence than MIL 8866 results. The results from the Appareo system coincided with MIL 8866, and those from the SEI system fell well below it.

For negative load factors, the results from the two recording systems agreed well. However, for positive load factors, the results from the Appareo system indicated higher frequencies of occurrence. Nonetheless, both recording systems indicated cumulative occurrences of maneuver load factors at, or below, MIL 8866.

Regarding the maneuver loads, there are two possible sources of error in the results shown in figure A-37. The first source could be from using the 2-second rule to separate the gust loads from the maneuver loads. This rule may not be applicable to such low-level flights. Therefore, if a shorter duration was to be used, it would result in fewer gust loads and more maneuver load counts. Consequently, in figure A-37, at least the results from the Appareo system would fall slightly above MIL 8866.

The second source of error could be due to the correction of the maneuver accelerations for the rotational degrees of freedom of the aircraft and the moment arm of the sensors relative to the CG. This type of correction involves numerical evaluation of the rotational accelerations from the recorded rotation rates. Such numerical differentiation invariably introduces some noise in the correction terms. The average amplitude of the correction terms was approximately ±0.025 g.

In any event, the placement of the sensors, discussed previously, resulted in higher counts of the maneuver load factors, stemming from the rotational degrees of freedom of the aircraft. Therefore, the results from the Appareo system shown here could be considered the worst-case scenario. The authors recommend moving the sensors closer to the aircraft CG and repeating this analysis after a few years.

The cumulative occurrences of maneuver load factors from the P2V fleet and the P3A fleet is the second set of comparisons, as shown in figure A-38. It is clear from this figure that the P3A results from the Appareo data agreed better with the P2V data from the SEI system. Again, all three sets of results fell well below MIL 8866.

5.2.3 Effect of Weight on Vertical Loads.

It is clear that the vertical accelerations that can be tolerated by the airframe depend on the instantaneous weight. The latter parameter was calculated for the Appareo data and was used to normalize the vertical maneuver loads. Vertical accelerations were multiplied by the ratio of the instantaneous weight to the gross takeoff weight. The result is shown in figure A-39. For the purpose of comparison, the results from reference 4 were also included in this figure, even though it was not clear how the weight was handled in that case. The data in figure A-39 shows a maximum difference of 0.25 g of load factor, as expected. Furthermore, in the case of maneuver loads, normalizing the vertical accelerations resulted in even bigger differences with MIL 8866, with the latter being higher. Therefore, the results shown throughout this report, at

least from the Appareo system, should be considered to be conservative, even though they fall at or below Hall's results [4].

6. CONCLUSIONS AND RECOMMENDATIONS.

Considering that the data was taken during actual field operations, the overall data quality was good. Furthermore, there was sufficient data volume to obtain reasonable statistical conclusions. Generally, the results from both P2V and P3A aircraft matched closely, reaffirming that they should be in the same category.

The statistical data formats used in this study allowed thorough examination of various parameters related to the life cycle of the air tankers. These results will be useful to the USFS and the operators in better understanding and controlling the issues that impact the airworthiness of these aircraft. Noteworthy findings are briefly discussed in the following paragraphs.

To a large extent, the aircraft usage results matched the expected outcomes. The altitudes, normal accelerations, and airspeeds did not reveal any operation outside the established boundaries. Although relatively large dive and roll angles were prominent during all phases of flight except the drop phase, they remained within the limits stated by the manufacturer or imposed by the Federal Aviation Administration Type Certificate Data Sheet. These trends were consistent with the cumulative occurrences of the maneuver loads during the drop and exit phases. However, despite such aggressive maneuvering, the load factors did not exceed the prescribed limits.

Average flight durations were approximately 45 minutes and were consistent with earlier findings. The majority of the flights had a single drop. Single-drop durations appeared to be proportional to the size of the retardant load.

Cumulative occurrences of incremental maneuver load factors did not show any significant altitude dependence. Except for the drop and the exit phases, these loads occurred at lower frequencies than those stated in MIL 8866.

Comparison of the incremental vertical maneuver load factors between the Systems and Electronics, Inc. and Appareo recording systems showed higher frequencies of occurrence from the Appareo system. It was speculated that this was the effect of the sensor placement. Nonetheless, the maneuver loads measured by the Appareo system were at or below those stated in MIL 8866 and well below those shown in other studies.

Several recommendations can be made as a result of this study:

- Standard operating procedures call for flap deployment during the entry and drop phases of flight. These two phases are also most susceptible to overspeeding due to pilot workload and the nature of the necessary maneuvers dictated by the terrain. Therefore, it is highly recommended that some form of flap deflection information be included among the recorded parameters.

- The location of the Appareo sensor led to recording additional occurrences of gust loads and necessitated the correction of the maneuver loads because the sensor was offset from the center of gravity. The former could be due to airframe vibration, while the latter was in response to the rotational degrees of freedom of the aircraft. The authors highly recommend moving the sensors closer to the center of gravity to minimize these effects.

- The 2-second rule was used for identification of the maneuver loads. This method was developed from detailed examination of loads on transport aircraft that typically fly at higher altitudes. It is unknown whether the 2-second rule is applicable to air tankers that fly at much lower altitudes. Therefore, the authors recommend re-evaluation of this method for low-altitude flying aircraft.

- This study was entirely focused on the airborne phases of flight. In most cases, these aircraft are operated at or near the gross weight before takeoff. The ground load experienced by the airframe may be as significant as those in the airborne phases. Therefore, it is recommended that the ground phases be included in any future studies.

- To ensure the integrity of the data, the authors recommend periodic calibration of the sensors.

After implementing the above recommendations, it is advisable to repeat this study in 2 to 3 years. Such duplication will

- remove any doubts concerning the integrity of the data used for the present report.
- result in quantifying any possible changes in aircraft usage.

7. REFERENCES.

1. Jewel, J.W., Morris, G.J., and Avery, D.E., "Operating Experiences of Retardant Bombers During Firefighting Operations," NASA TM X-72622, November 1974.

2. National Transportation Safety Board, Safety Recommendations A-04-29 through -33, April 23, 2004.

3. Nelson, J., "U.S. Forest Service Operational Loads Monitoring Program," *11th Joint FAA/DoD/NASA Aging Aircraft Conference*, Phoenix, AZ, April 22, 2008.

4. Hall, S.R., "Consolidation and Analysis of Loading Data in Firefighting Operations – Analysis of Existing Data and Definition of Preliminary Air Tanker and Lead Aircraft Spectra," FAA Report DOT/FAA/AR-05/35, October 2005.

5. Misencik, D., Riccio, T., and Burd, J., "Service Life Evaluation Program–Fatigue and Damage Tolerance Analysis for the U.S. Navy P2V-5/-7 Wing," Avenger Aircraft Services, AAS-SSR-05-004, May 23, 2005.

6. Pritchard, D.M., Riccio, T., and Burd, J., "P2V-5/-7 Aerial Dispersion Mission Configuration, Usage and Load History for Fatigue Loads," Avenger Aircraft Services, AAS-SSR-05-023, November 15, 2005.

7. Gibson, H., Riccio, T., and Burd, J., "P2V-5/-7 Aerial Dispersion External Fatigue Loads," Avenger Aircraft Services, AAS-SSR-06-008, February 23, 2006.

8. Burd, J., Misencik, D., Riccio, T., Nelson, J., and Brosnan, L., "Operational Service Life Evaluation for the United States Forest Service P2V-5/-7," *9th Joint FAA/DoD/NASA Aging Aircraft Conference*, Atlanta, Georgia, March 2006.

9. Gibson, H., Riccio, T., and Burd, J., "P2V-5/-7 Aerial Dispersion With 2005-2006 Tanker Data Fatigue and Damage Tolerance Report," Avenger Aircraft Services, AAS-SSR-06-071, December 20, 2006.

10. Farrell, P. and Burd, J., "USFS DC-3/TP67 Usage Report," Avenger Aircraft Services, AAS-OLM-08-001, September 9, 2008.

11. Burd, J., "Operational Service Life Evaluation for the United States Forest Service P-3 Aircraft," *2007 Aircraft Structural Integrity Conference*, Palm Springs, California, December 2007.

12. United States Air Force, *Flight Manual Handbook, Navy Model P2V-5 and P2V-5F Aircraft*, Document AN 01-75EDA-1, published January 15, 1955, revised April 15, 1958.

13. Naval Air Systems Command, *NATOPS Flight Manual, Navy Model P3A/B/C Aircraft*, Document NAVAIR 01-75PAC-1, published June 1, 1996, revised February 15, 1999.

14. Miner, J., "ADAPT System Interface Specification: SEI Flight Recorder System," Celeris Aerospace Canada, Inc., September 2003.

15. Schade, M.O., Braun, J.F., and Hall, Stephen R., "A Structural Health Management Installation Plan for the Lockheed P2-V7 Aircraft Operating in the Aerial Firefighting Role," Celeris Aerospace Canada Inc./Systems and Electronics, Inc., Technical Report CAC/TR/03-025, October 2003.

16. Schade, M.O., Braun, J.F., and Hall, Stephen R., "A Structural Health Management Installation Plan for P-3 Aircraft Operating in the Aerial Firefighting Role," Celeris Aerospace Canada Inc./Systems and Electronics, Inc., Technical Report CAC/TR/03-016 Revision 1, November 2003.

17. Tipps, D.O., Skinn, D.A., Rustenburg, J.W., and Zeiler, T.A., "Statistical Loads Data for BE-1900D Aircraft in Commuter Operations," FAA Report DOT/FAA/AR-00/11, April 2000.

18. Airplane Strength and Rigidity Reliability Requirements, Repeated Loads, Fatigue, and Damage Tolerance, MIL-1-8866C(AS), 20 May 1987.

19. Rustenburg, J.W., Skinn, D.A., and Tipps, D.O., "An Evaluation of Methods to Separate Maneuver and Gust Load Factors From Measured Acceleration Time Histories," FAA Report DOT/FAA/AR-99/14, April 1999.

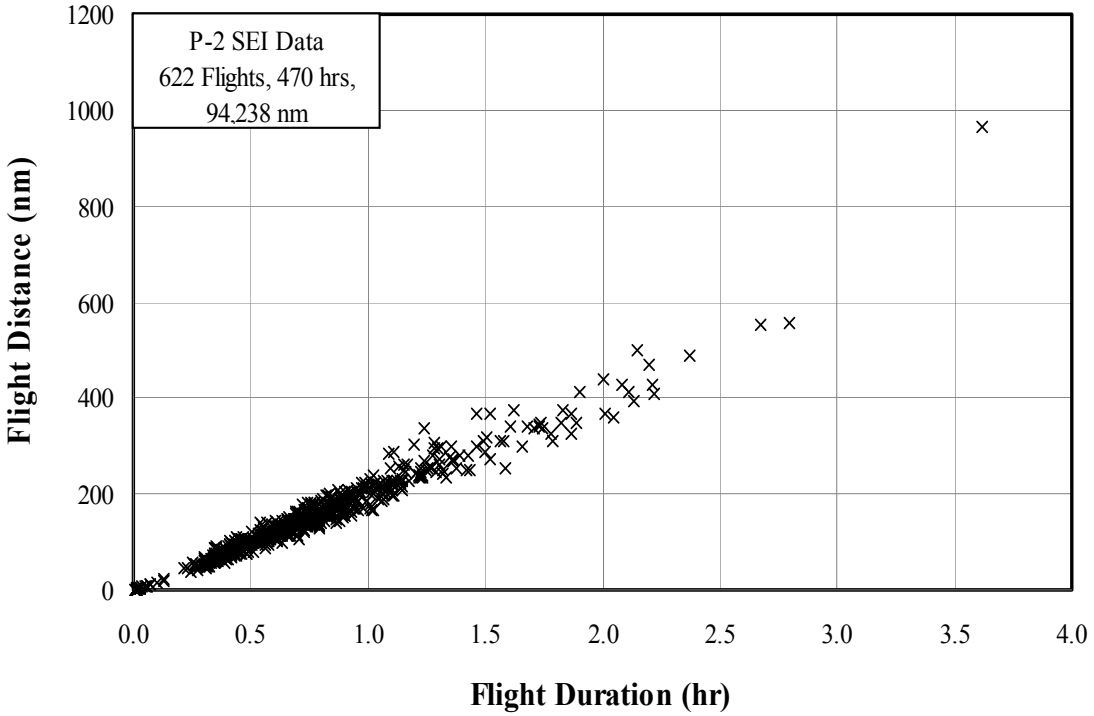

(a) P2V—Systems and Electronics, Inc. System

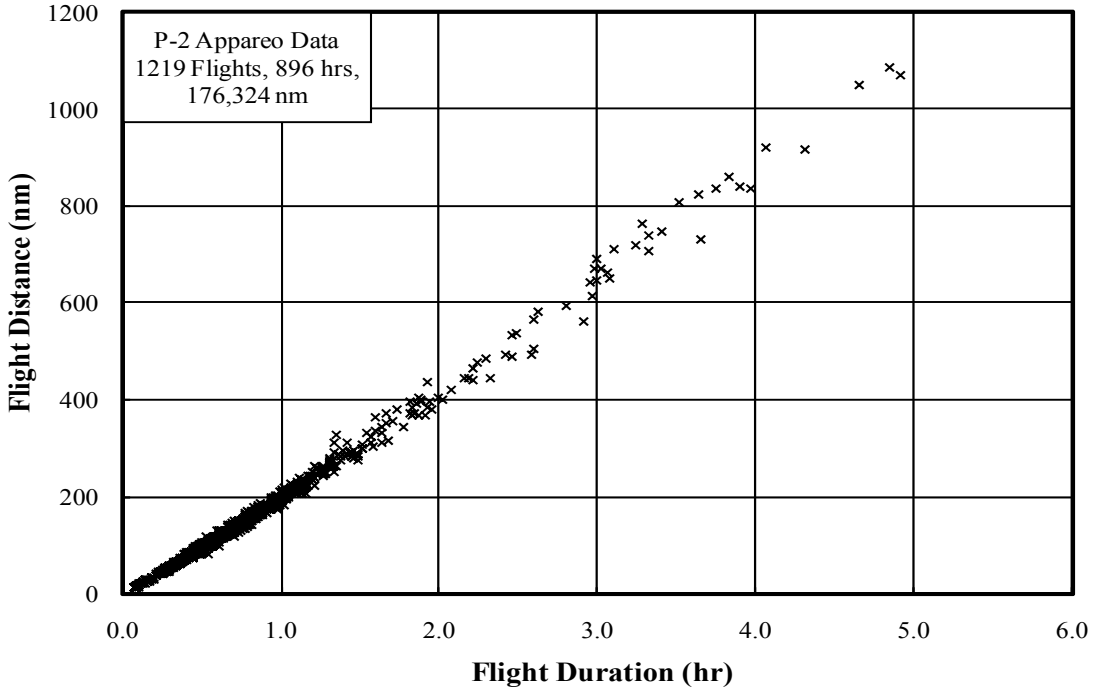

(b) P2V—Appareo System

Figure A-1. Correlation of Flight Distance and Flight Duration, all Phases

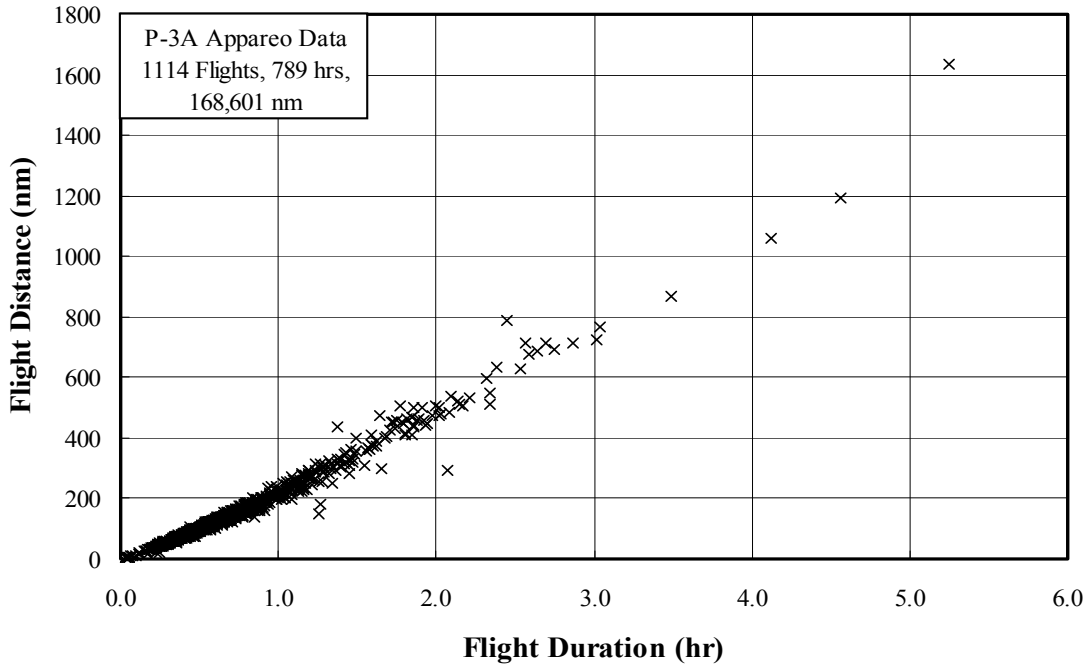

(c) P3A—Appareo System

Figure A-1. Correlation of Flight Distance and Flight Duration, all Phases (Continued)

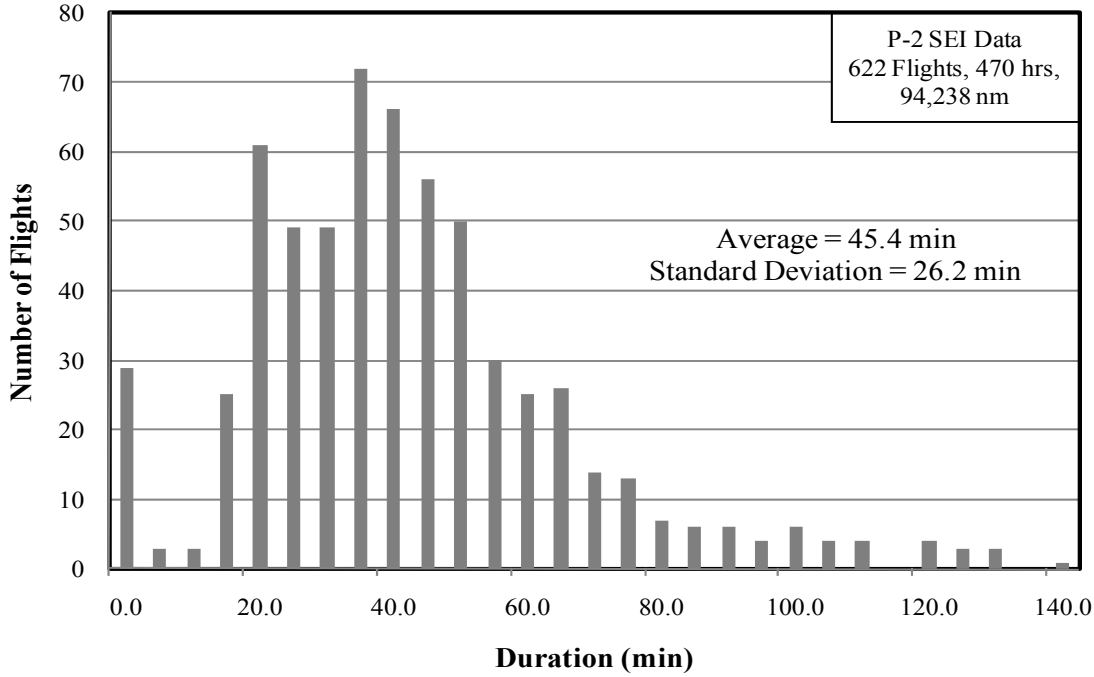

(a) P2V—Systems and Electronics, Inc. System

Figure A-2. Distribution of Flight Durations, all Phases

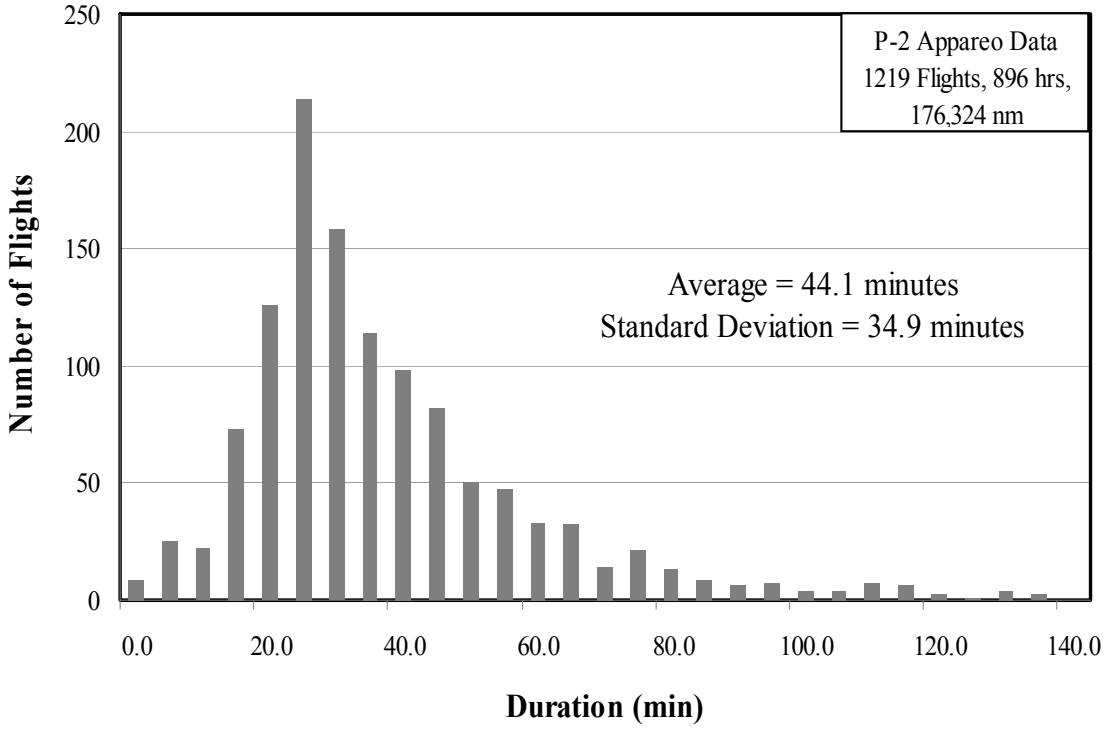

(b) P2V—Appareo System

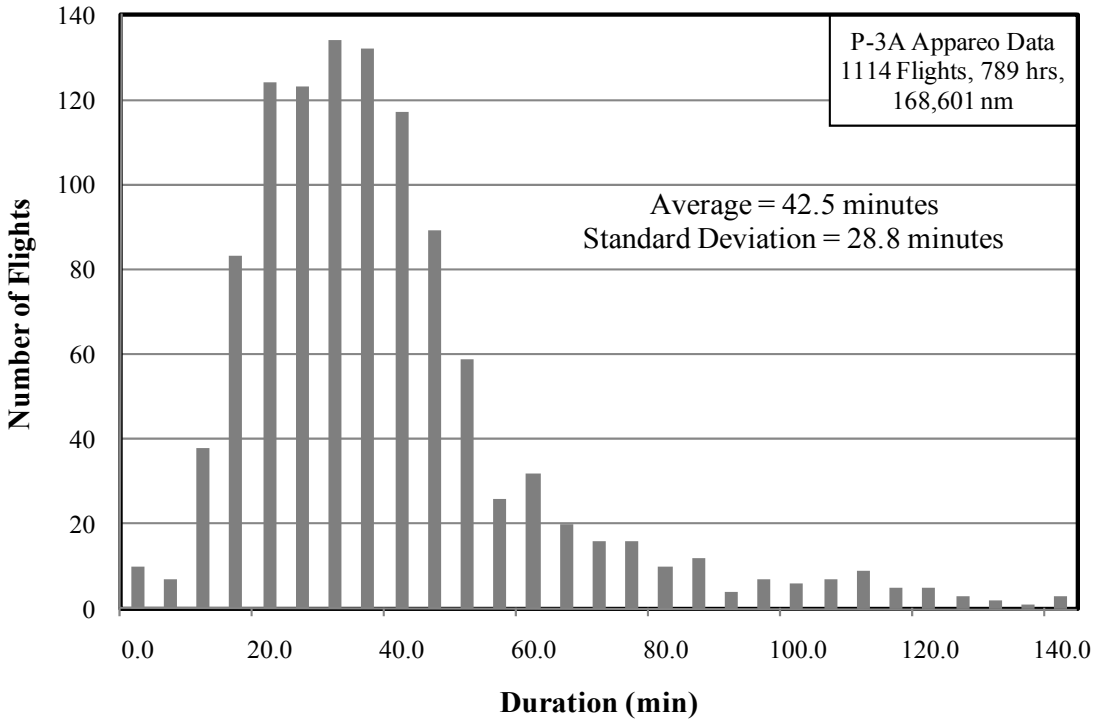

(c) P3A—Appareo System

Figure A-2. Distribution of Flight Durations, all Phases (Continued)

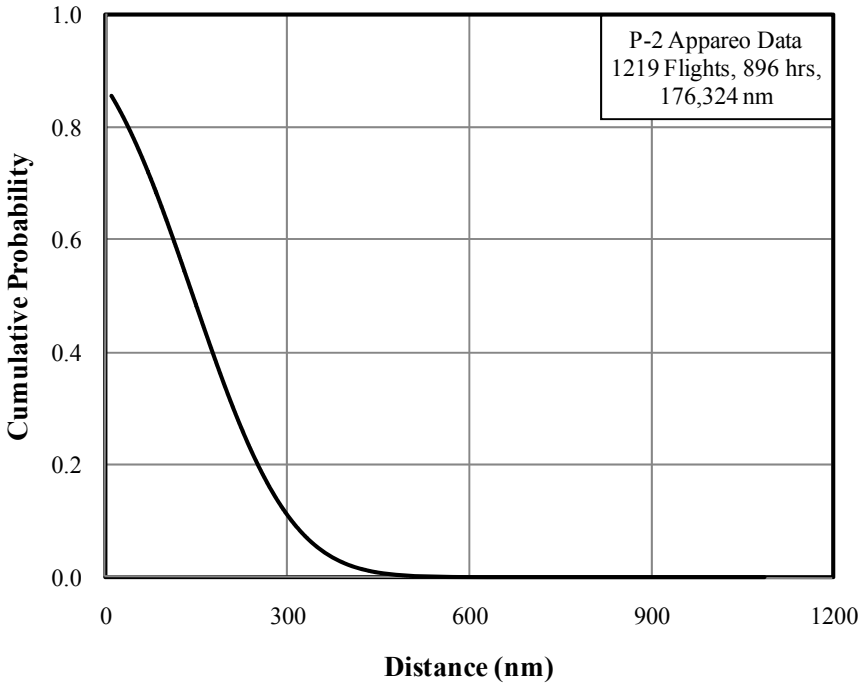

(a) P2V—Appareo System

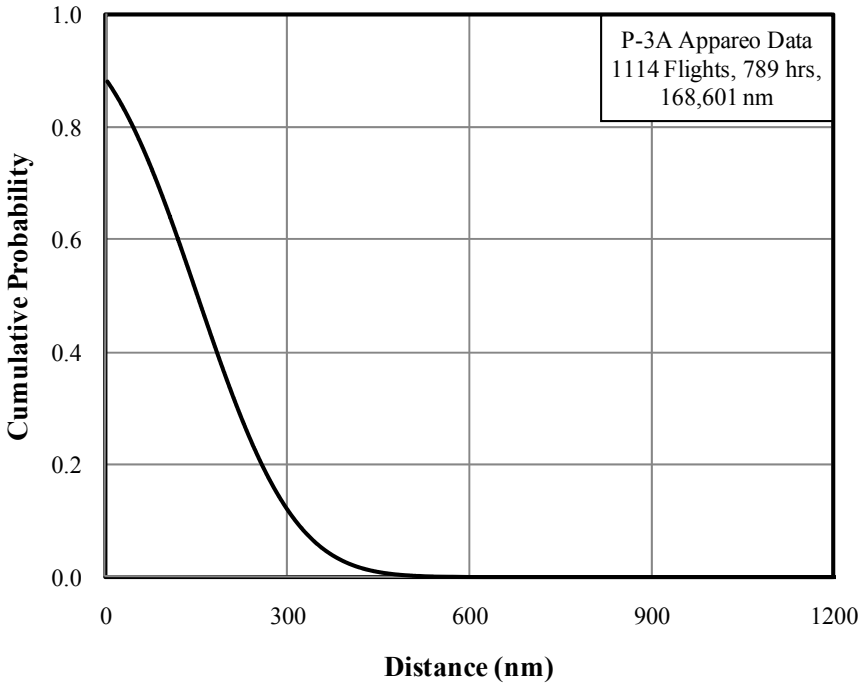

(b) P3A—Appareo System

Figure A-3. Cumulative Probability of Flight Distance, all Phases

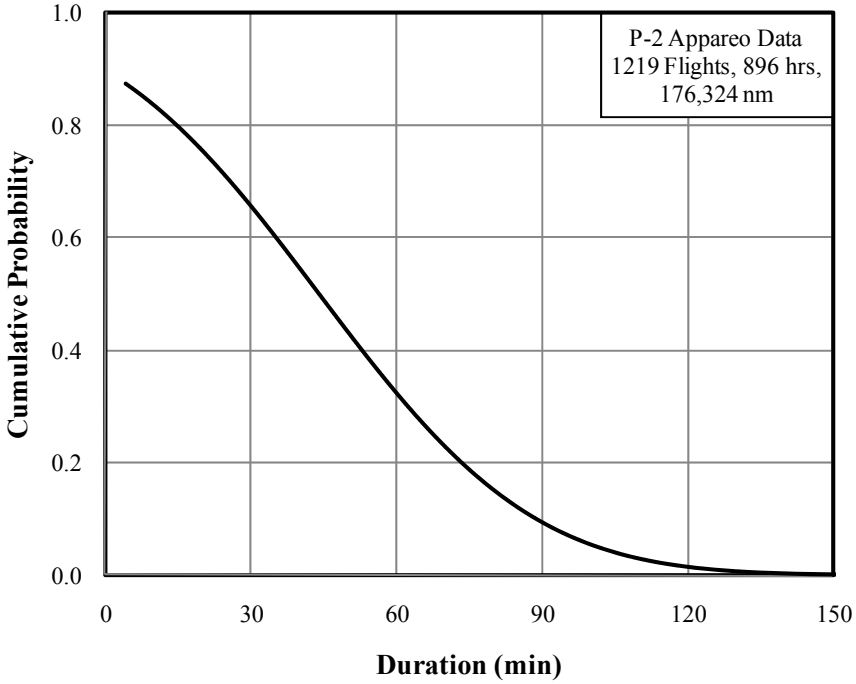

(a) P2V—Appareo System

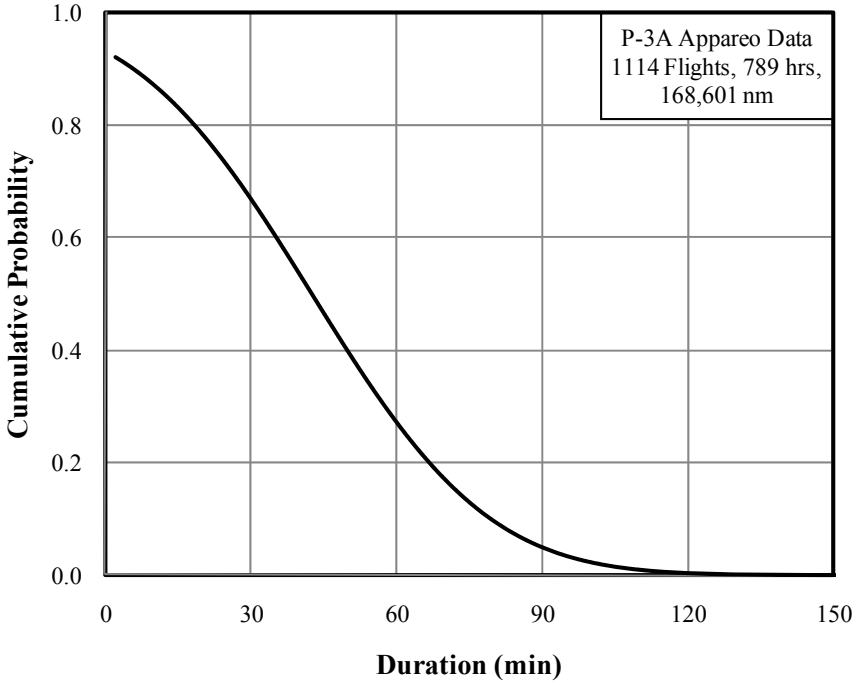

(b) P3A—Appareo System

Figure A-4. Cumulative Probability of Flight Duration, all Phases

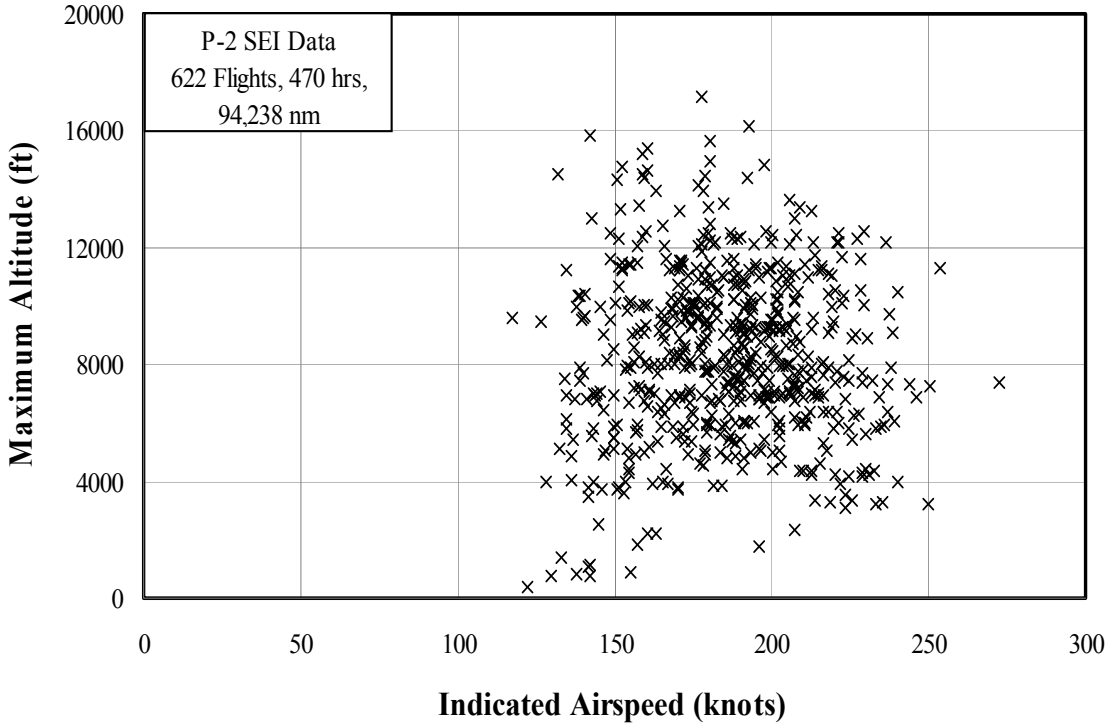

(a) P2V—Systems and Electronics, Inc. System

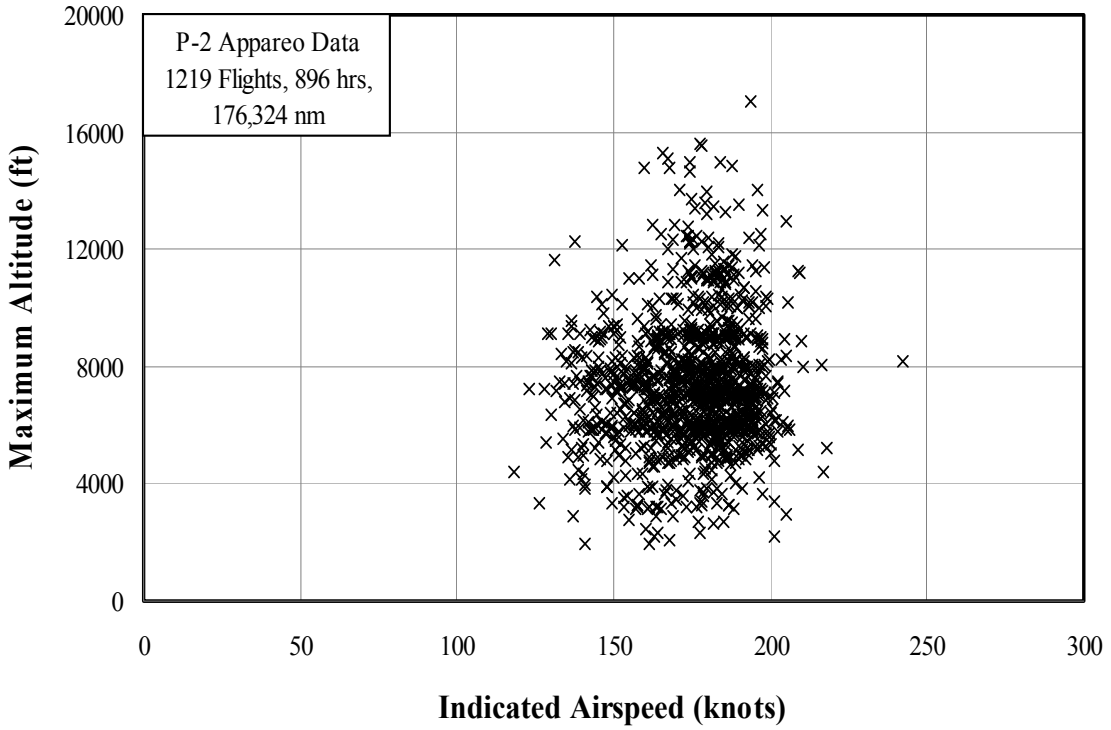

(b) P2V—Appareo System

Figure A-5. Maximum Above Ground Level Altitude and Coincident Indicated Airspeed, all Phases

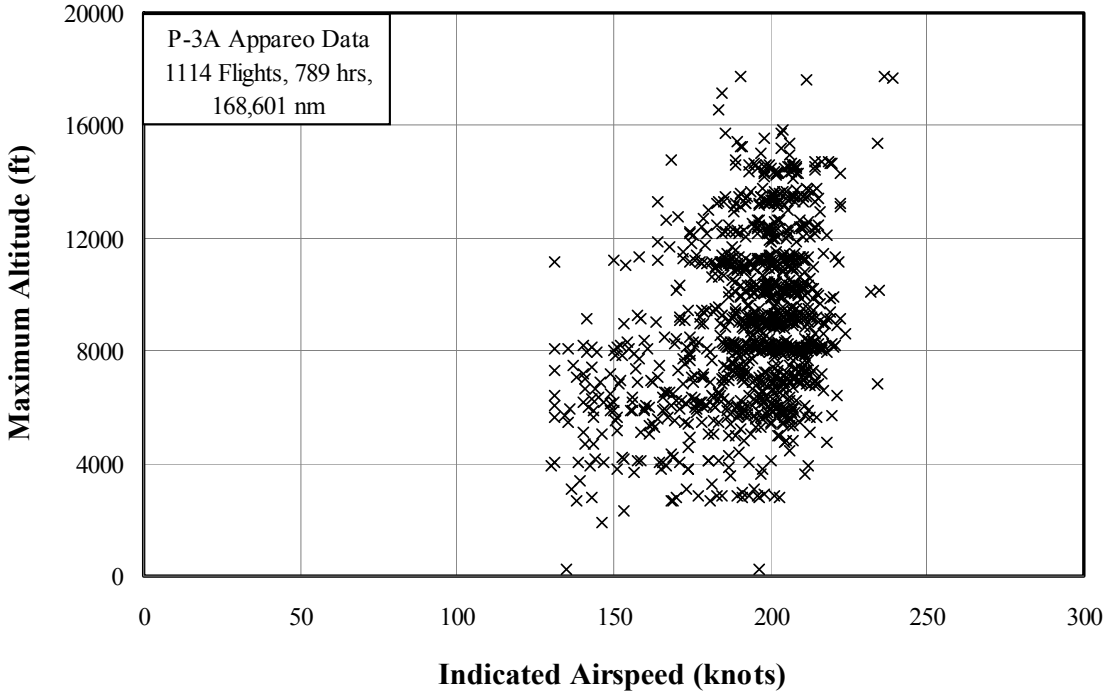

(c) P3A—Appareo System

Figure A-5. Maximum Above Ground Level Altitude and Coincident Indicated Airspeed, all Phases (Continued)

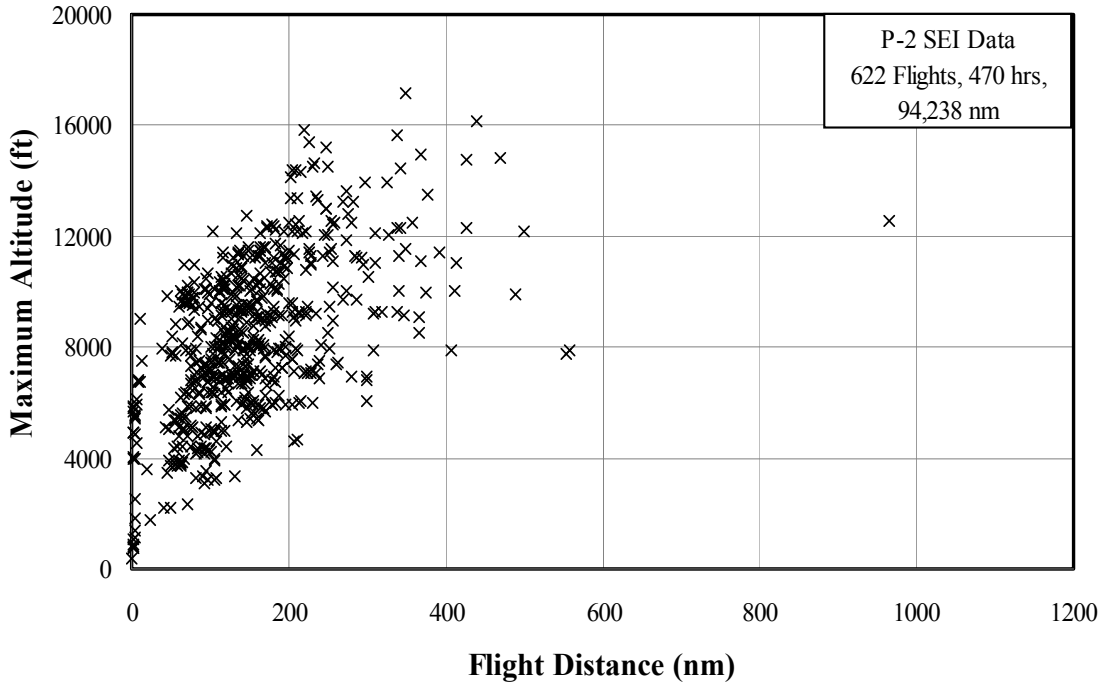

(a) P2V—Systems and Electronics, Inc. System

Figure A-6. Correlation of Maximum Above Ground Altitude and Flight Duration, all Phases

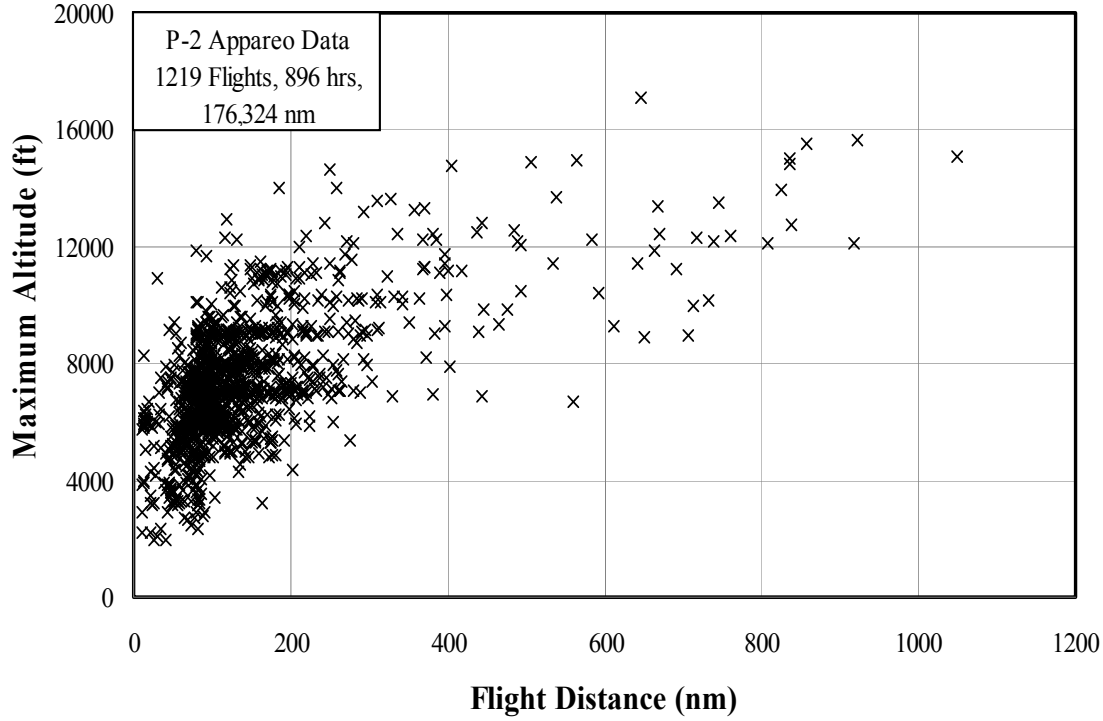

(b) P2V—Appareo System

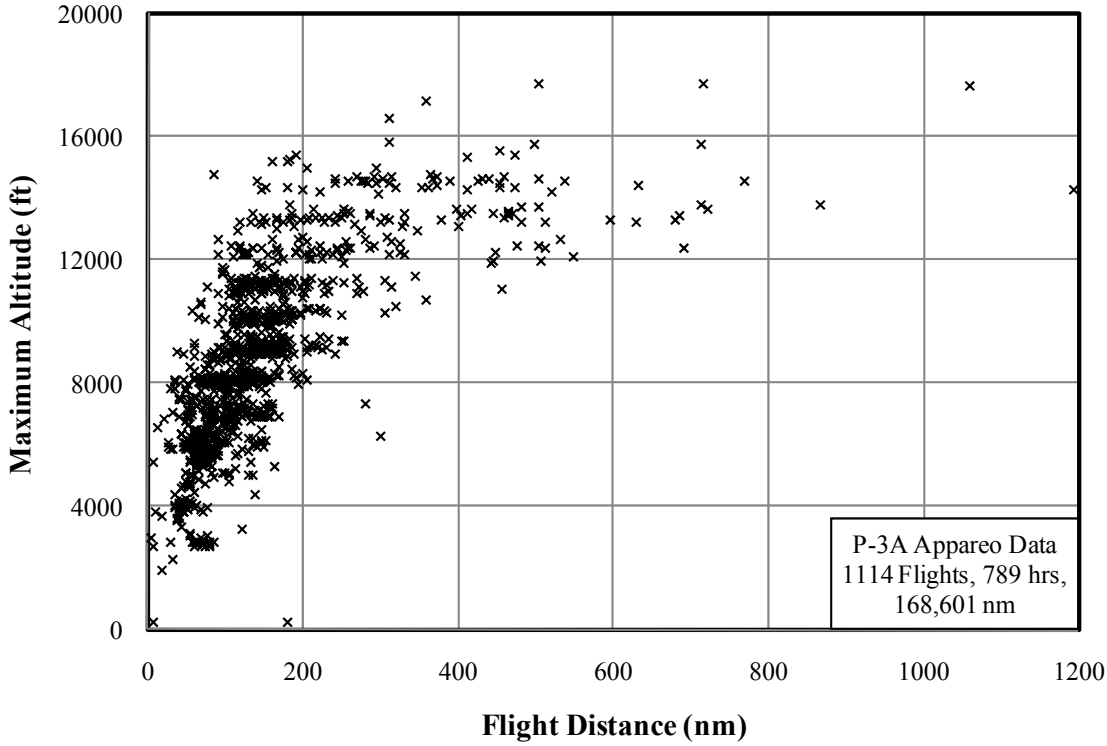

(c) P3A—Appareo System

Figure A-6. Correlation of Maximum Above Ground Altitude and Flight Distance, all Phases (Continued)

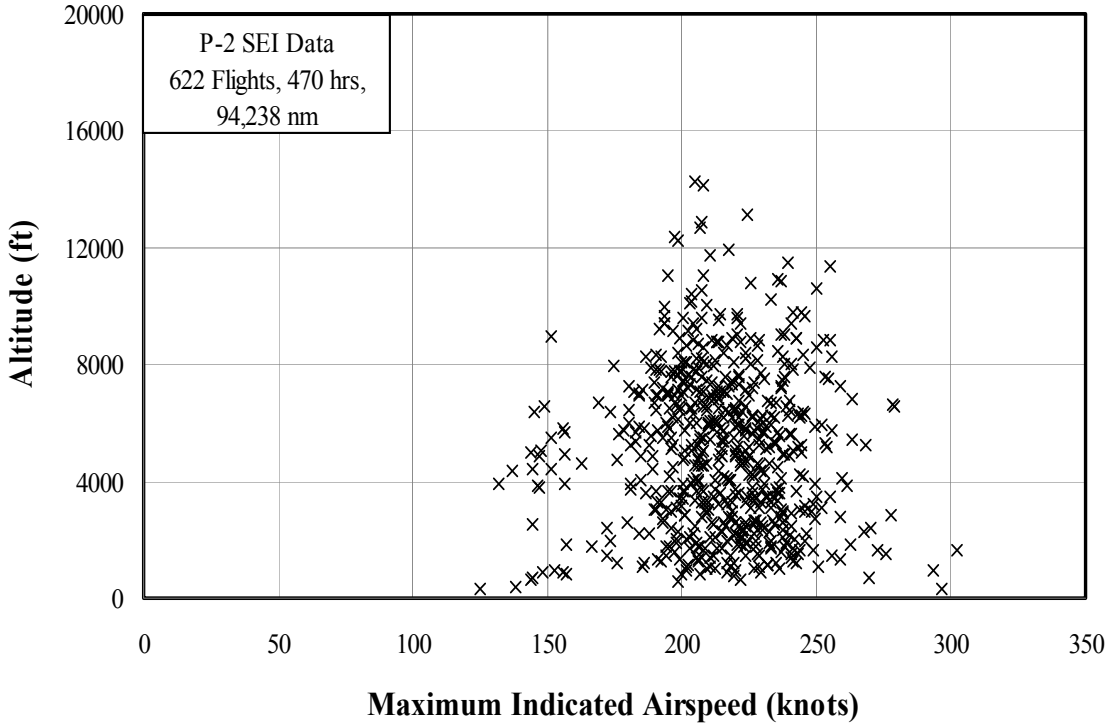

(a) P2V—Systems and Electronics, Inc. System

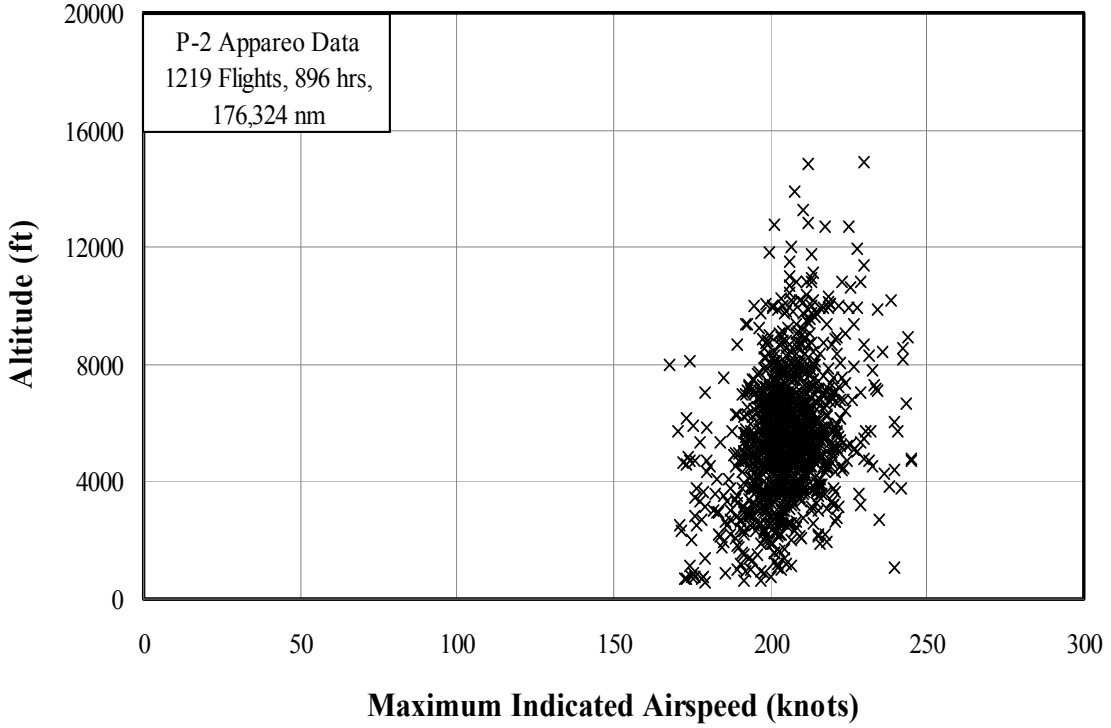

(b) P2V—Appareo System

Figure A-7. Maximum Airspeed and Coincident Above Ground Level Altitude, all Phases

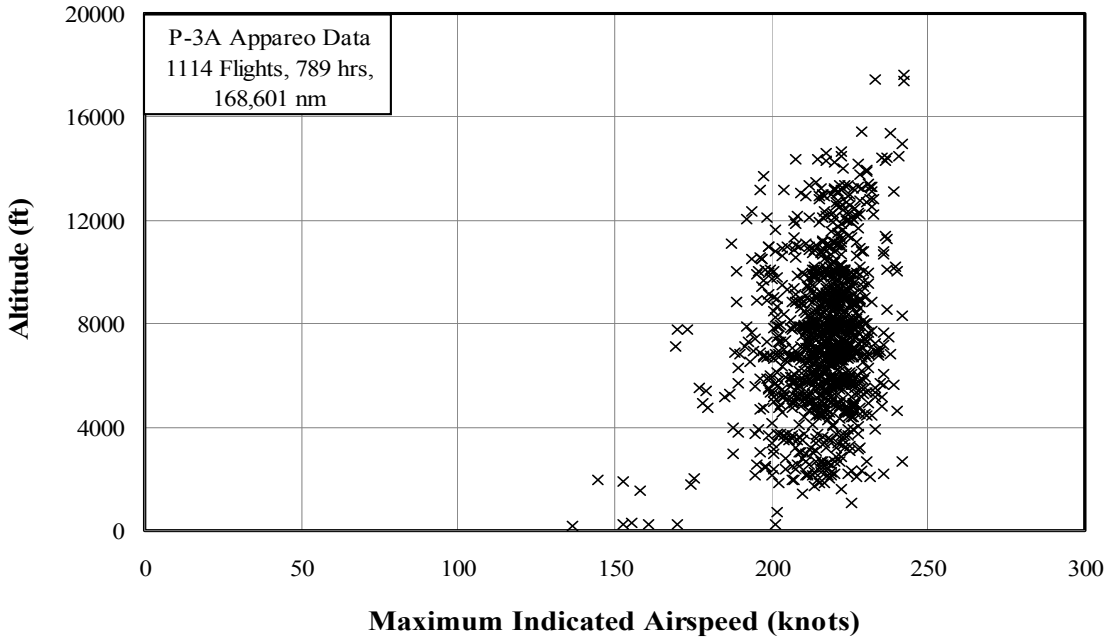

(c) P3A—Appareo System

Figure A-7. Maximum Airspeed and Coincident Above Ground Level Altitude, all Phases (Continued)

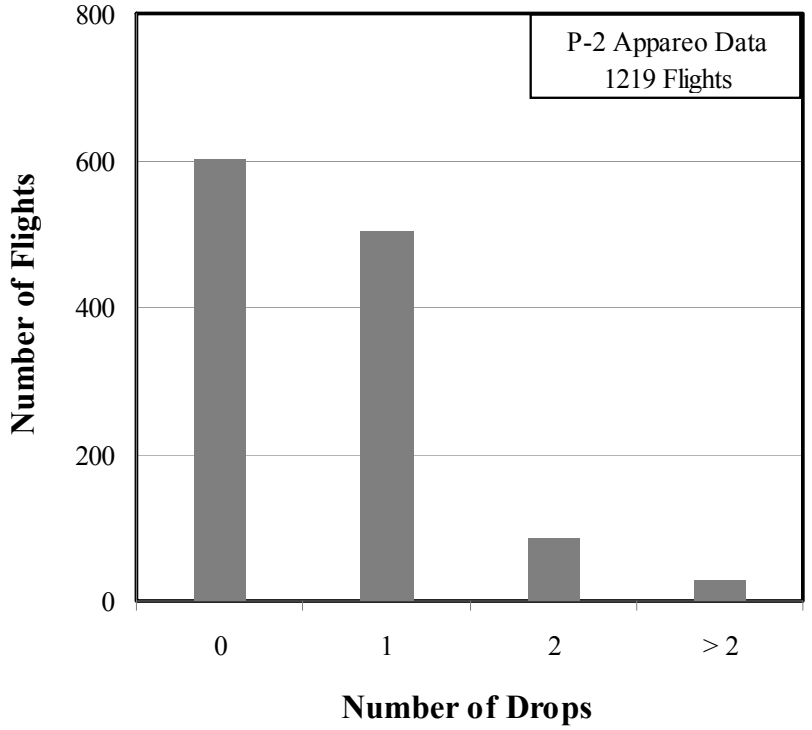

(a) P2V—Appareo System, all Flights

Figure A-8. Number of Flights and Associate Drops

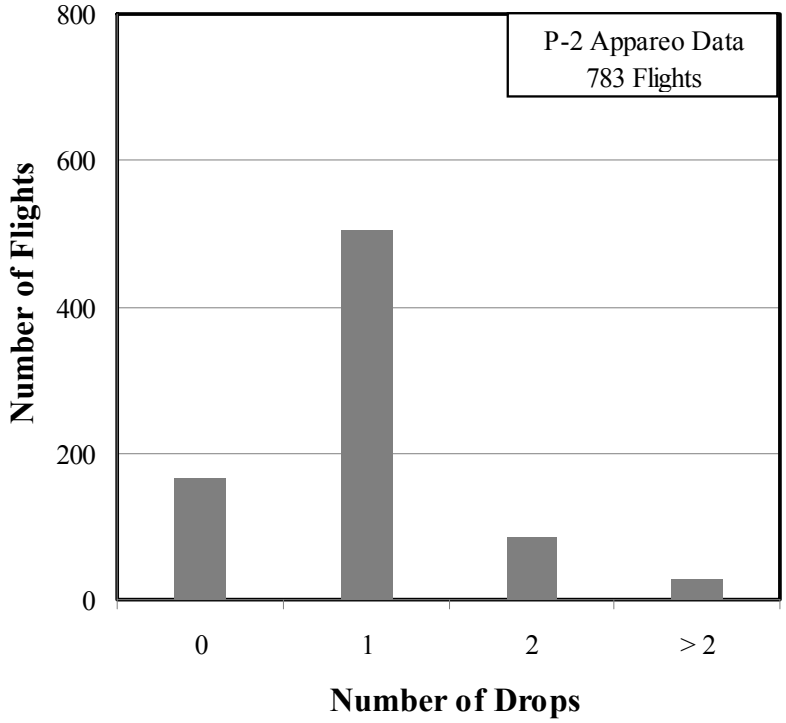

(b) P2V—Appareo System, Excluding Aircraft 5

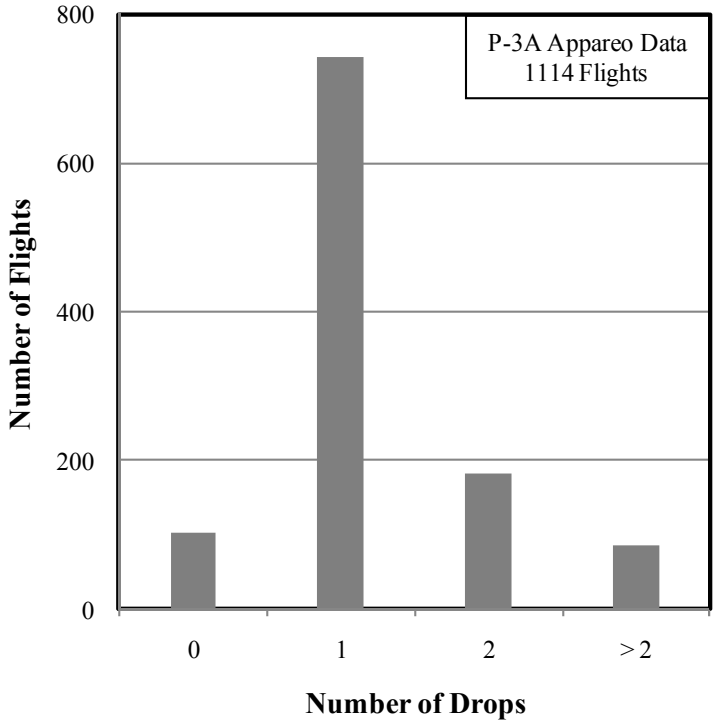

(c) P3A—Appareo System

Figure A-8. Number of Flights and Associated Drops (Continued)

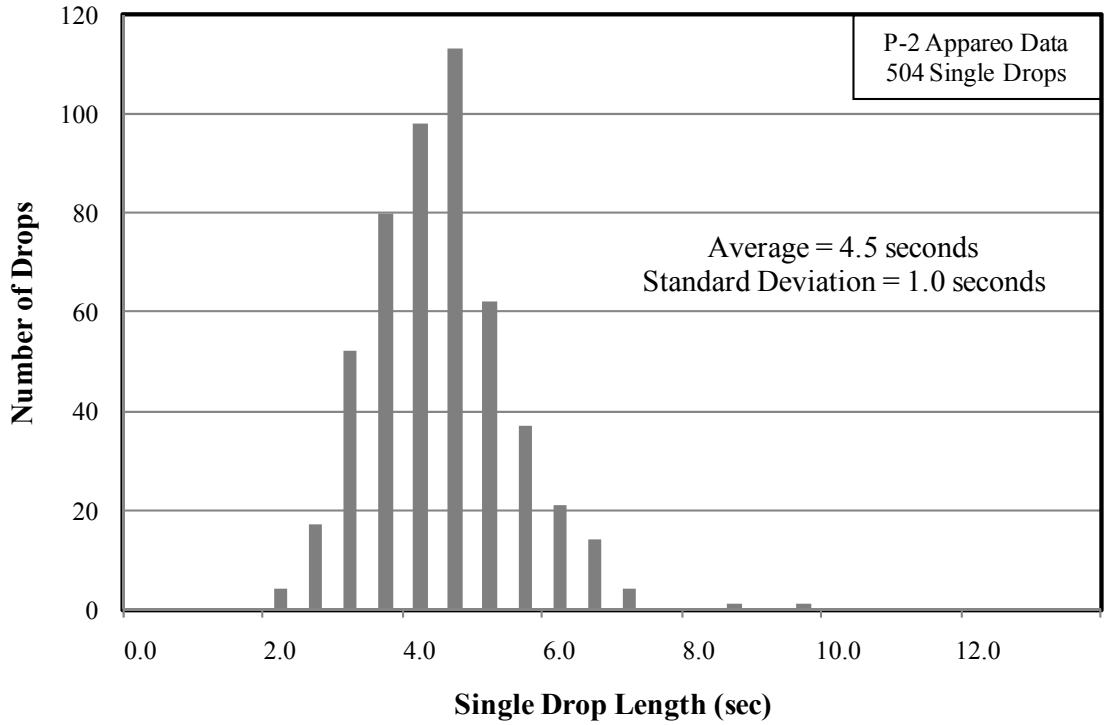

(a) P2V—Appareo System

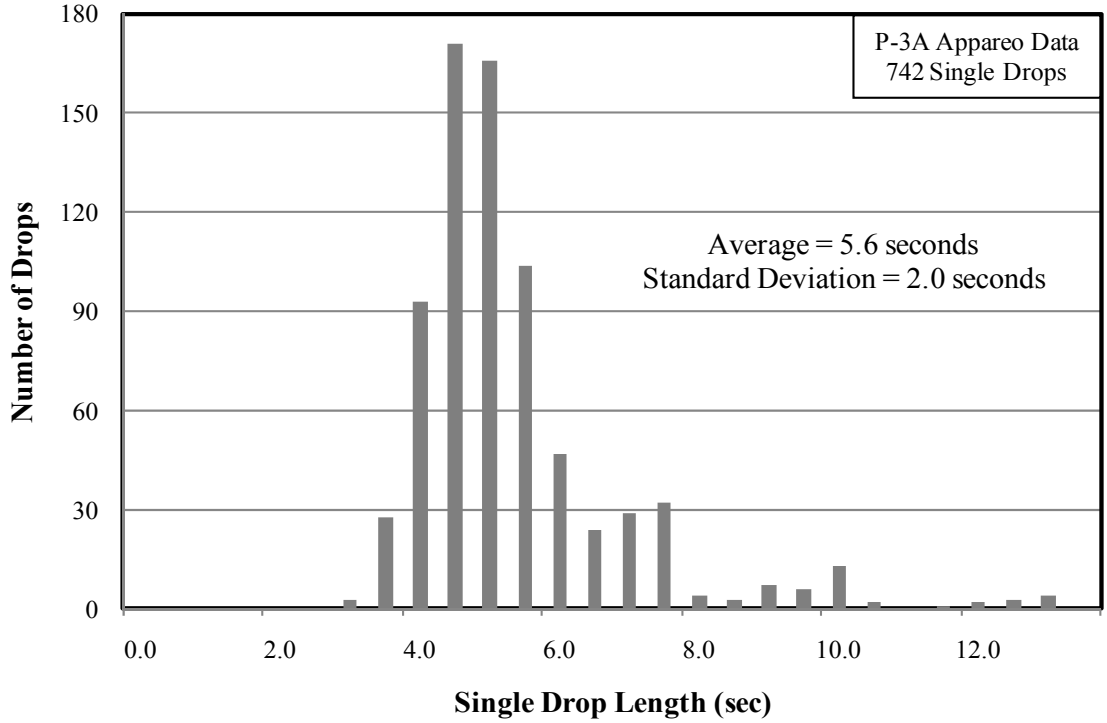

(b) P3A—Appareo System

Figure A-9. Distribution of Single-Drop Durations

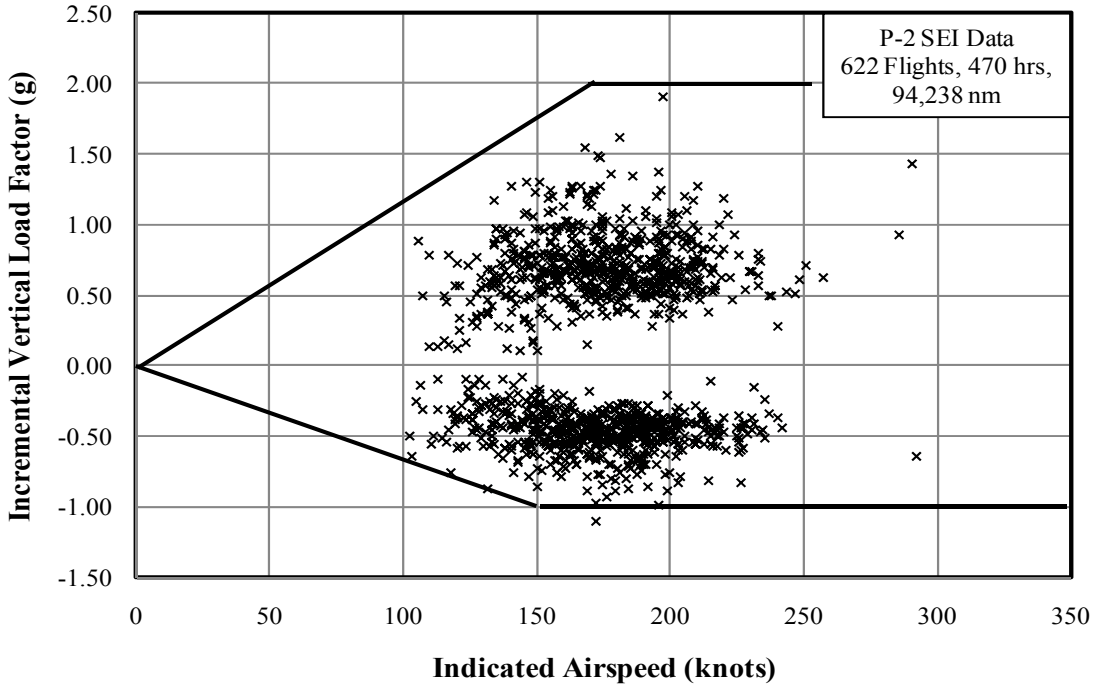

(a) P2V— Systems and Electronics, Inc. System with P3A limits

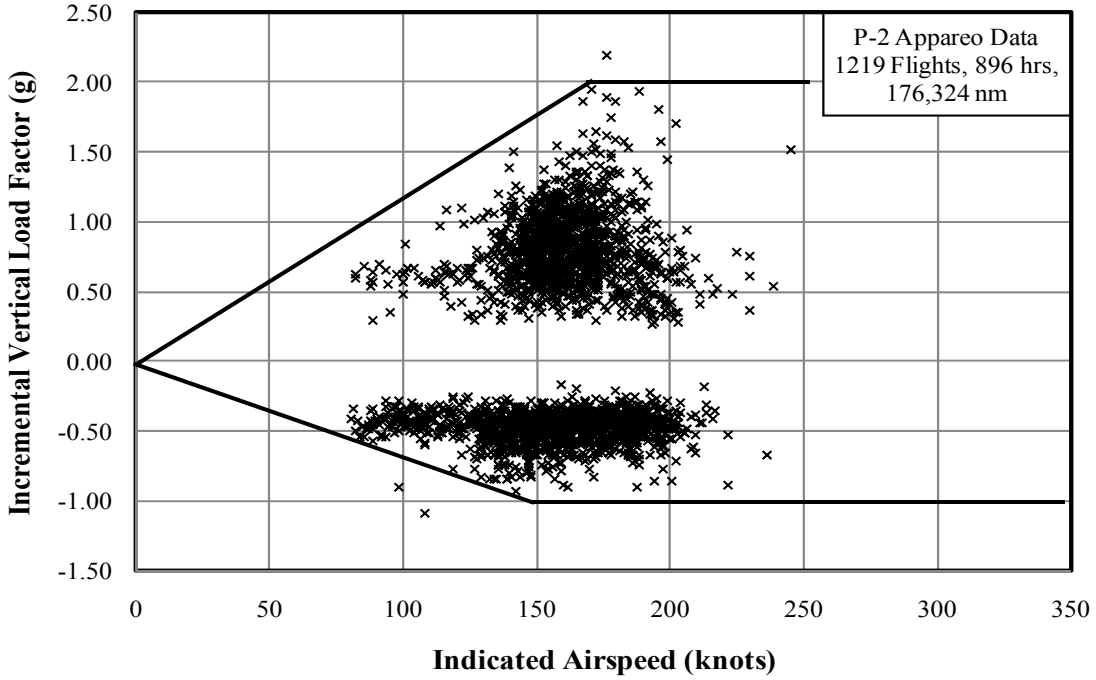

(b) P2V—Appareo System with P3A limits

Figure A-10. Maximum Incremental Vertical Load Factor and Coincident Indicated Airspeed, all Phases

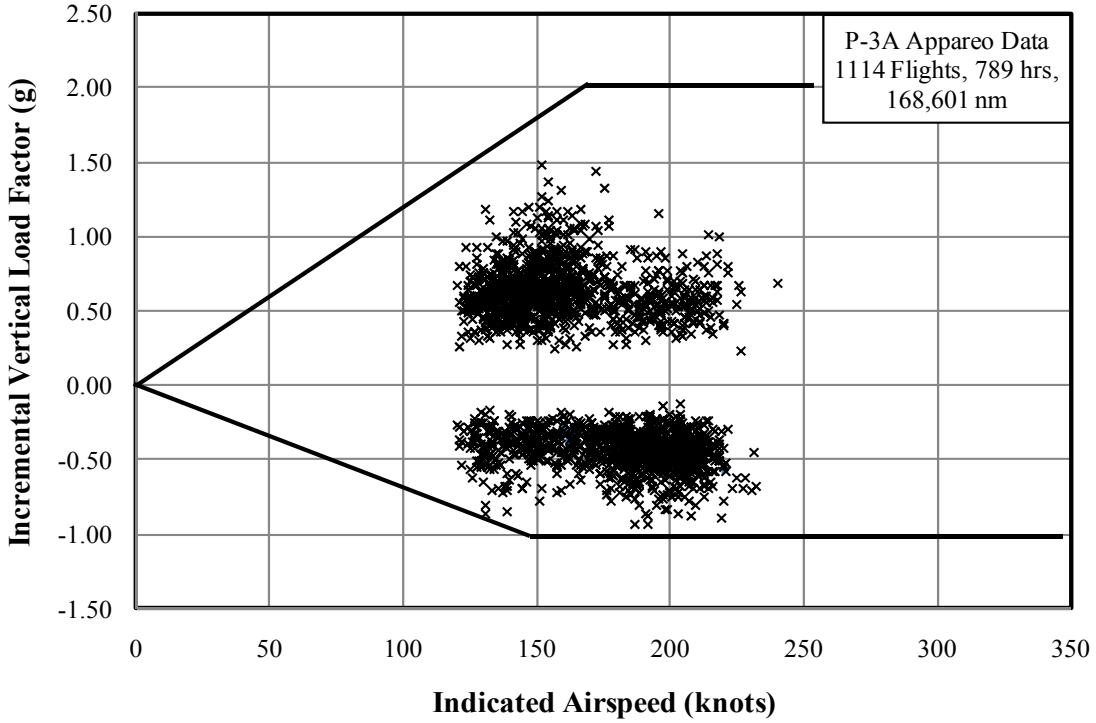

(c) P3A—Appareo System

Figure A-10. Maximum Incremental Vertical Load Factor and Coincident Indicated Airspeed, all Phases (Continued)

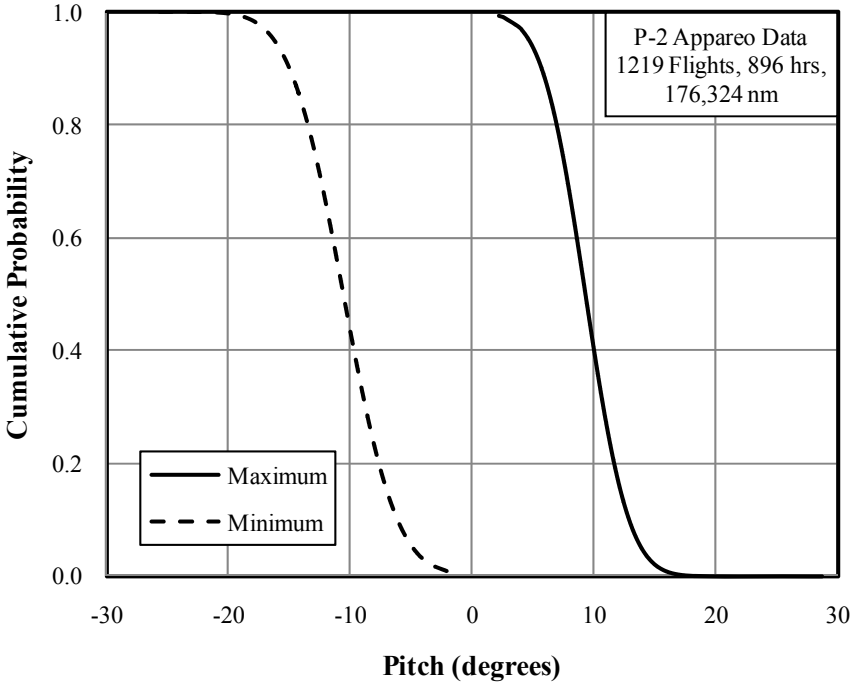

(a) P2V—Appareo System

Figure A-11. Cumulative Probability of the Maximum/Minimum Pitch Angle, all Phases

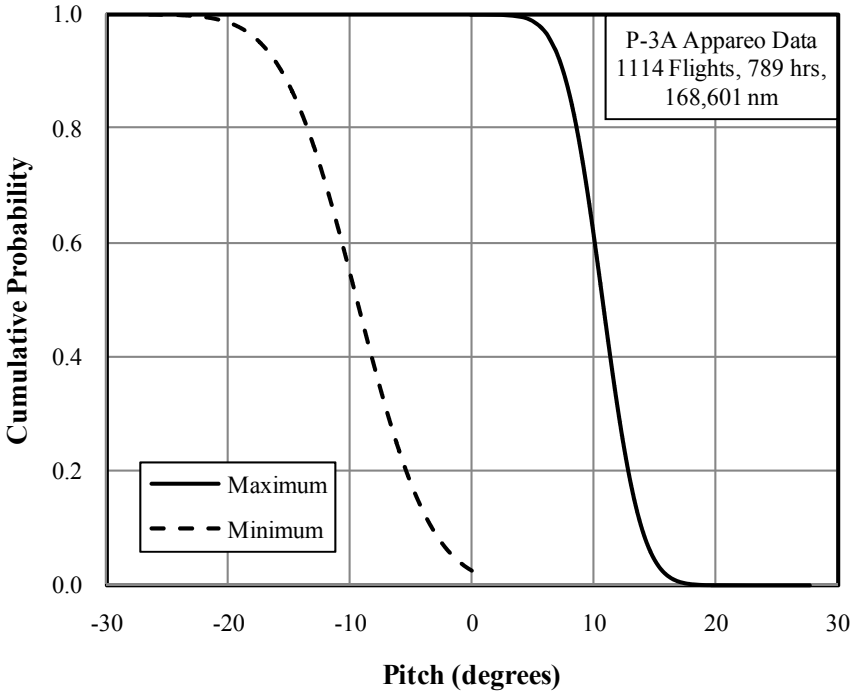

(b) P3A—Appareo System

Figure A-11. Cumulative Probability of the Maximum/Minimum Pitch Angle, all Phases (Continued)

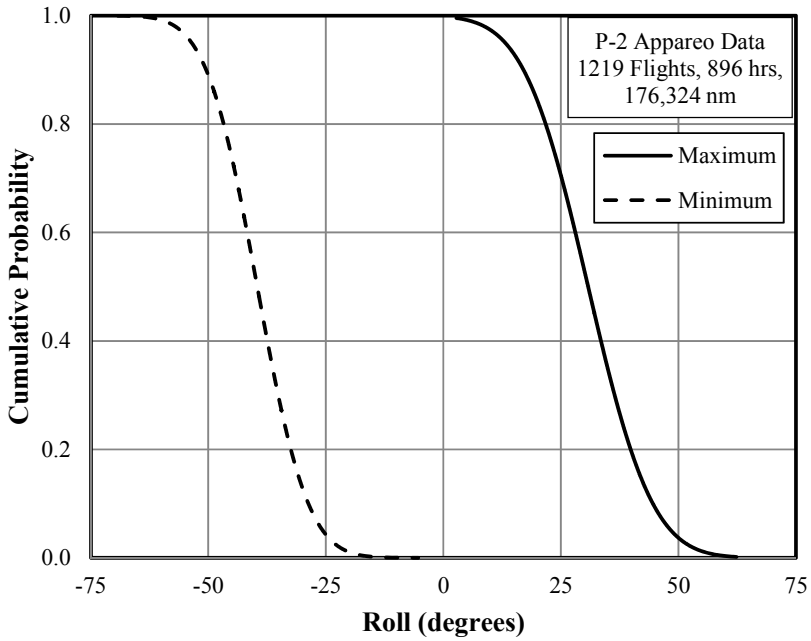

(a) P2V—Appareo System

Figure A-12. Cumulative Probability of the Maximum/Minimum Bank Angle, all Phases

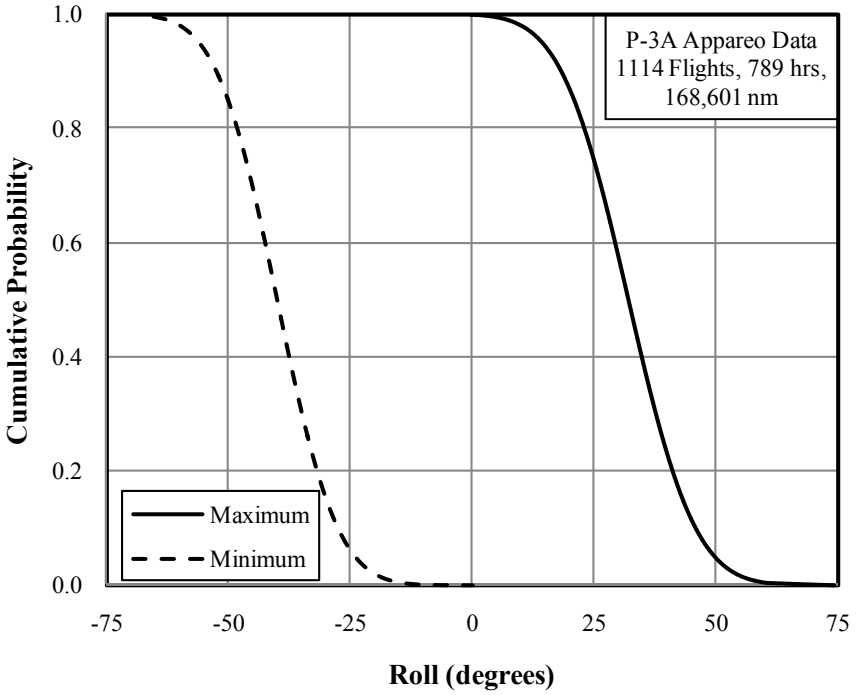

(b) P3A—Appareo System

Figure A-12. Cumulative Probability of the Maximum/Minimum Bank Angle, all Phases (Continued)

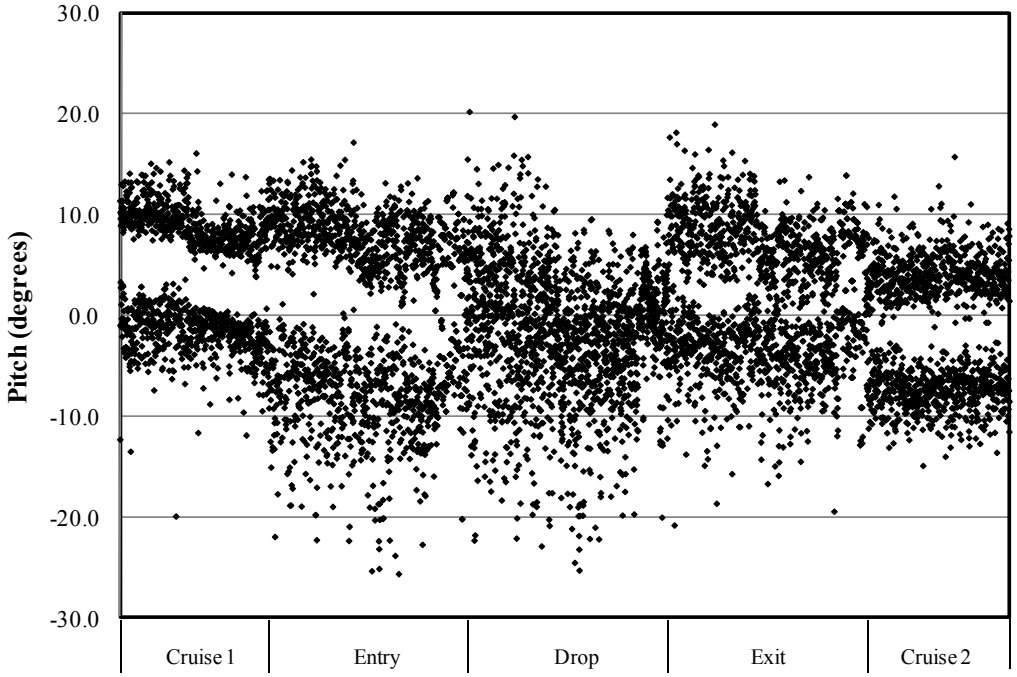

(a) P2V—Appareo System

Figure A-13. Extreme Values of Pitch Angle Correlated With Flight Phase

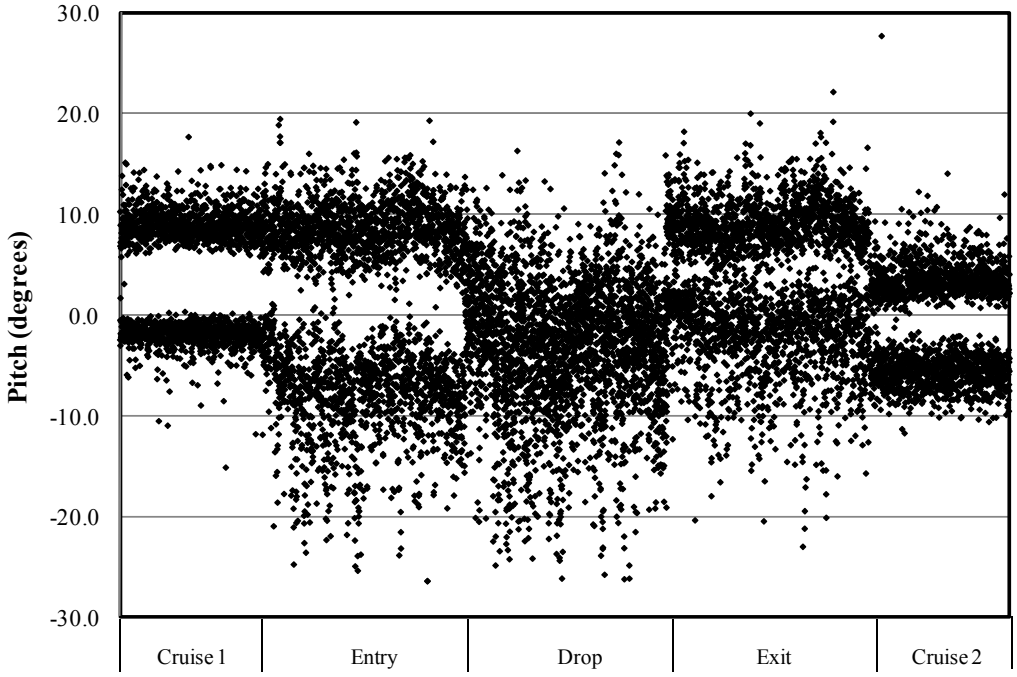

(b) P3A—Appareo System

Figure A-13. Extreme Values of Pitch Angle Correlated With Flight Phase (Continued)

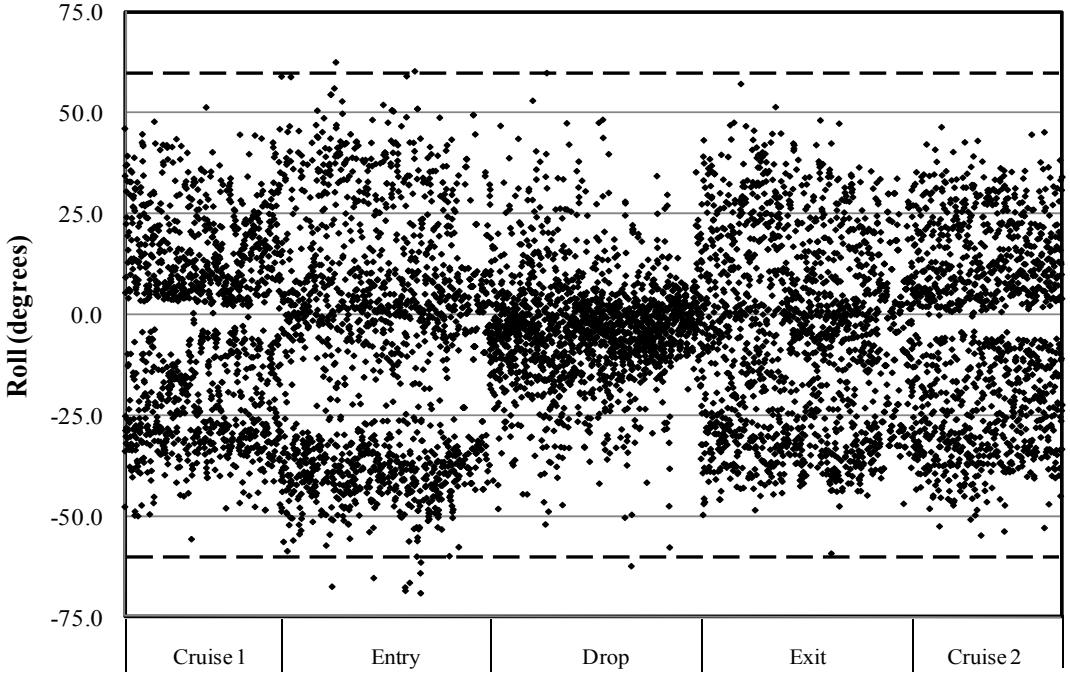

(a) P2V—Appareo System

Figure A-14. Extreme Values of Roll Angle Correlated With Flight Phase

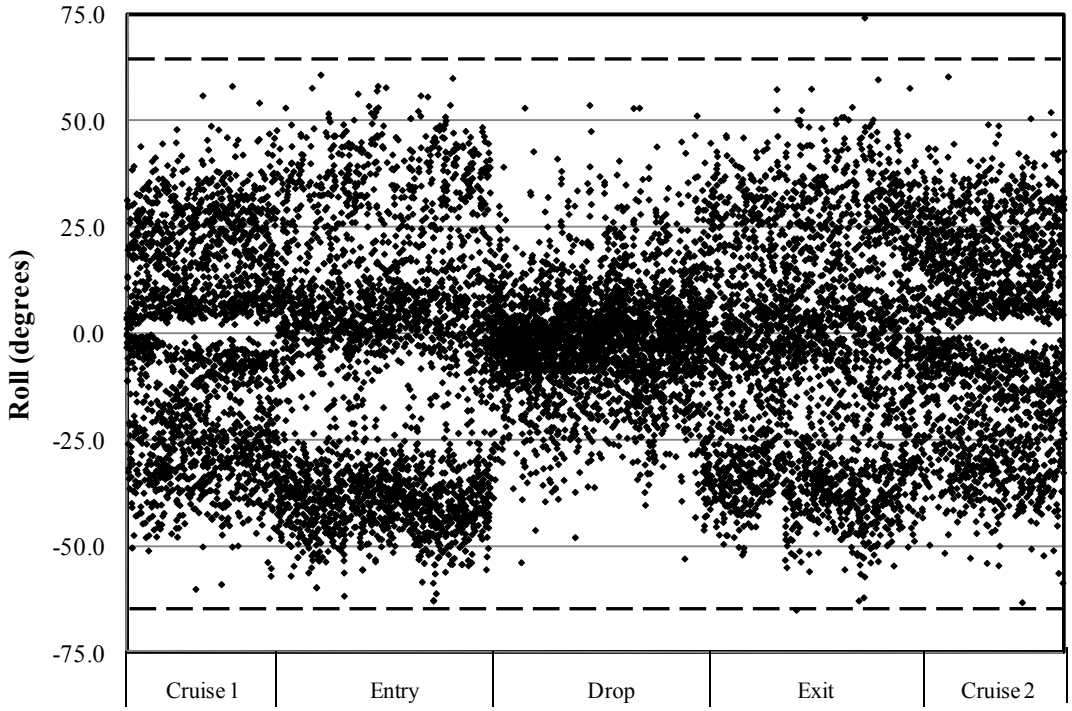

(b) P3A—Appareo System

Figure A-14. Extreme Values of Roll Angle Correlated With Flight Phase (Continued)

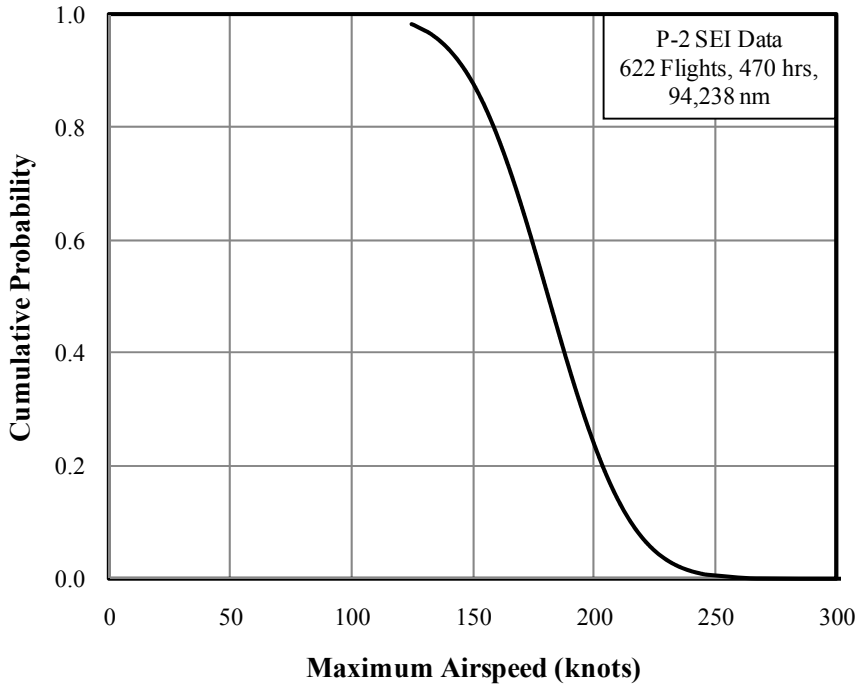

Figure A-15. Cumulative Probability of Maximum Airspeed With at Least one bay Door Open, all Phases, P2V, Systems and Electronics, Inc. System

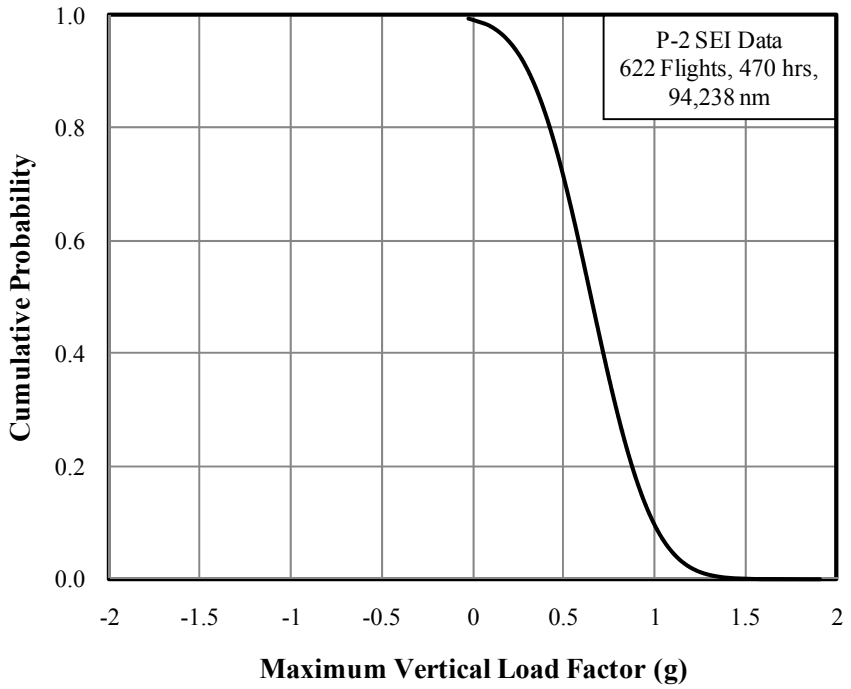

Figure A-16. Cumulative Probability of Maximum Incremental Vertical Load Factor With at Least one bay Door Open, all Phases, P2V, Systems and Electronics, Inc. System

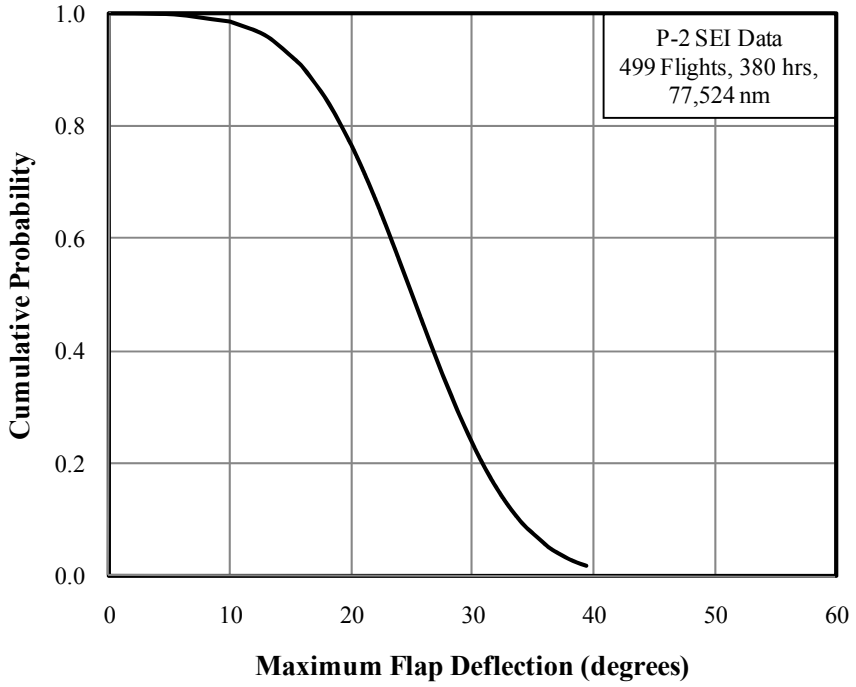

Figure A-17. Cumulative Probability of any Flap Deflection With at Least one bay Door Open, all Phases, P2V, Systems and Electronics, Inc. System

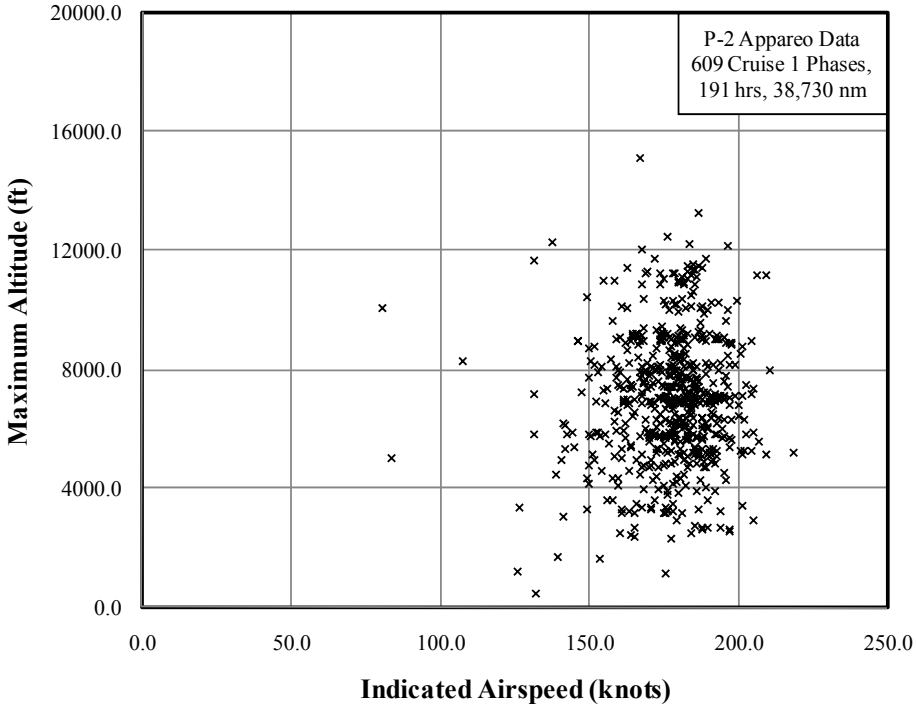

(a) Cruise 1—P2V, Appareo System

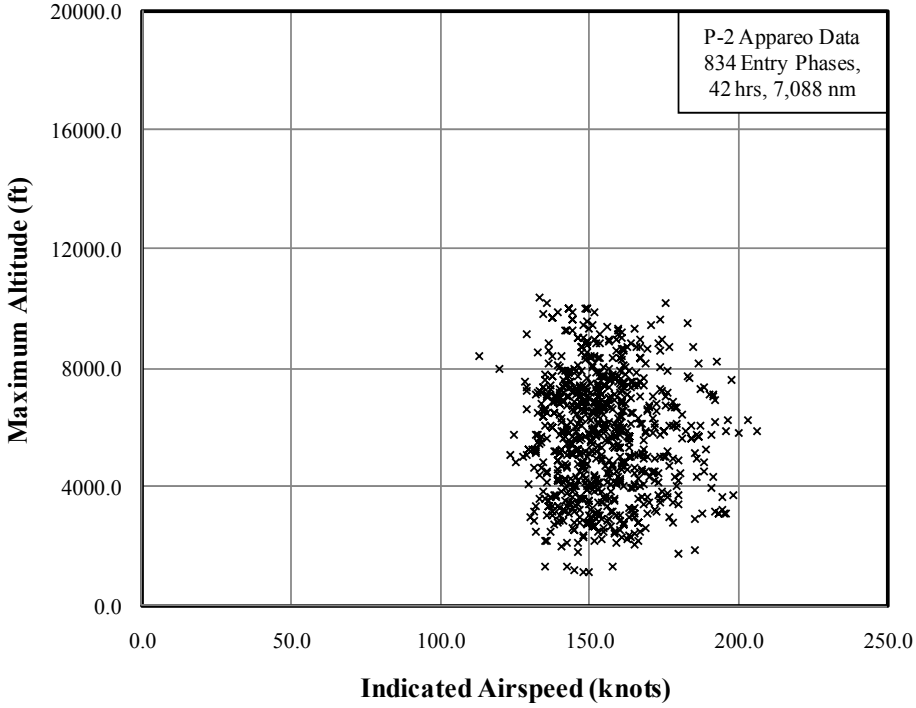

(b) Entry—P2V, Appareo System

Figure A-18. Maximum Above Ground Level Altitude and Coincident Indicated Airspeed, P2V Aircraft

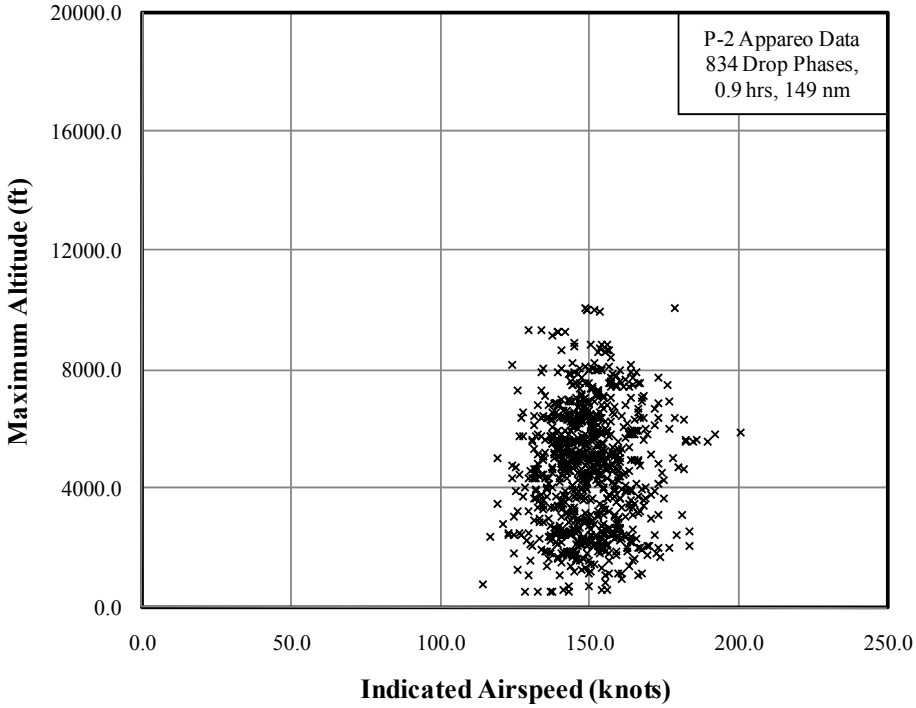

(c) Drop—P2V, Appareo System

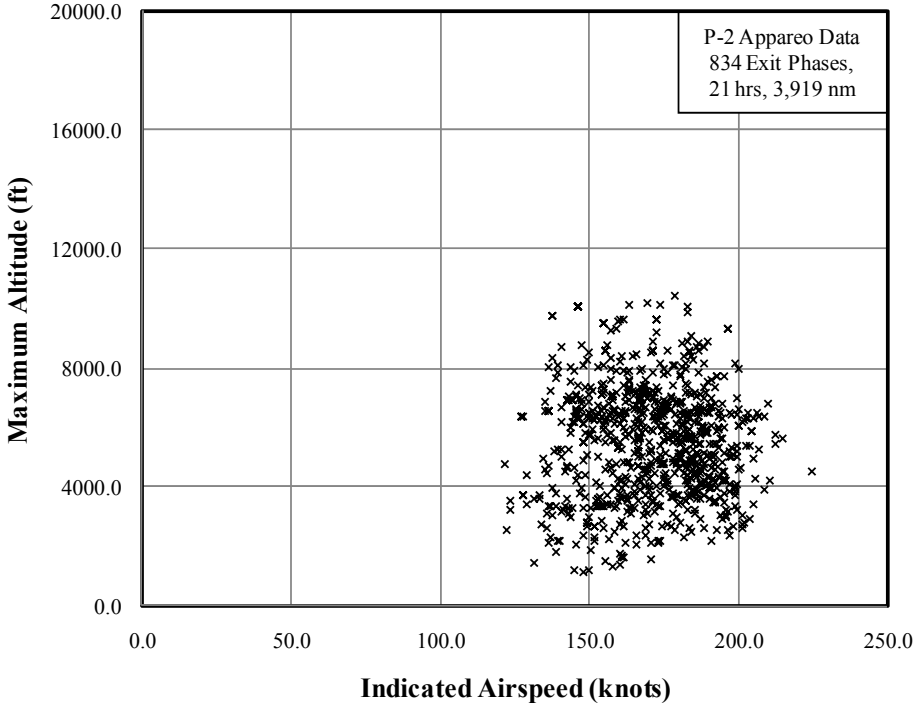

(d) Exit—P2V, Appareo System

Figure A-18. Maximum Above Ground Level Altitude and Coincident Indicated Airspeed, P2V Aircraft (Continued)

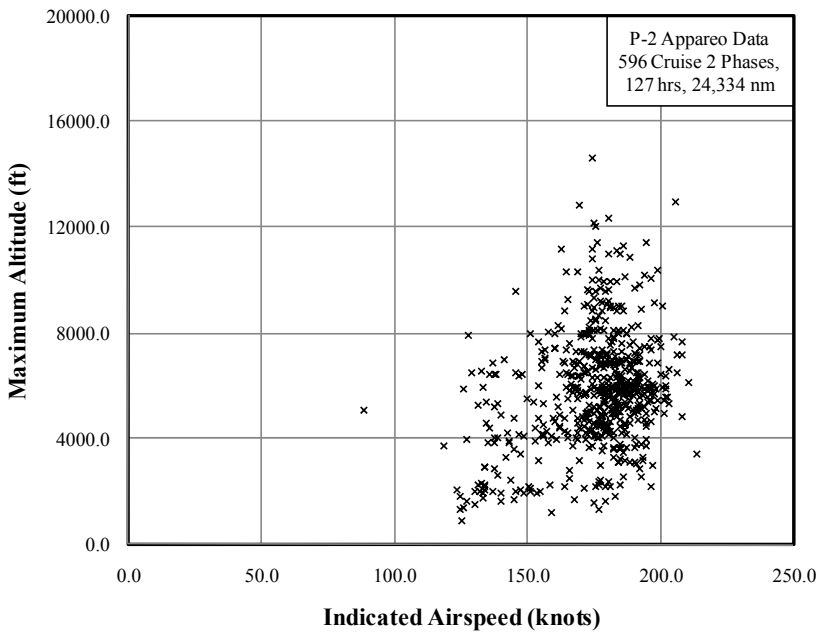

(e) Cruise 2—P2V, Appareo System

Figure A-18. Maximum Above Ground Level Altitude and Coincident Indicated Airspeed, P2V Aircraft (Continued)

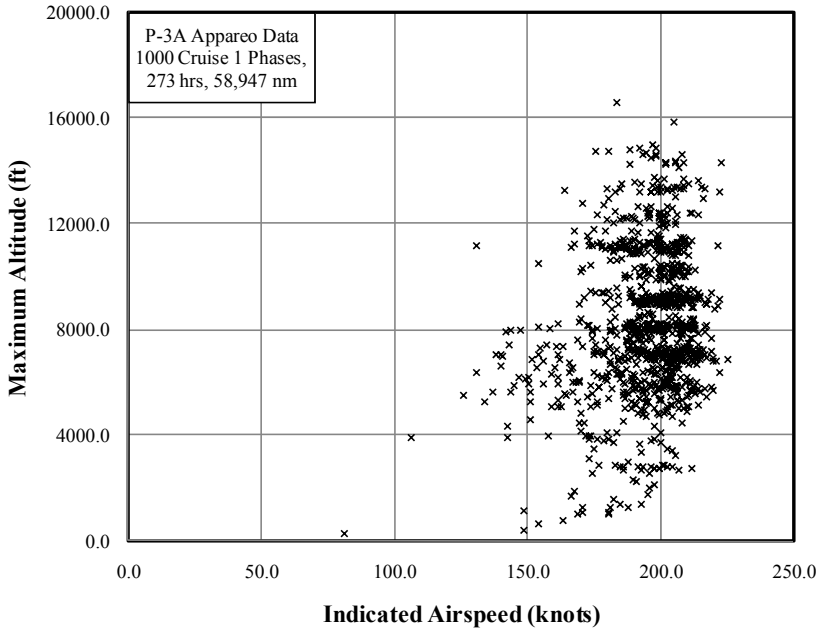

(a) Cruise 1—P3A, Appareo System

Figure A-19. Maximum Above Ground Level Altitude and Coincident Indicated Airspeed, P3A Aircraft

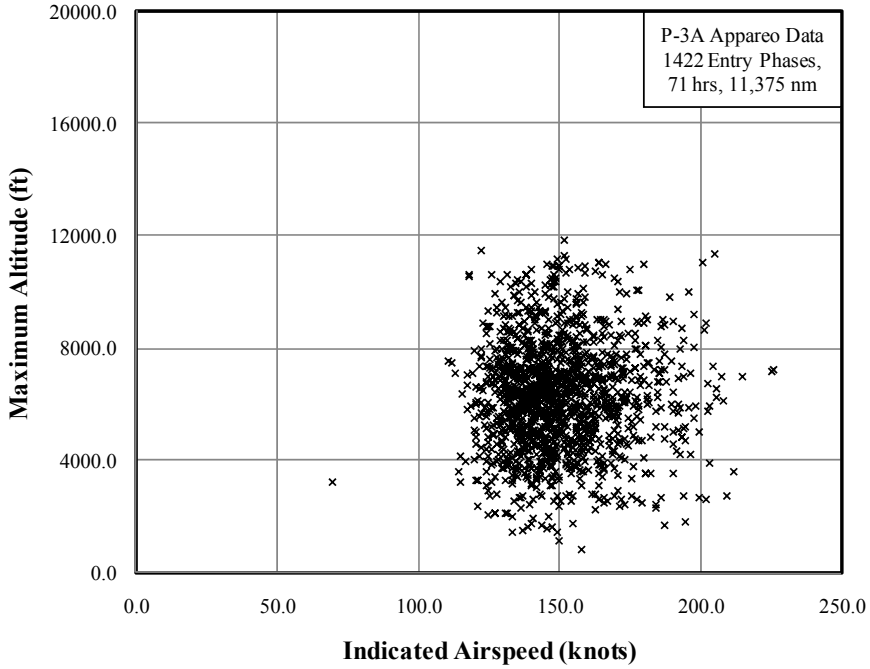

(b) Entry—P3A, Appareo System

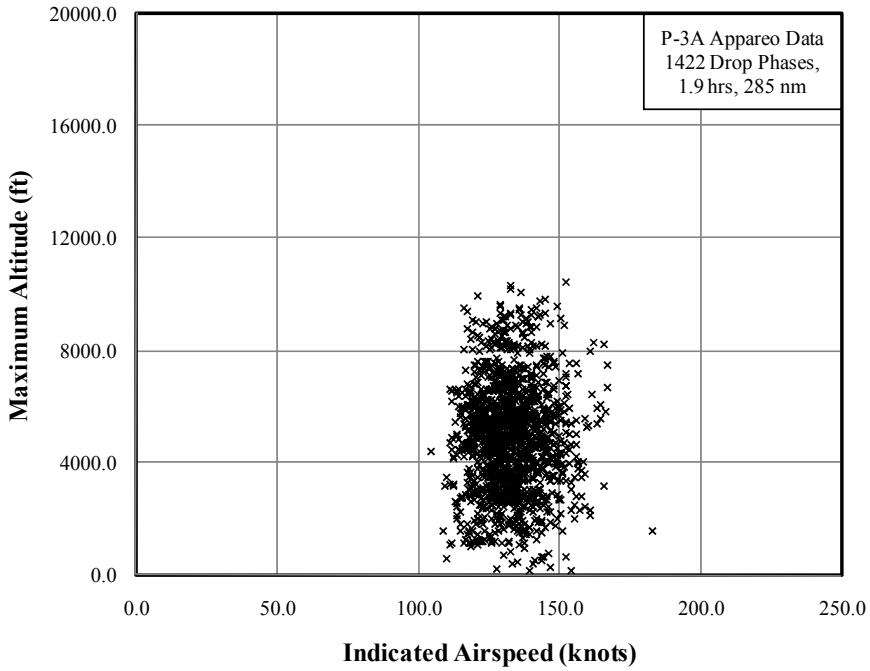

(c) Drop—P3A, Appareo System

Figure A-19. Maximum Above Ground Level Altitude and Coincident Indicated Airspeed, P3A Aircraft (Continued)

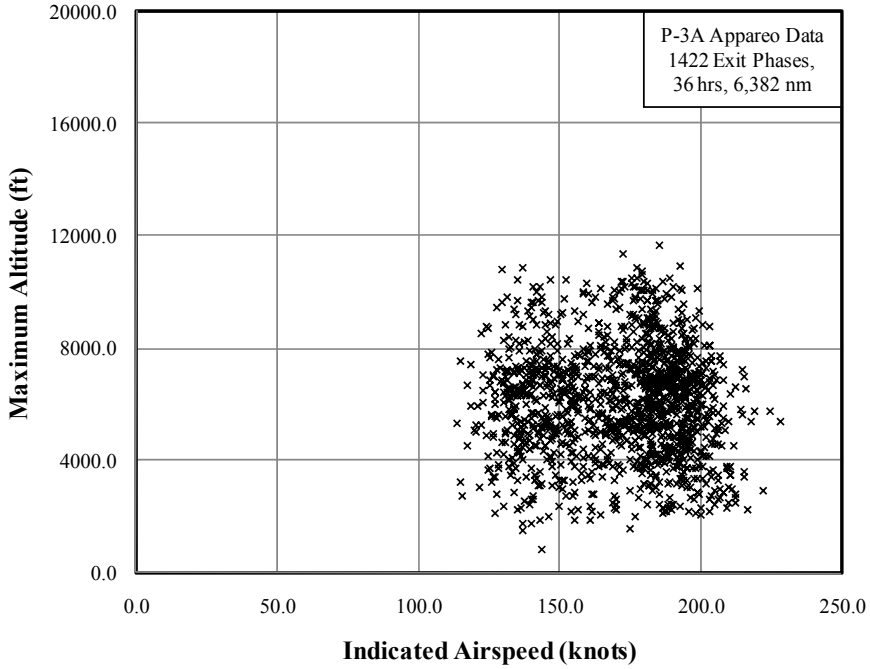

(d) Exit—P3A, Appareo System

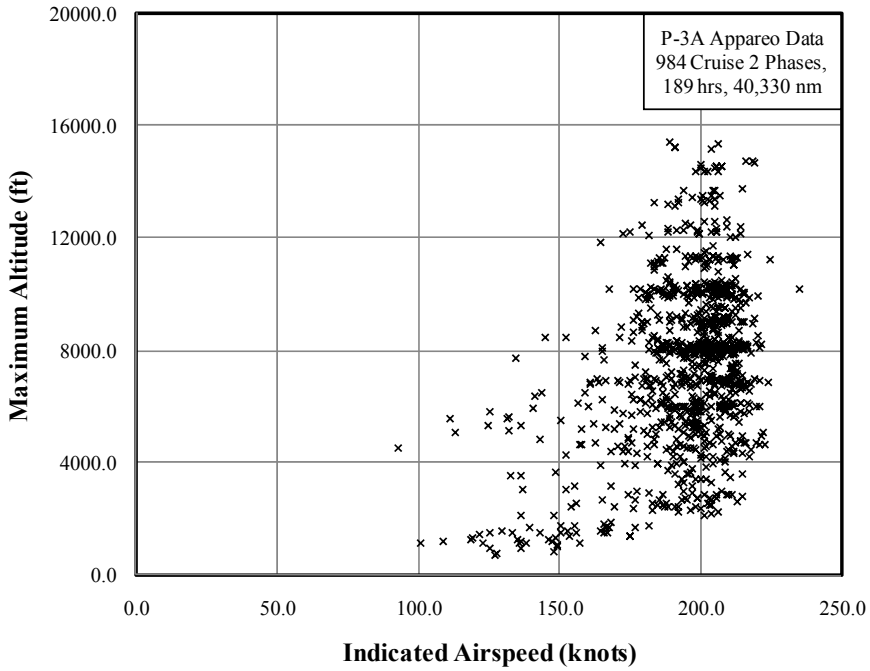

(e) Cruise 2—P3A, Appareo System

Figure A-19. Maximum Above Ground Level Altitude and Coincident Indicated Airspeed, P3A Aircraft (Continued)

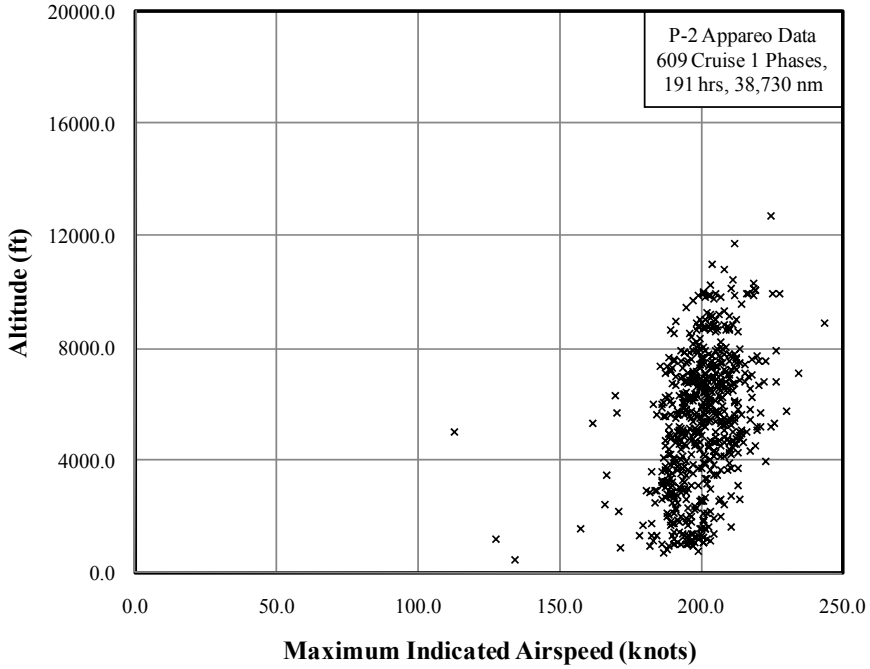

(a) Cruise 1—P2V, Appareo System

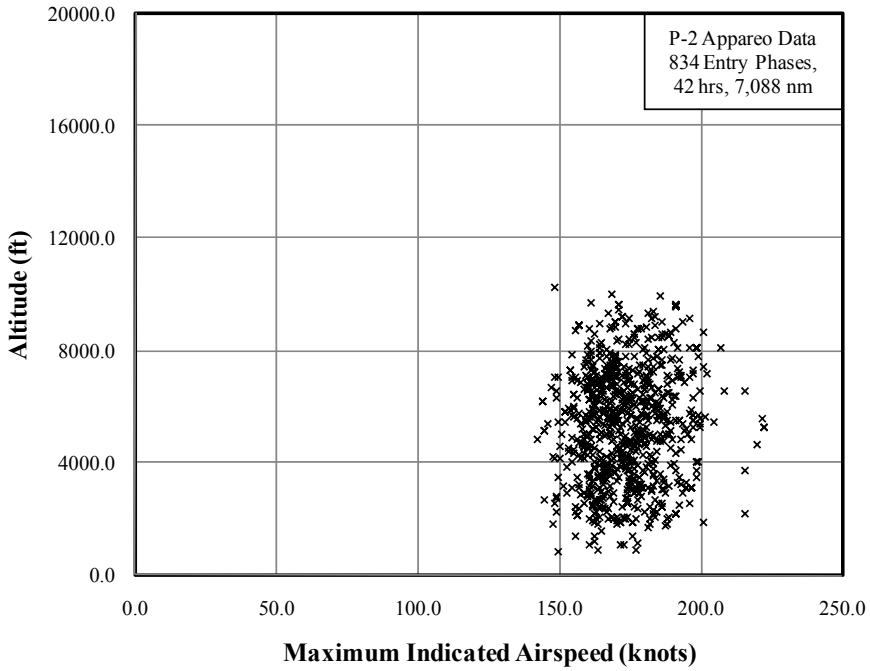

(b) Entry—P2V, Appareo System

Figure A-20. Maximum Indicated Airspeed and Coincident Above Ground Level Altitude, P2V Aircraft

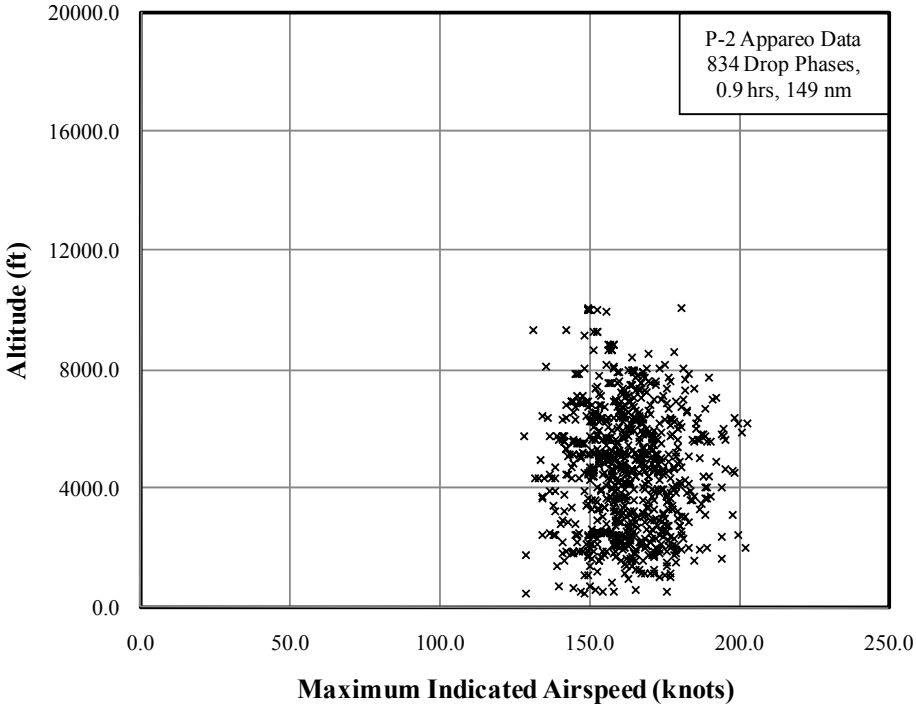

(c) Drop—P2V, Appareo System

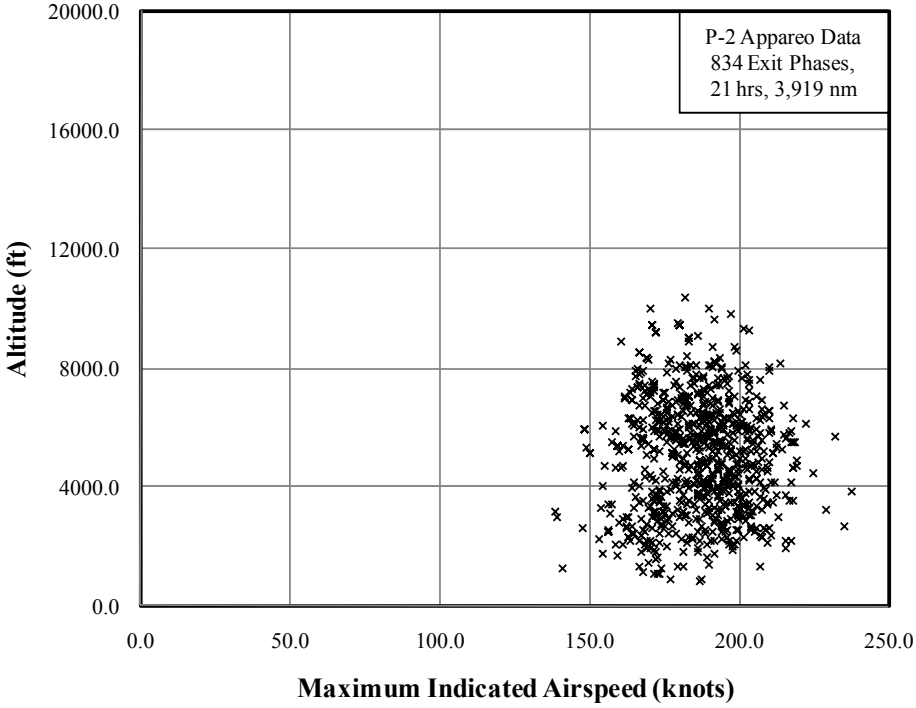

(d) Exit—P2V, Appareo System

Figure A-20. Maximum Indicated Airspeed and Coincident Above Ground Level Altitude, P2V Aircraft (Continued)

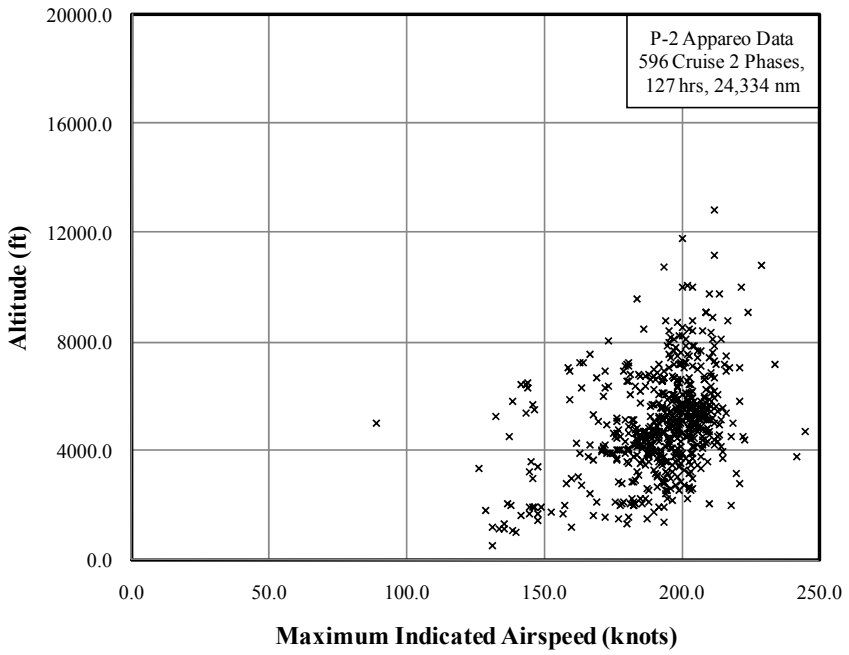

(e) Cruise 2—P2V, Appareo System

Figure A-20. Maximum Indicated Airspeed and Coincident Above Ground Level Altitude, P2V Aircraft (Continued)

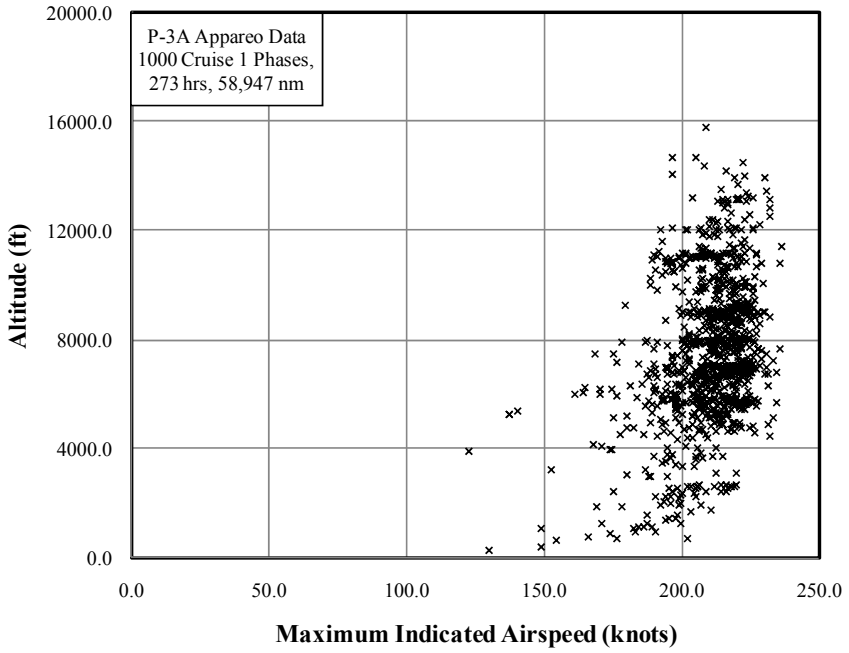

(a) Cruise 1—P3A, Appareo System

Figure A-21. Maximum Airspeed and Coincident Above Ground Level Altitude, P3A Aircraft

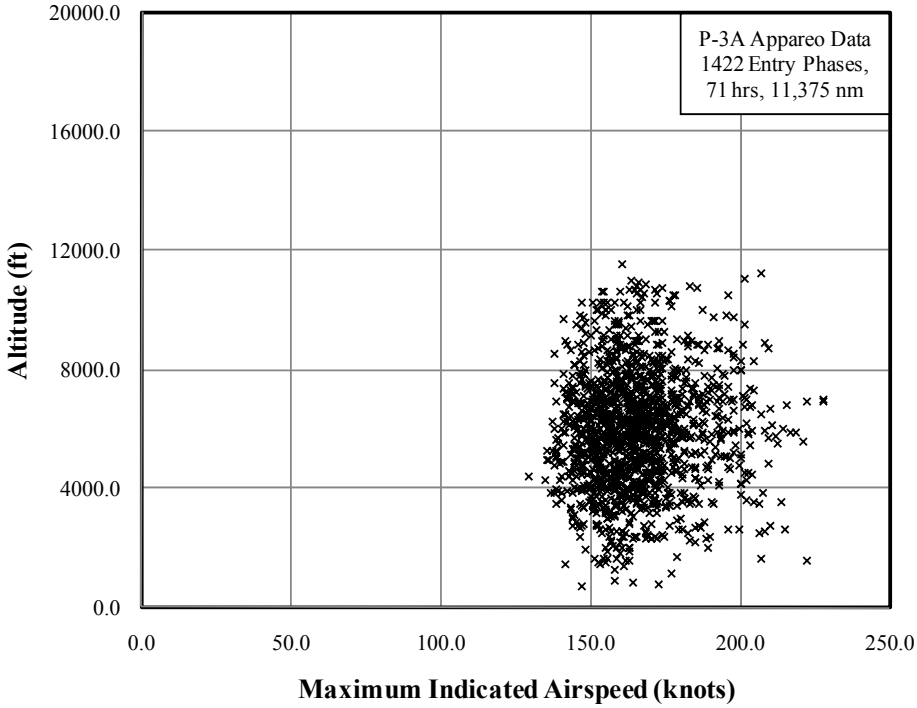

(b) Entry—P3A, Appareo System

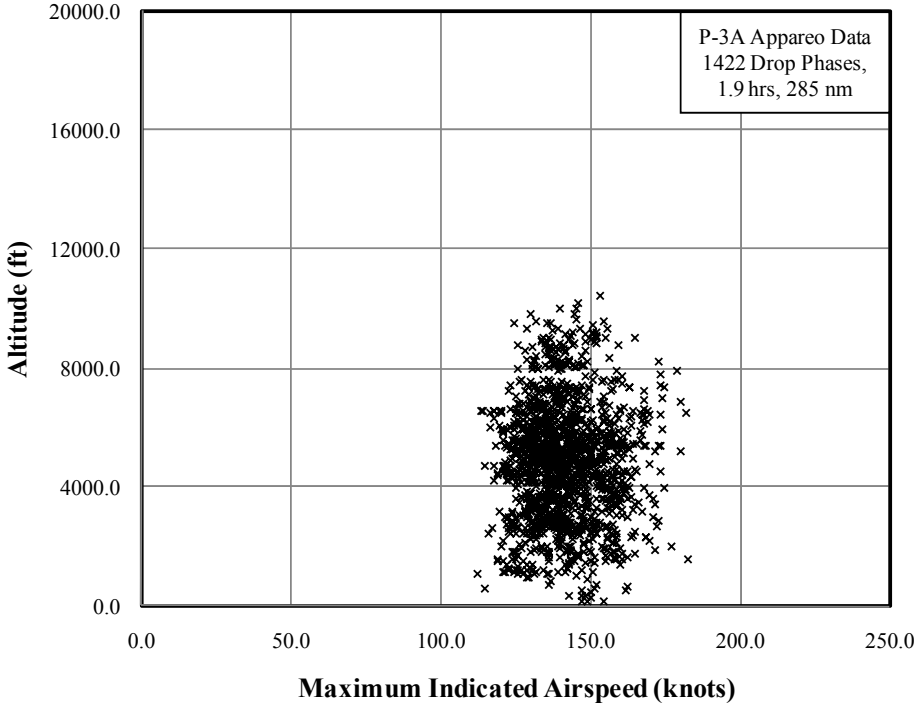

(c) Drop—P3A, Appareo System

Figure A-21. Maximum Airspeed and Coincident Above Ground Level Altitude, P3A Aircraft (Continued)

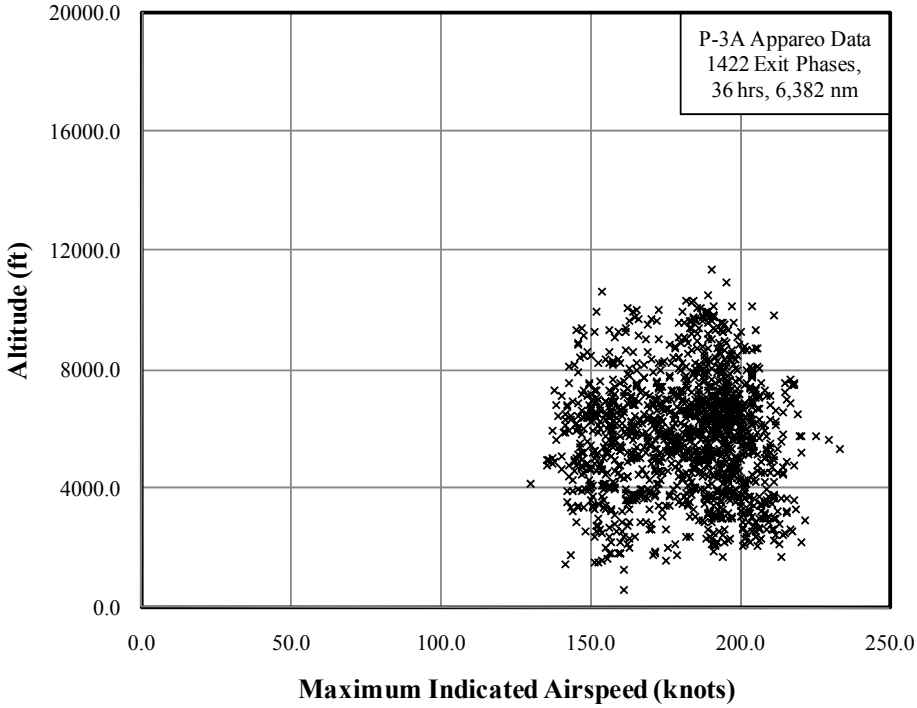

(d) Exit—P3A, Appareo System

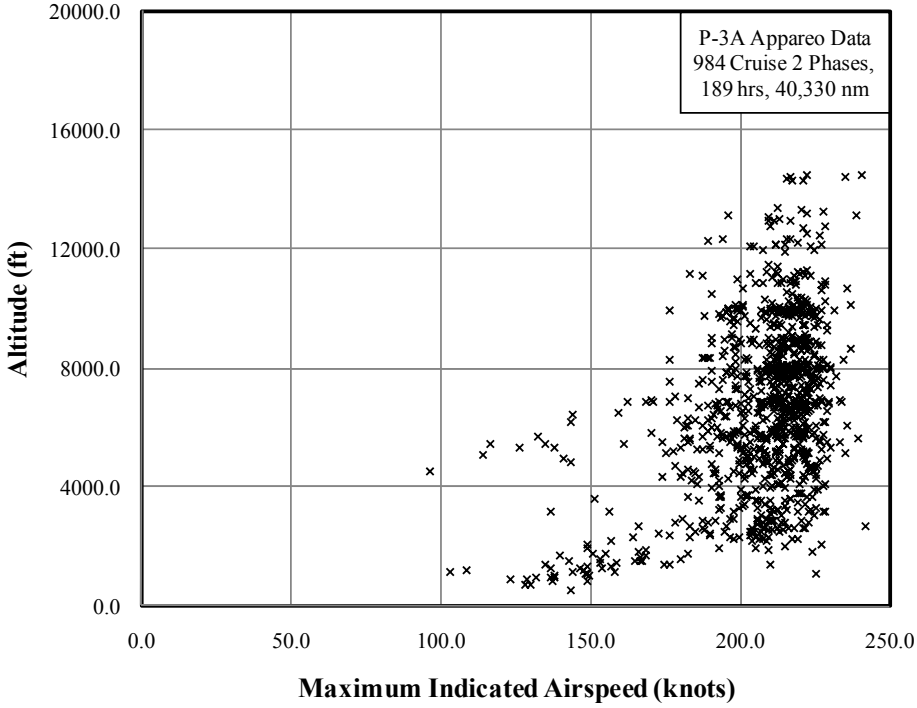

(e) Cruise 2—P3A, Appareo System

Figure A-21. Maximum Airspeed and Coincident Above Ground Level Altitude, P3A Aircraft (Continued)

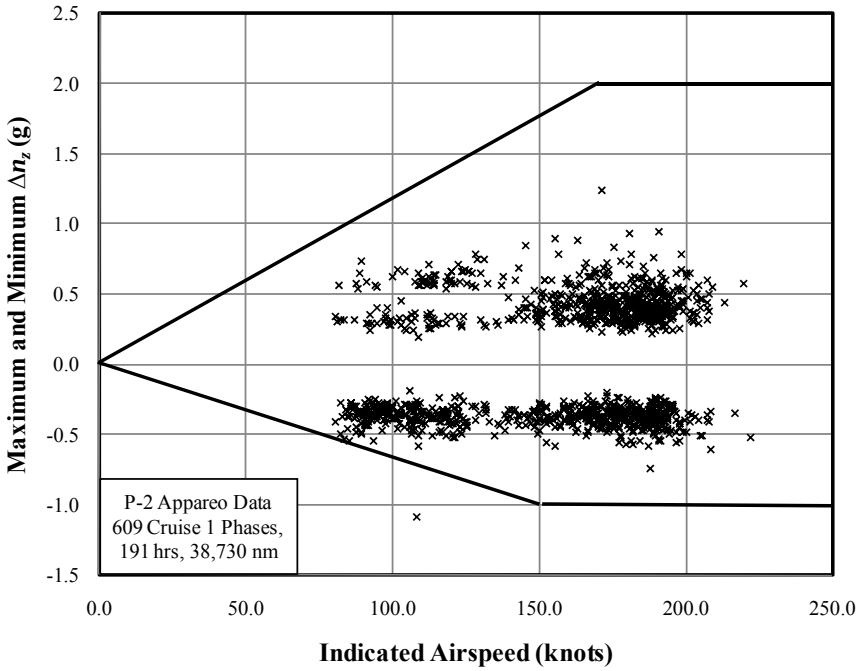

(a) Cruise 1—P2V, Appareo System

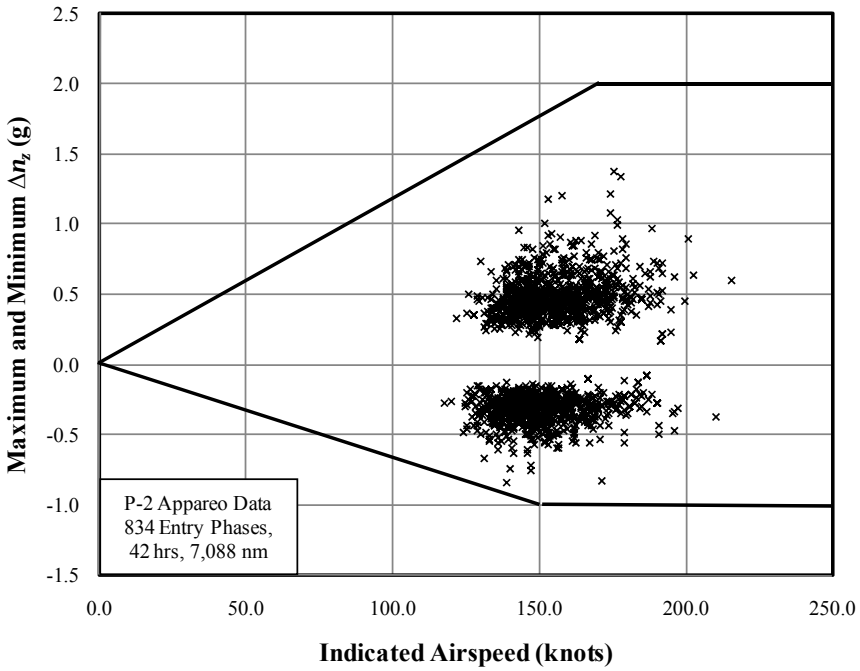

(b) Entry—P2V, Appareo System

Figure A-22. Maximum Incremental Vertical Load Factor and Coincident Indicated Airspeed, P2V Aircraft With P3A Limits

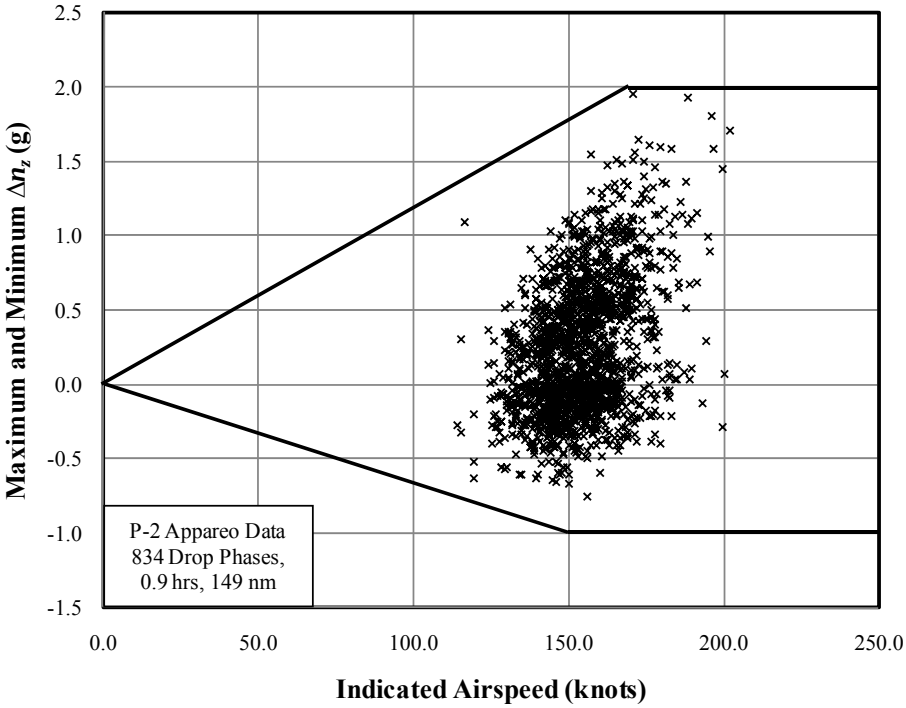

(c) Drop—P2V, Appareo System

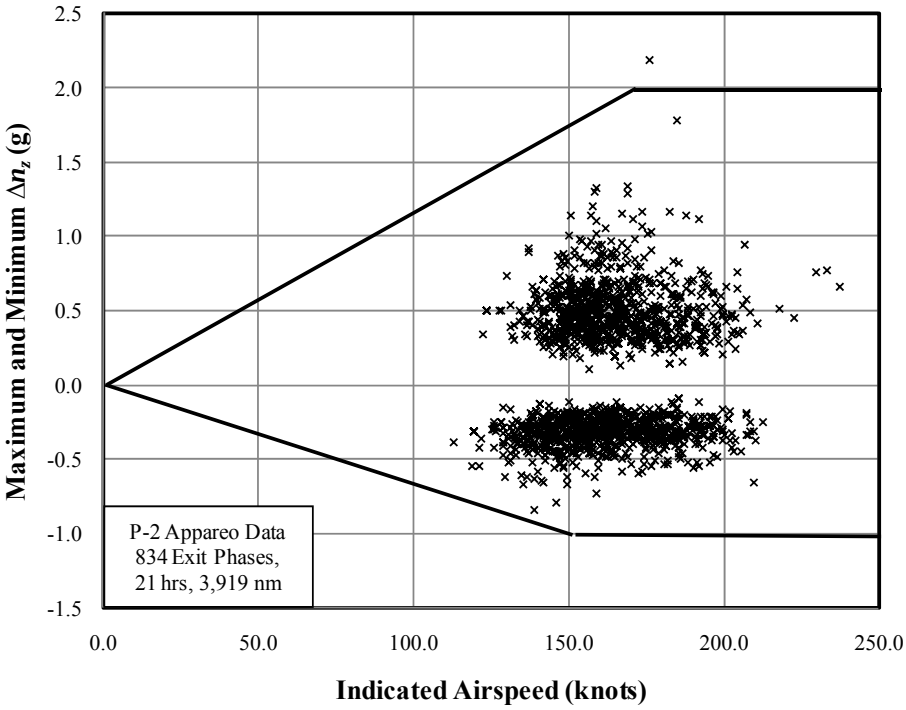

(d) Exit—P2V, Appareo System

Figure A-22. Maximum Incremental Vertical Load Factor and Coincident Indicated Airspeed, P2V Aircraft With P3A Limits (Continued)

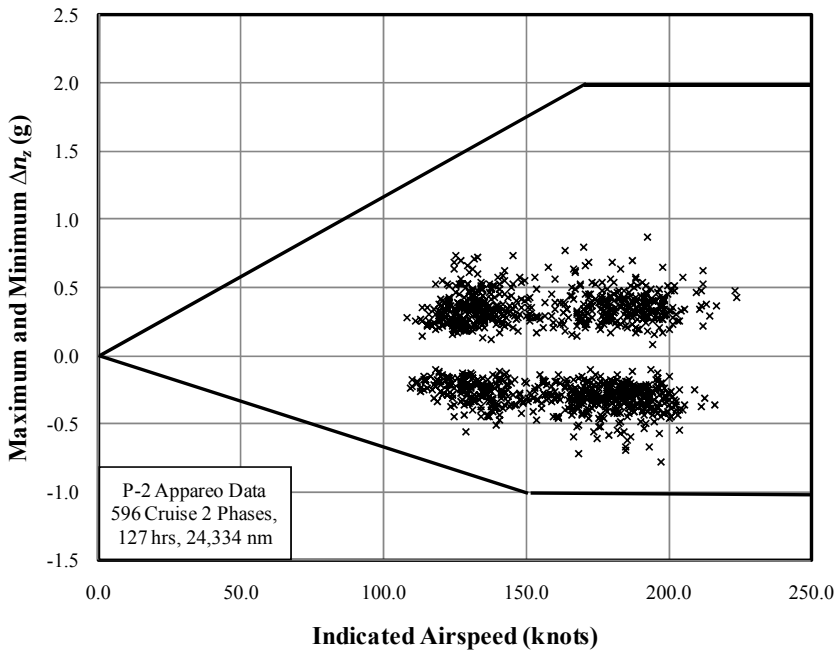

(e) Cruise 2—P2V, Appareo System

Figure A-22. Maximum Incremental Vertical Load Factor and Coincident Indicated Airspeed, P2V Aircraft With P3A Limits (Continued)

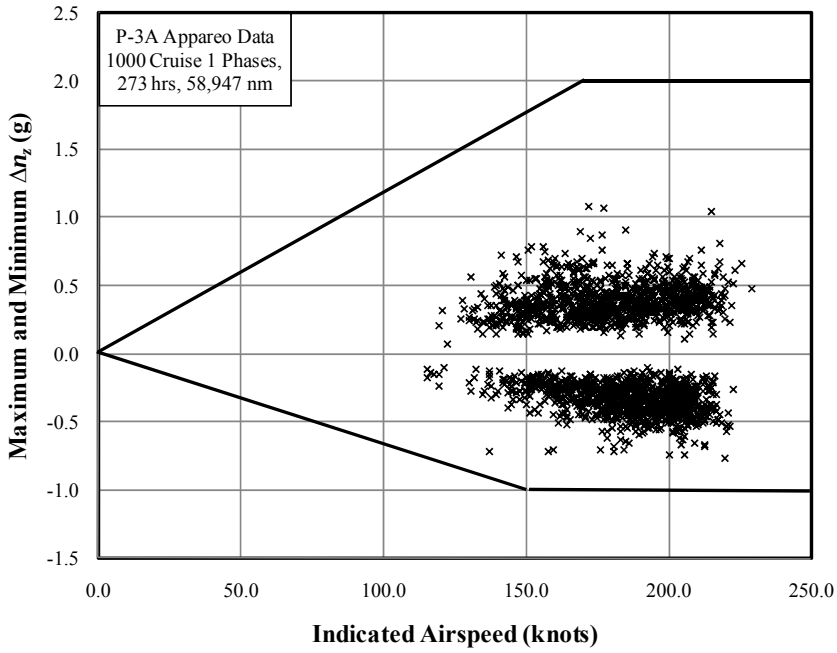

(a) Cruise 1—P3A, Appareo System

Figure A-23. Maximum Incremental Vertical Load Factor and Coincident Indicated Airspeed, P3A Aircraft

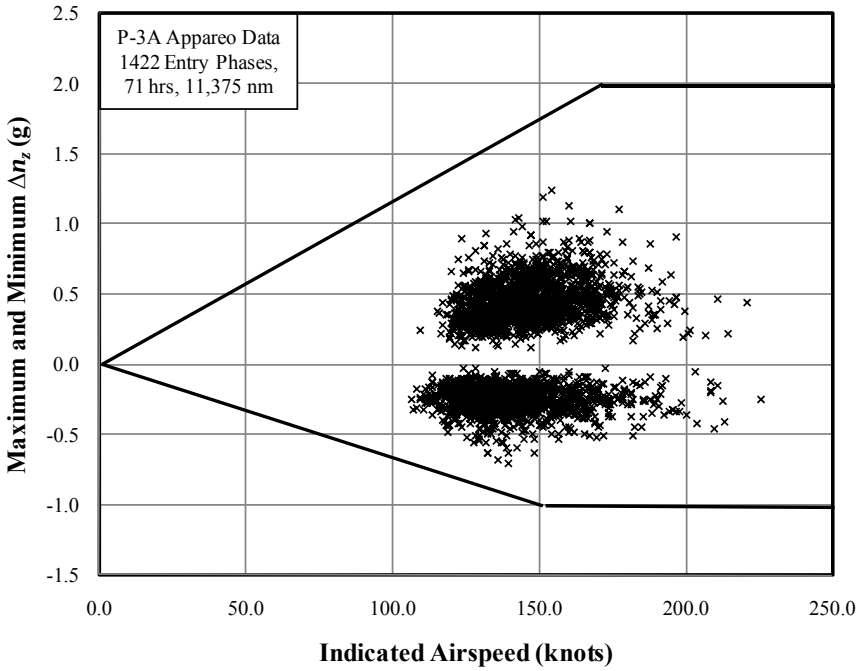

(b) Entry—P3A, Appareo System

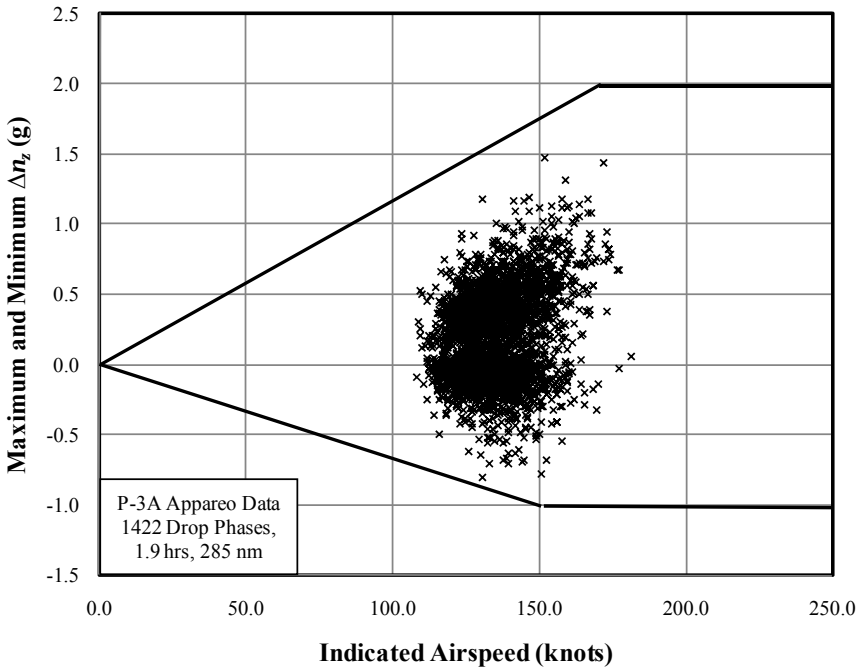

(c) Drop—P3A, Appareo System

Figure A-23. Maximum Incremental Vertical Load Factor and Coincident Indicated Airspeed, P3A Aircraft (Continued)

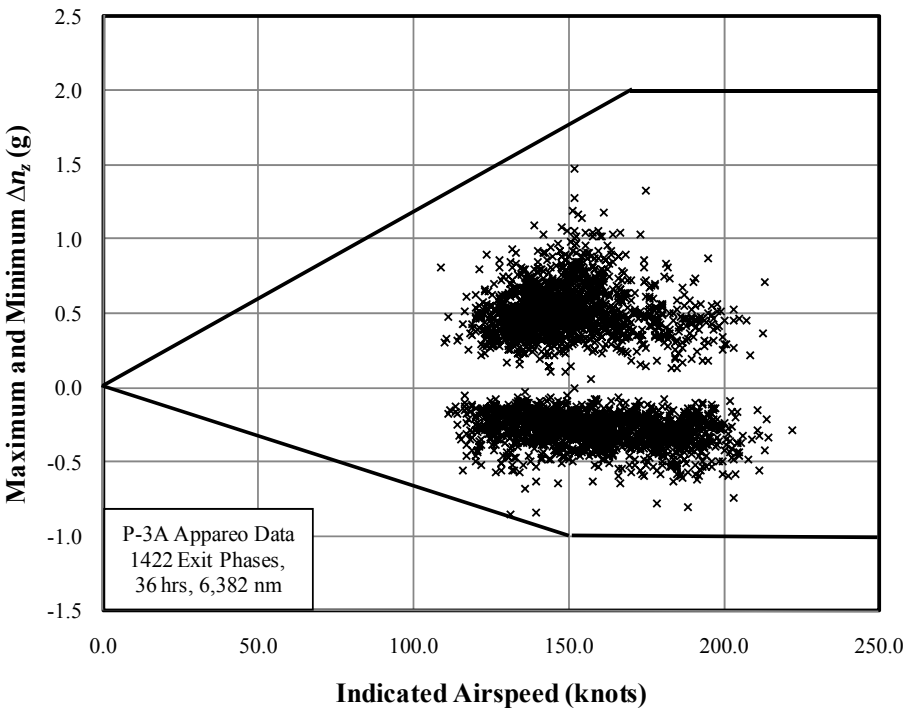

(d) Exit—P3A, Appareo System

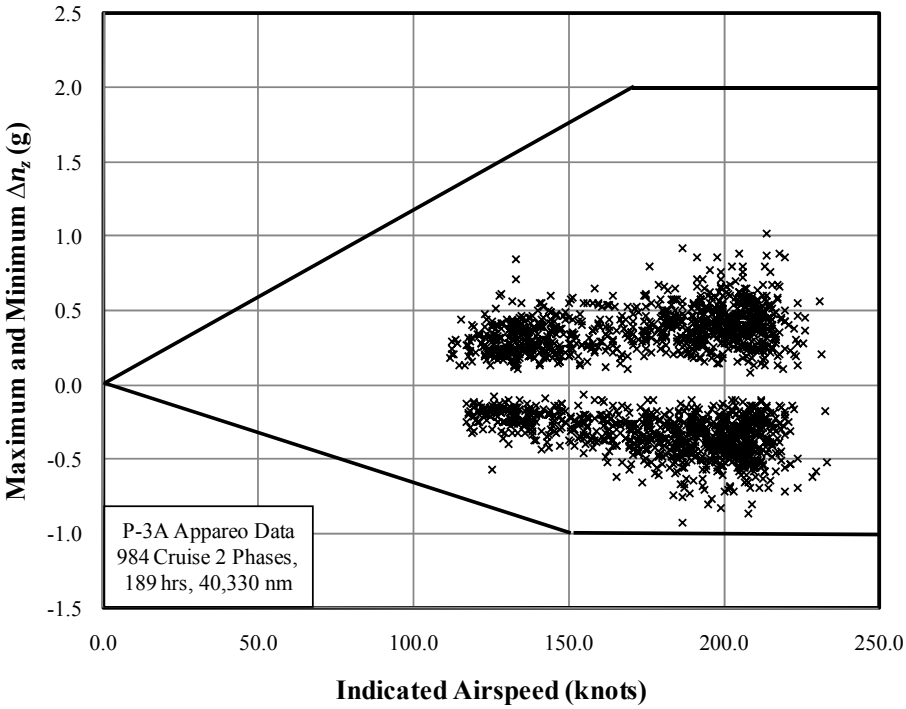

(e) Cruise 2—P3A, Appareo System

Figure A-23. Maximum Incremental Vertical Load Factor and Coincident Indicated Airspeed, P3A Aircraft (Continued)

Values	Pitch Angle (deg)				
	Cruise 1	Entry	Drop	Exit	Cruise 2
Average maximum	9.0	7.9	1.6	7.4	4.2
Standard deviation	2.1	2.7	5.2	3.2	2.2
Average minimum	-1.7	-7.8	-5.2	-4.0	-7.6
Standard deviation	2.4	4.5	6.0	3.4	2.1
Values	Roll Angle (deg)				
	Cruise 1	Entry	Drop	Exit	Cruise 2
Average maximum	16.8	15.1	1.9	14.0	15.8
Standard deviation	10.7	16.0	12.3	13.7	10.6
Average minimum	-24.1	-32.5	-9.2	-23.3	-25.0
Standard deviation	11.1	14.7	12.4	13.0	11.8

Figure A-24. Average Maximums and Minimums and Standard Deviations of Pitch and Roll Angles, P2V Aircraft, Appareo System

Values	Pitch Angle (deg)				
	Cruise 1	Entry	Drop	Exit	Cruise 2
Average maximum	8.9	8.6	0.4	9.1	3.7
Standard deviation	1.6	2.7	5.5	2.6	2.0
Average minimum	-2.0	-7.9	-6.3	-2.5	-5.8
Standard deviation	1.3	4.6	6.2	4.2	1.7
Values	Roll Angle (deg)				
	Cruise 1	Entry	Drop	Exit	Cruise 2
Average maximum	18.9	16.2	4.7	16.3	18.6
Standard deviation	11.1	16.1	11.2	15.2	10.6
Average minimum	-21.7	-35.2	-7.6	-26.2	-20.1
Standard deviation	13.2	13.5	11.2	14.8	12.8

Figure A-25. Average Maximums and Minimums and Standard Deviations of Pitch and Roll Angles, P3A Aircraft, Appareo System

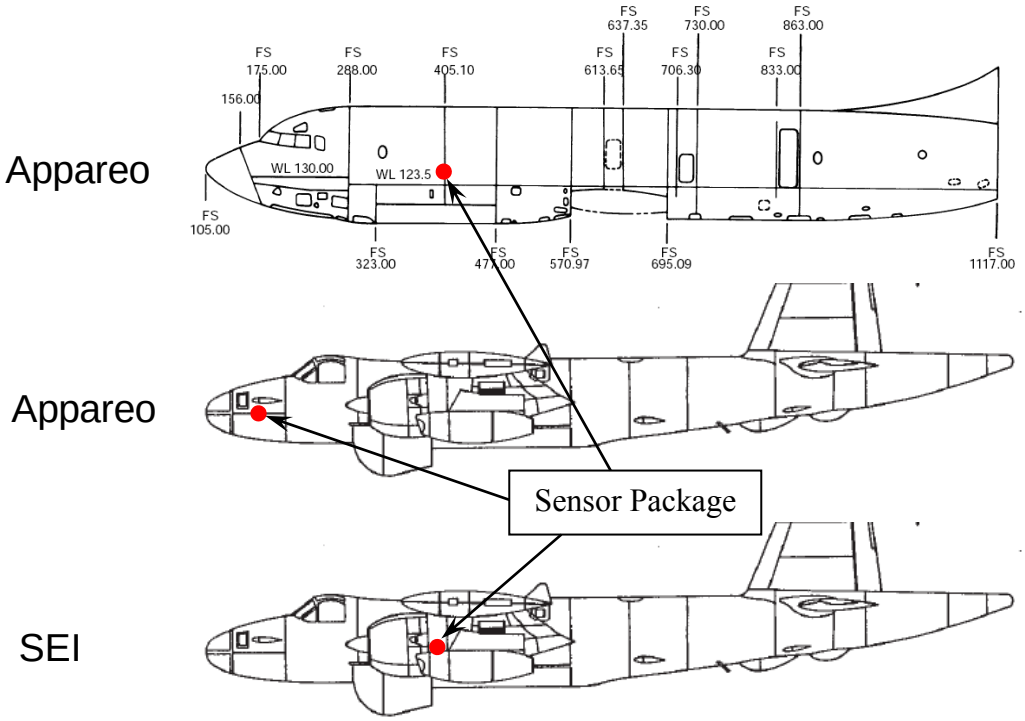

Figure A-26. Sensor Locations

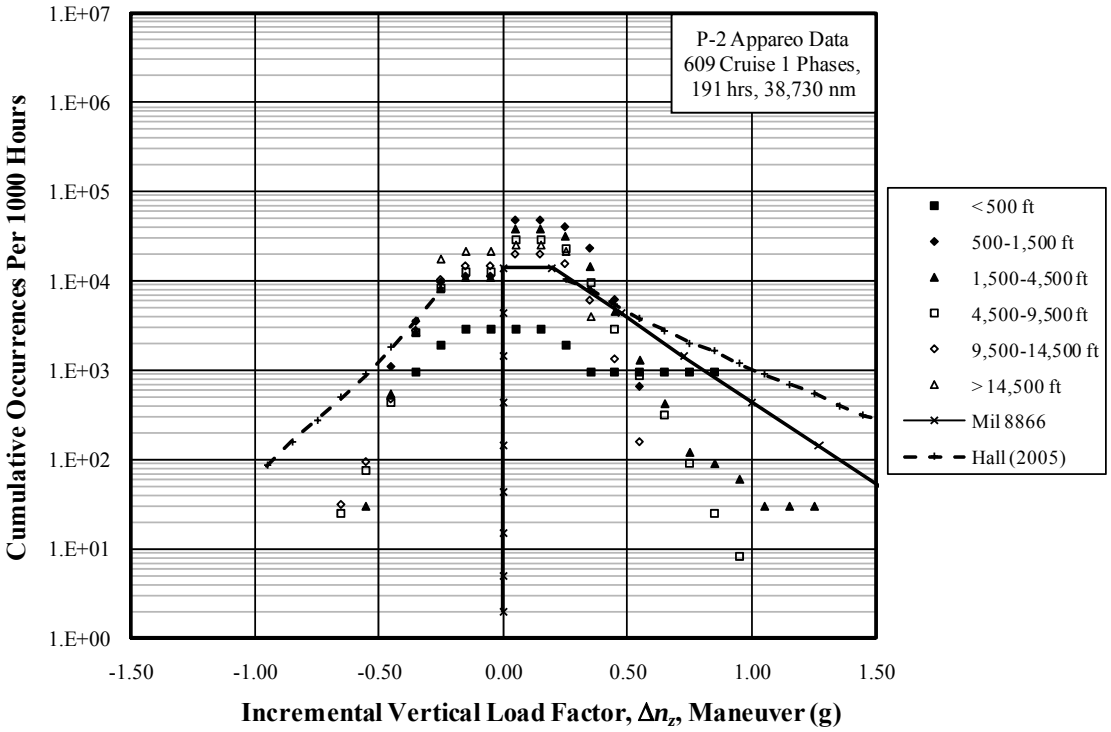

(a) Per 1000 hours

Figure A-27. Cumulative Occurrences of Incremental Maneuver Vertical Load Factor, Cruise 1, P2V, Appareo Data for Various Mean Sea Level Altitudes

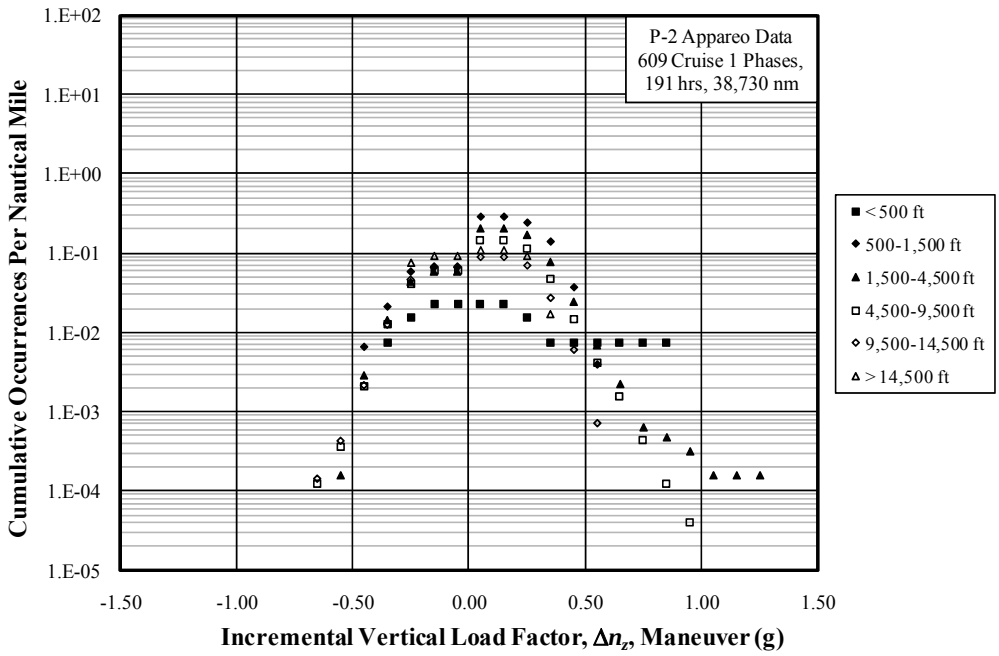

(b) Per nautical mile

Figure A-27. Cumulative Occurrences of Incremental Maneuver Vertical Load Factor, Cruise 1, P2V, Appareo Data for Various Mean Sea Level Altitudes (Continued)

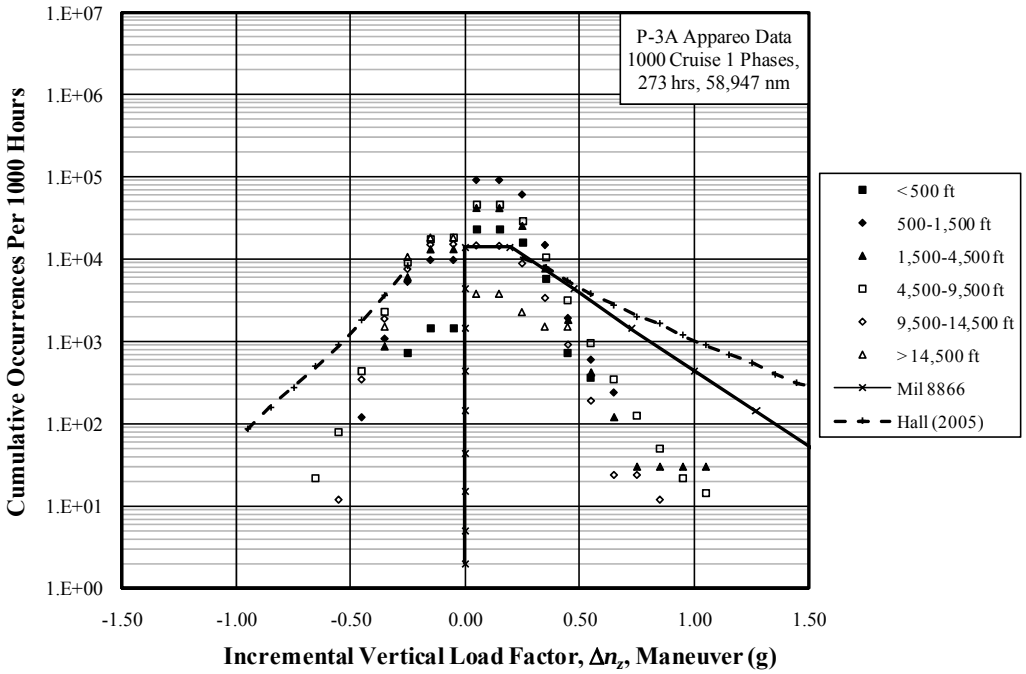

(a) Per 1000 hours

Figure A-28. Cumulative Occurrences of Incremental Maneuver Vertical Load Factor, Cruise 1, P3A, Appareo Data for Various Mean Sea Level Altitudes

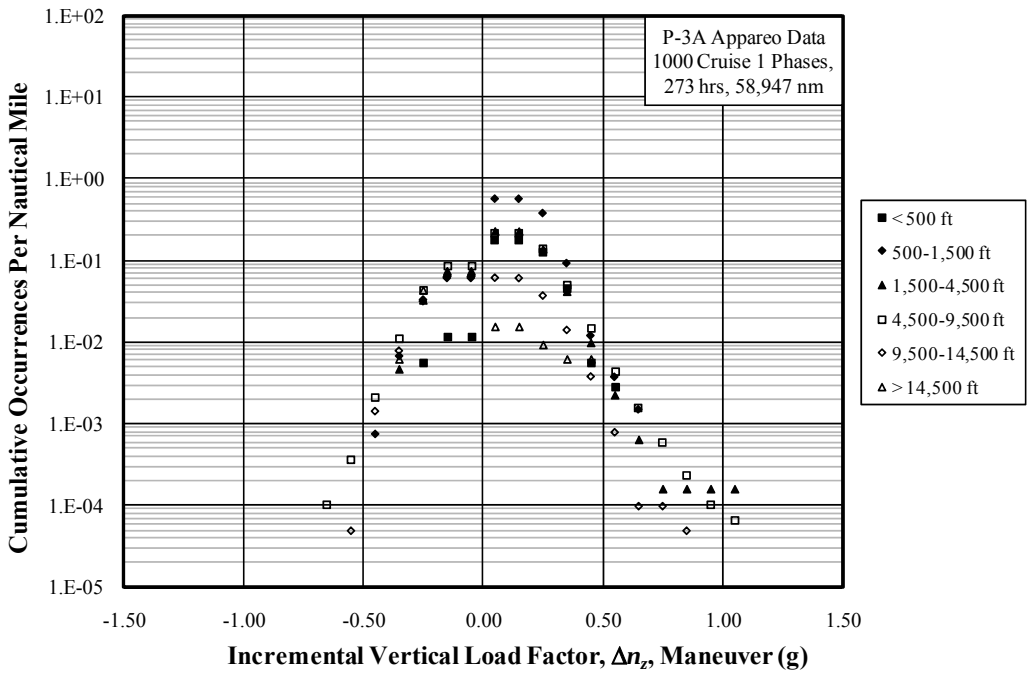

(b) Per nautical mile

Figure A-28. Cumulative Occurrences of Incremental Maneuver Vertical Load Factor, Cruise 1, P3A, Appareo Data for Various Mean Sea Level Altitudes (Continued)

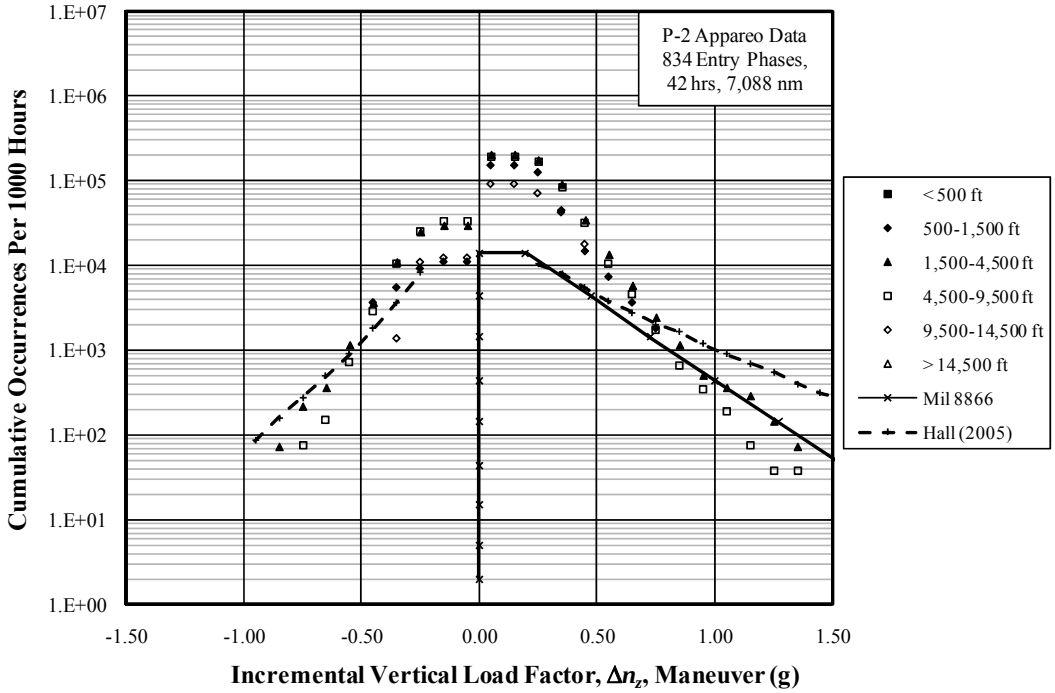

(a) Per 1000 hours

Figure A-29. Cumulative Occurrences of Incremental Maneuver Vertical Load Factor, Entry, P2V, Appareo Data for Various Mean Sea Level Altitudes

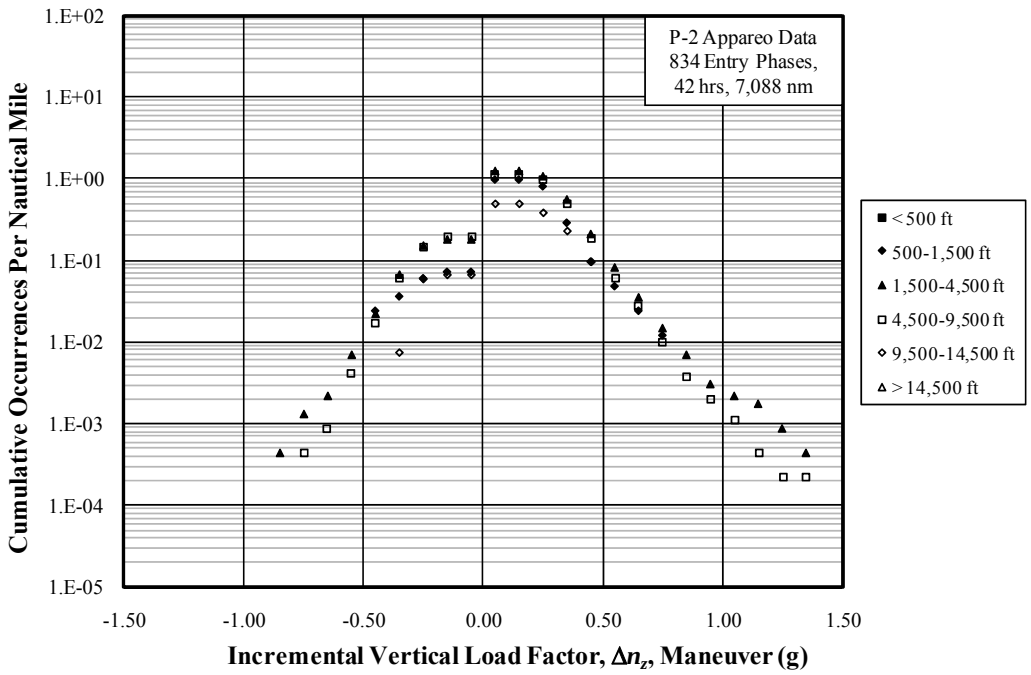

(b) Per nautical mile

Figure A-29. Cumulative Occurrences of Incremental Maneuver Vertical Load Factor, Entry, P2V, Appareo Data for Various Mean Sea Level Altitudes (Continued)

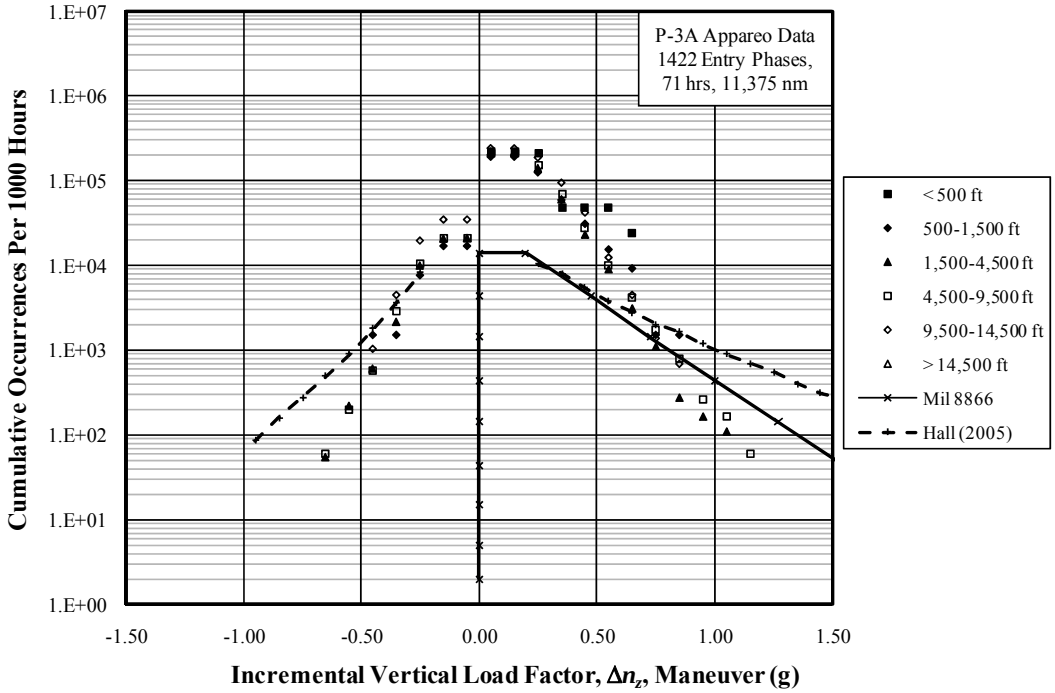

(a) Per 1000 hours

Figure A-30. Cumulative Occurrences of Incremental Maneuver Vertical Load Factor, Entry, P3A, Appareo Data for Various Mean Sea Level Altitudes

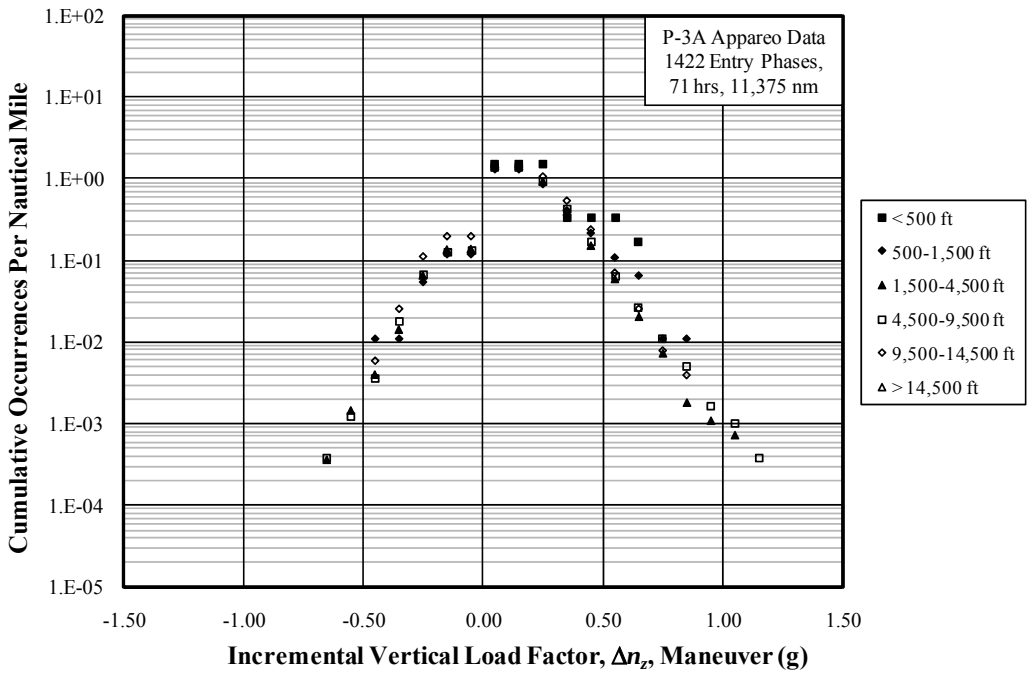

(b) Per nautical mile

Figure A-30. Cumulative Occurrences of Incremental Maneuver Vertical Load Factor, Entry, P3A, Appareo Data for Various Mean Sea Level Altitudes (Continued)

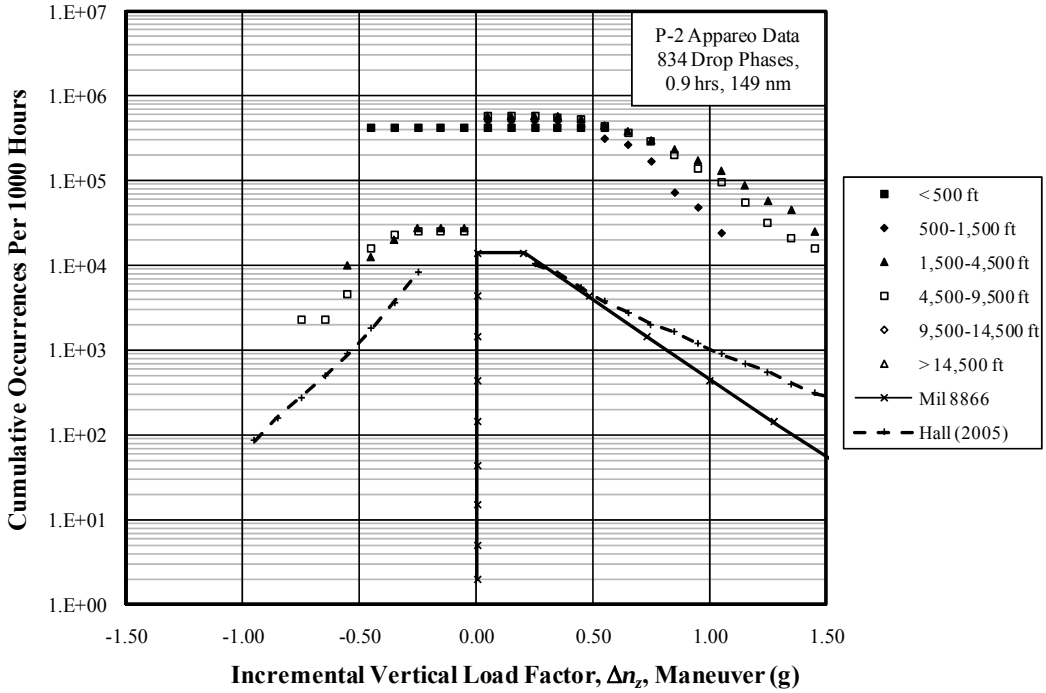

(a) Per 1000 hours

Figure A-31. Cumulative Occurrences of Incremental Maneuver Vertical Load Factor, Drop, P2V, Appareo Data for Various Mean Sea Level Altitudes

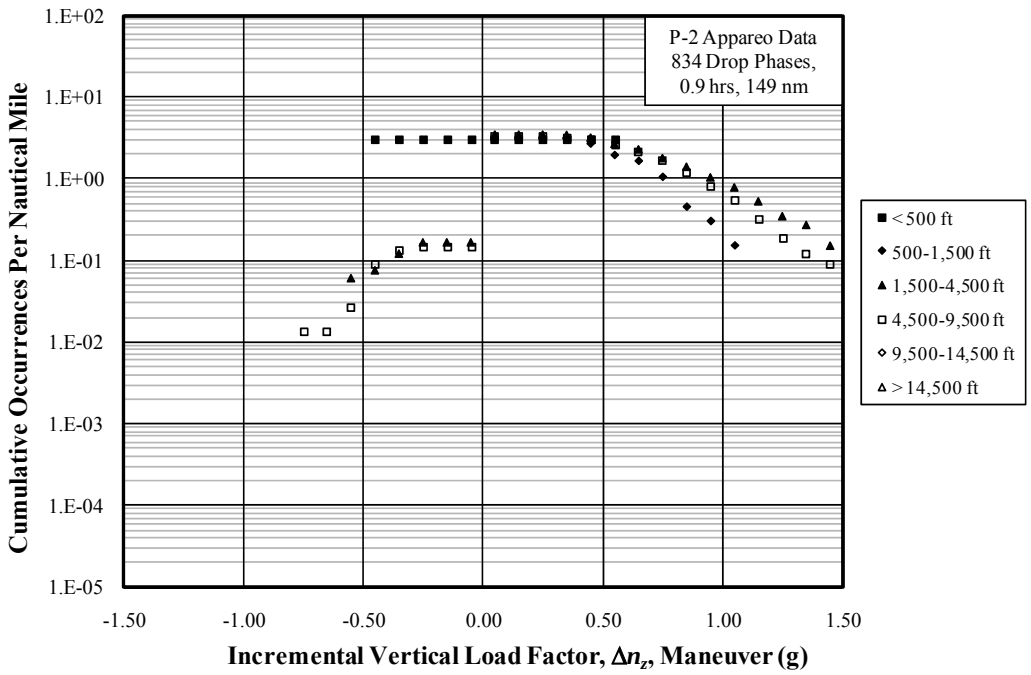

(b) Per nautical mile

Figure A-31. Cumulative Occurrences of Incremental Maneuver Vertical Load Factor, Drop, P2V, Appareo Data for Various Mean Sea Level Altitudes (Continued)

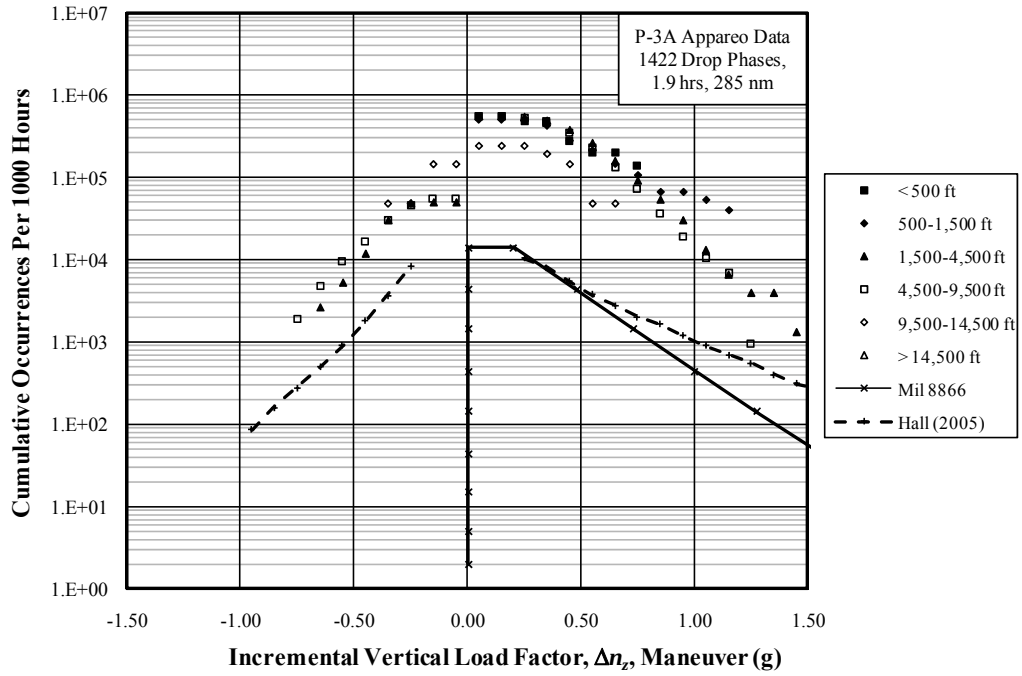

(a) Per 1000 hours

Figure A-32. Cumulative Occurrences of Incremental Maneuver Vertical Load Factor, Drop, P3A, Appareo Data for Various Mean Sea Level Altitudes

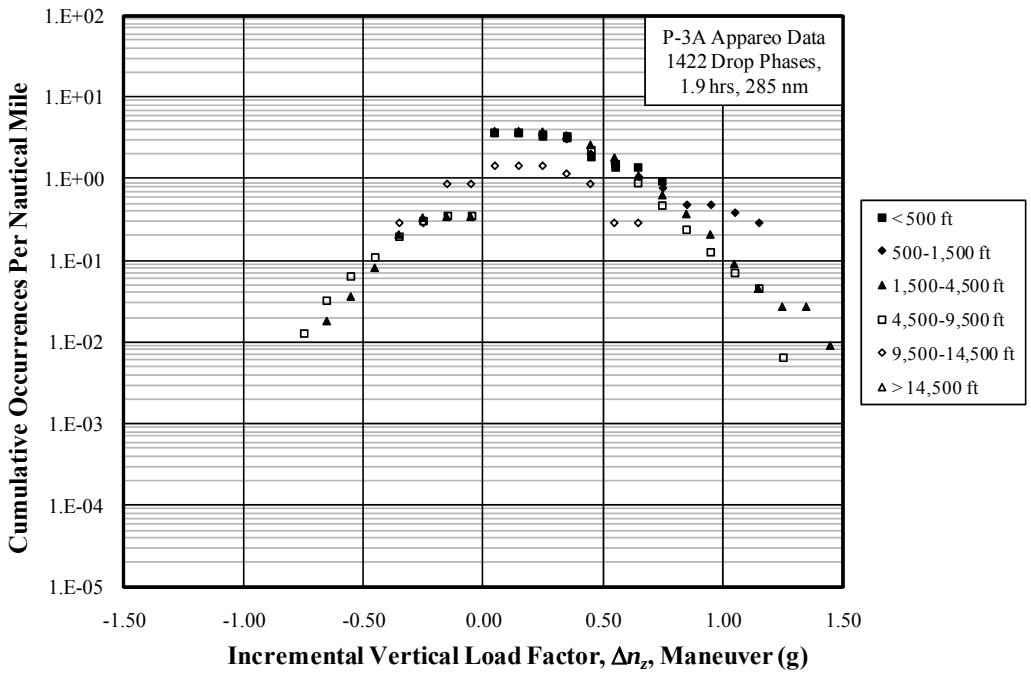

(b) Per nautical mile

Figure A-32. Cumulative Occurrences of Incremental Maneuver Vertical Load Factor, Drop, P3A, Appareo Data for Various Mean Sea Level Altitudes (Continued)

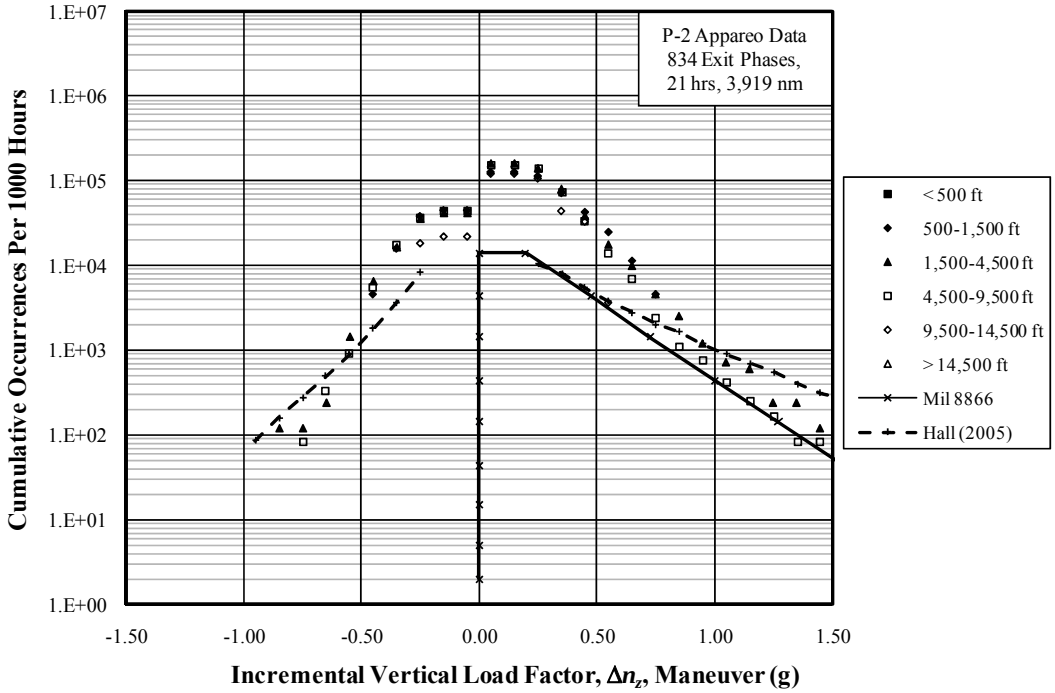

(a) Per 1000 hours

Figure A-33. Cumulative Occurrences of Incremental Maneuver Vertical Load Factor, Exit, P2V, Appareo Data for Various Mean Sea Level Altitudes

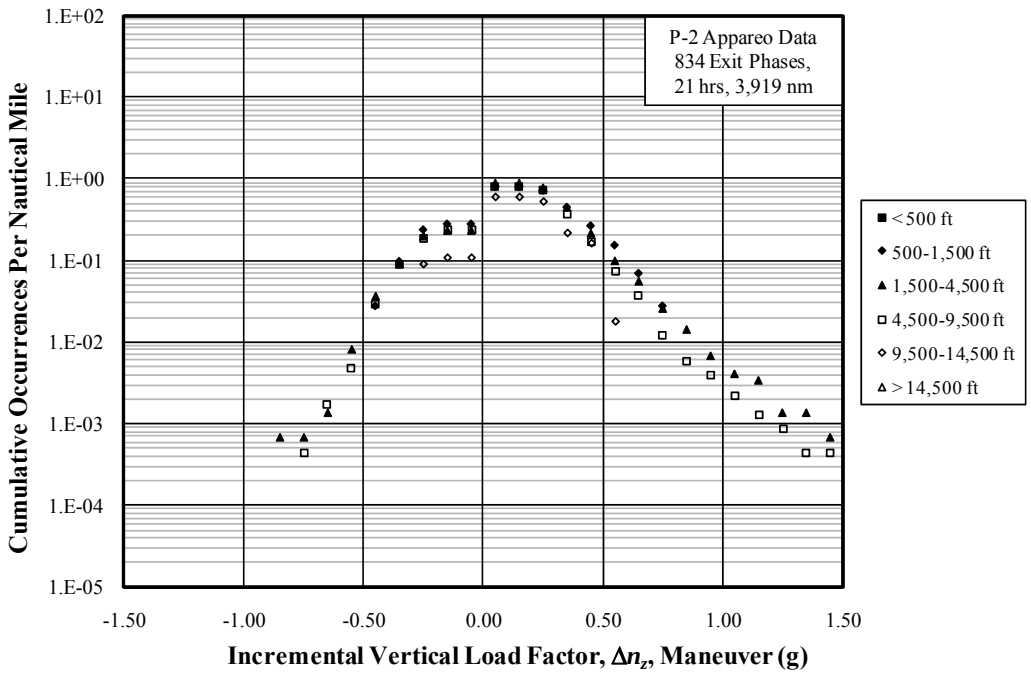

(b) Per nautical mile

Figure A-33. Cumulative Occurrences of Incremental Maneuver Vertical Load Factor, Exit, P2V, Appareo Data for Various Mean Sea Level Altitudes (Continued)

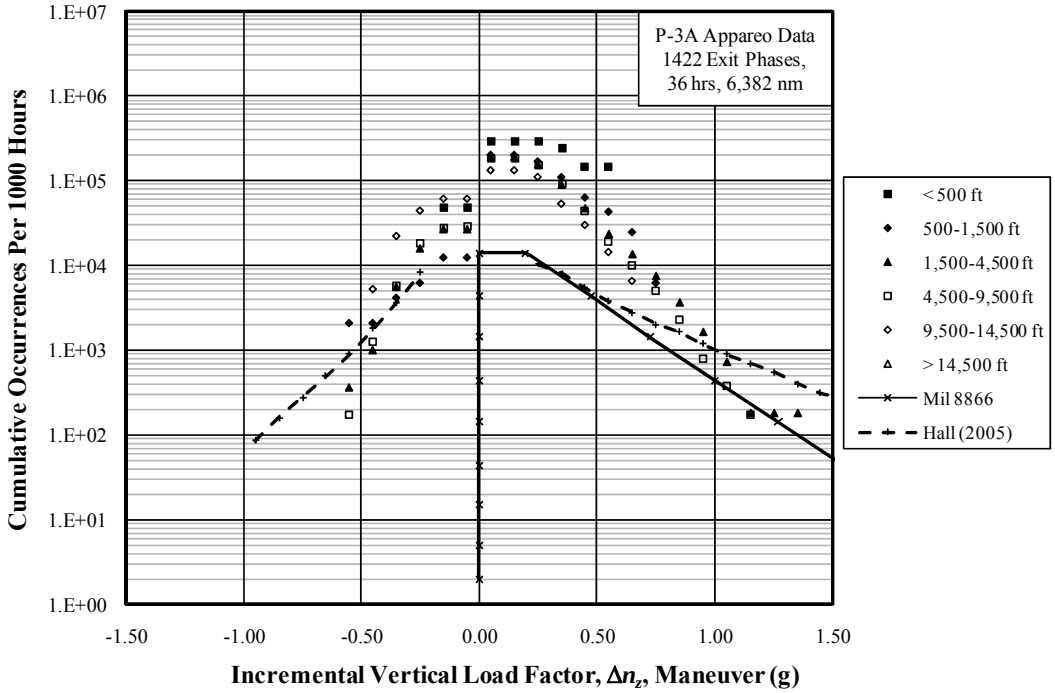

(a) Per 1000 hours

Figure A-34. Cumulative Occurrences of Incremental Maneuver Vertical Load Factor, Exit, P3A, Appareo Data for Various Mean Sea Level Altitudes

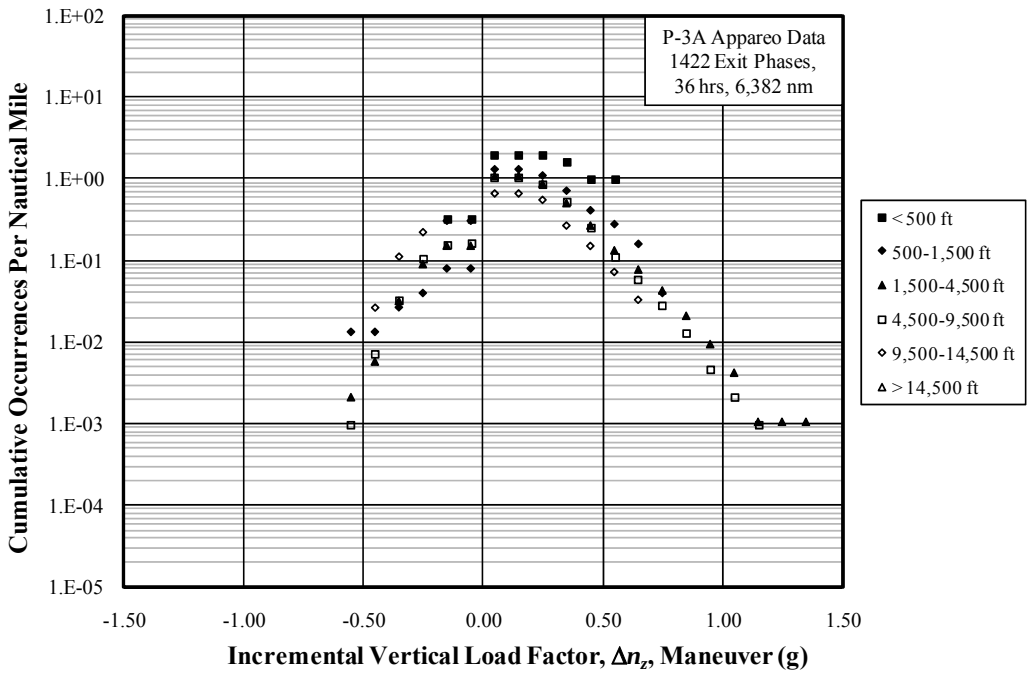

(b) Per nautical mile

Figure A-34. Cumulative Occurrences of Incremental Maneuver Vertical Load Factor, Exit, P3A, Appareo Data for Various Mean Sea Level Altitudes (Continued)

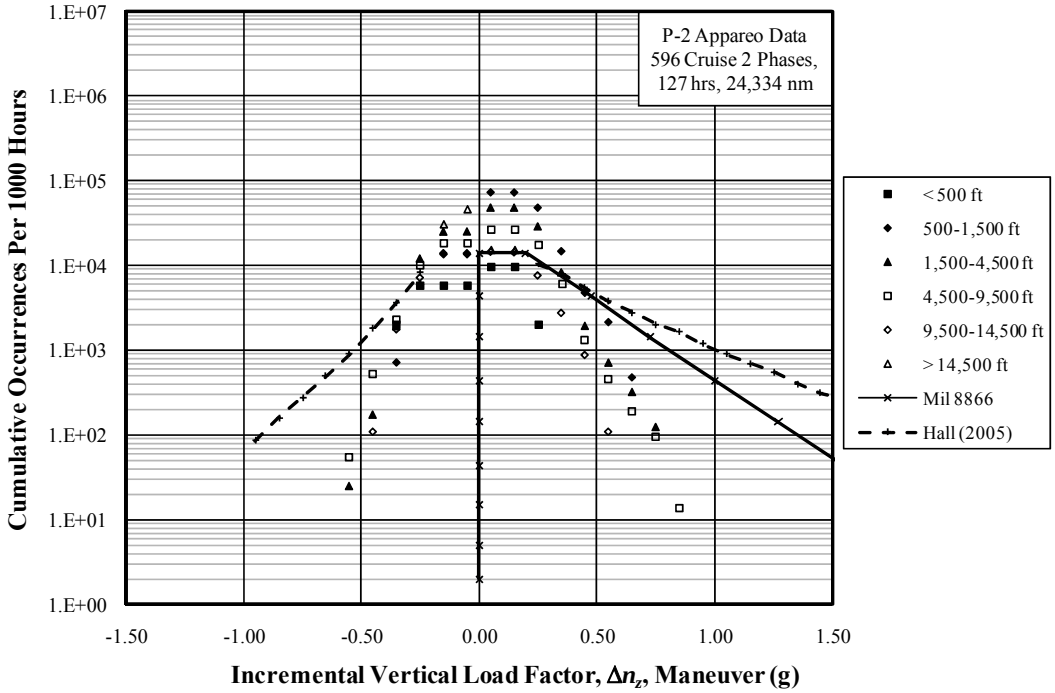

(a) Per 1000 hours

Figure A-35. Cumulative Occurrences of Incremental Maneuver Vertical Load Factor, Cruise 2, P2V, Appareo Data for Various Mean Sea Level Altitudes

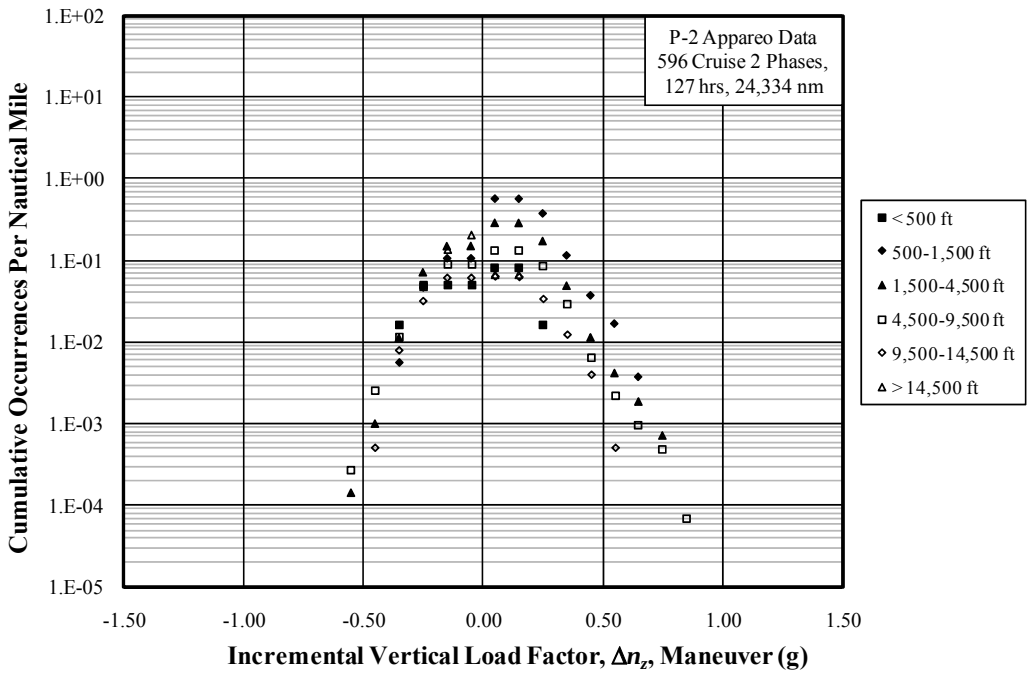

(b) Per nautical mile

Figure A-35. Cumulative Occurrences of Incremental Maneuver Vertical Load Factor, Cruise 2, P2V, Appareo Data for Various Mean Sea Level Altitudes (Continued)

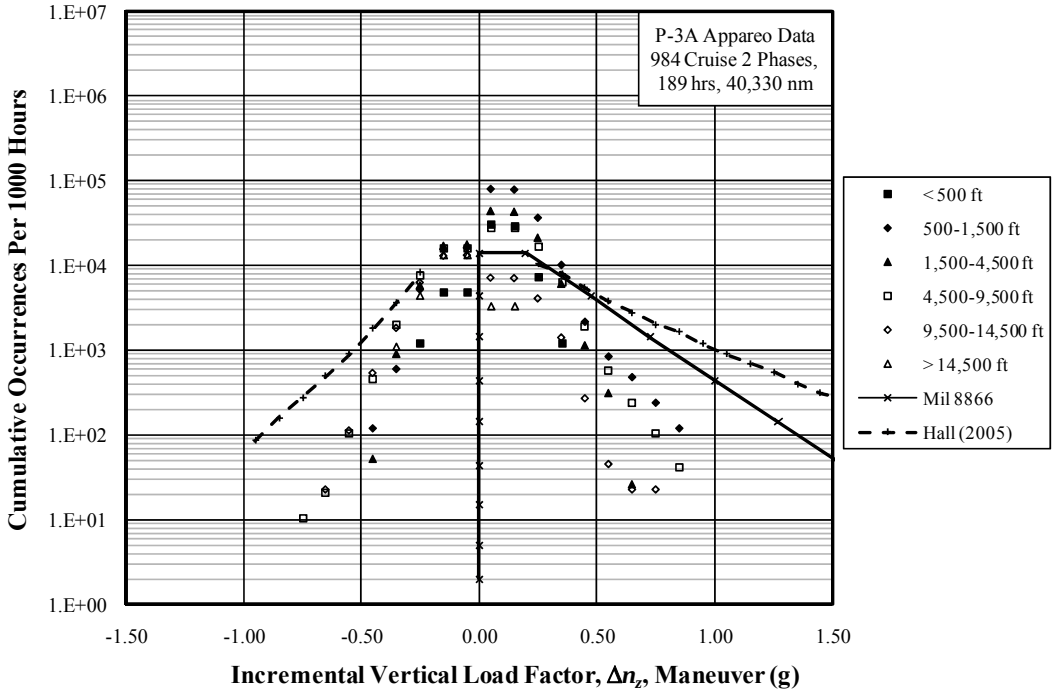

(a) Per 1000 hours

Figure A-36. Cumulative Occurrences of Incremental Maneuver Vertical Load Factor, Cruise 2, P3A, Appareo Data for Various Mean Sea Level Altitudes

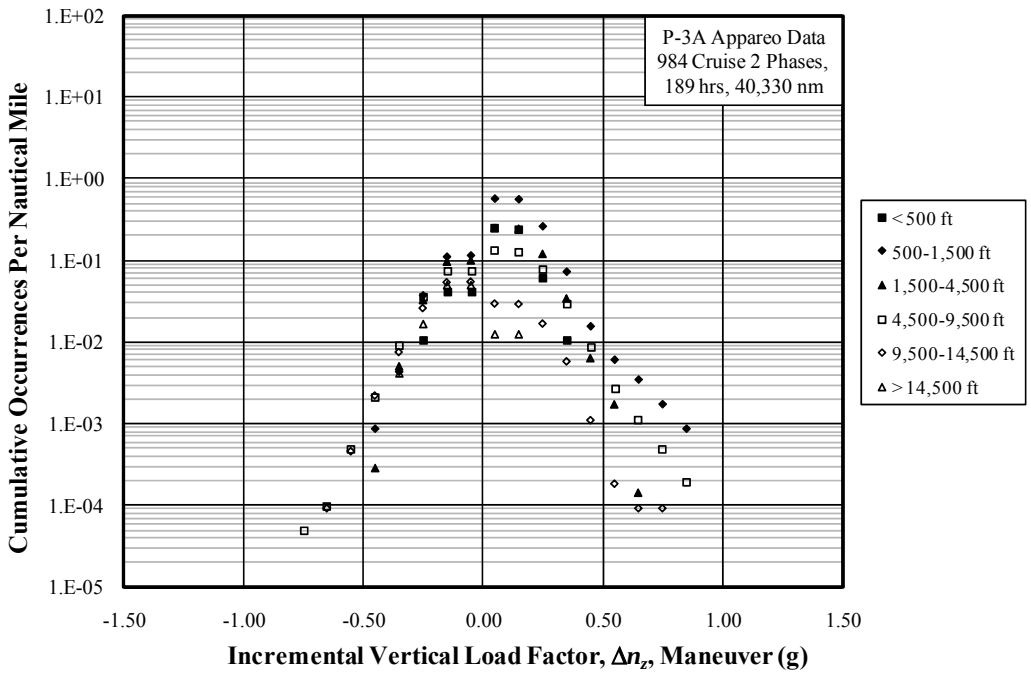

(b) Per nautical mile

Figure A-36. Cumulative Occurrences of Incremental Maneuver Vertical Load Factor, Cruise 2, P3A, Appareo Data for Various Mean Sea Level Altitudes (Continued)

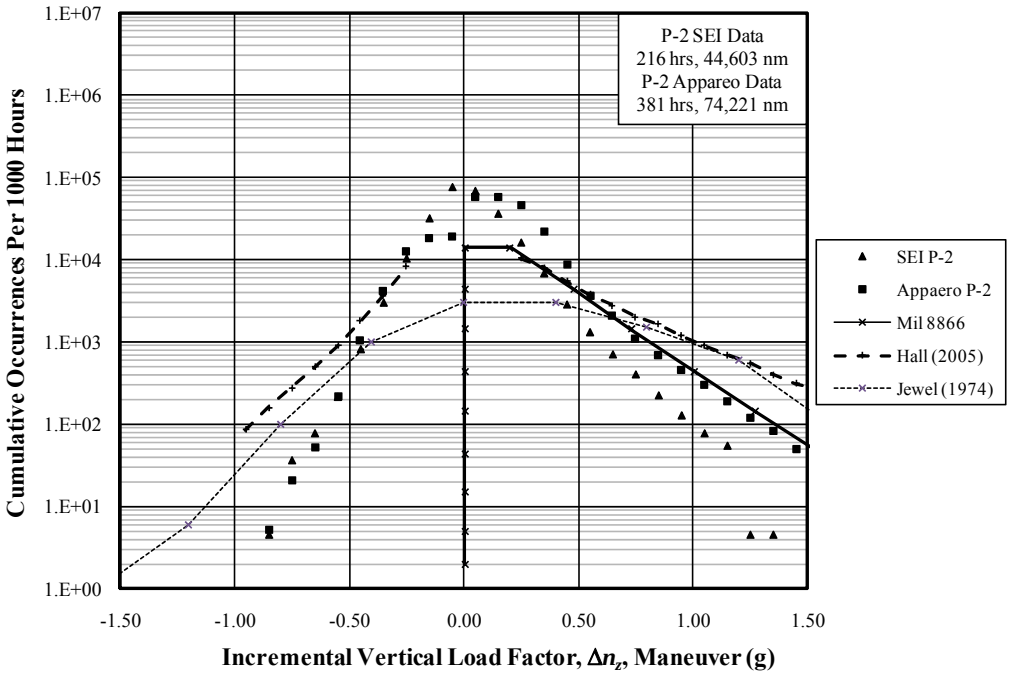

Figure A-37. Cumulative Occurrences of Incremental Vertical Maneuver Load Factor, Systems and Electronics, Inc. and Appareo Systems, Compared With Other Sources, P2V, all Phases

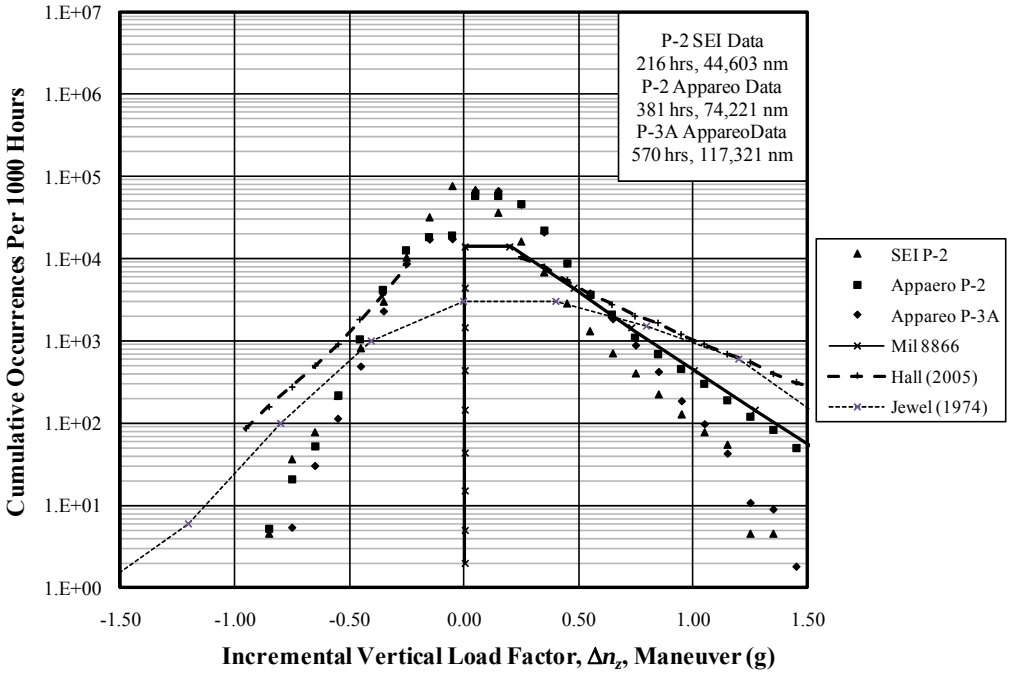

Figure A-38. Cumulative Occurrences of Incremental Vertical Maneuver Load Factor, P2V From Systems and Electronics, Inc. and Appareo Systems Compared With P3A, all Phases

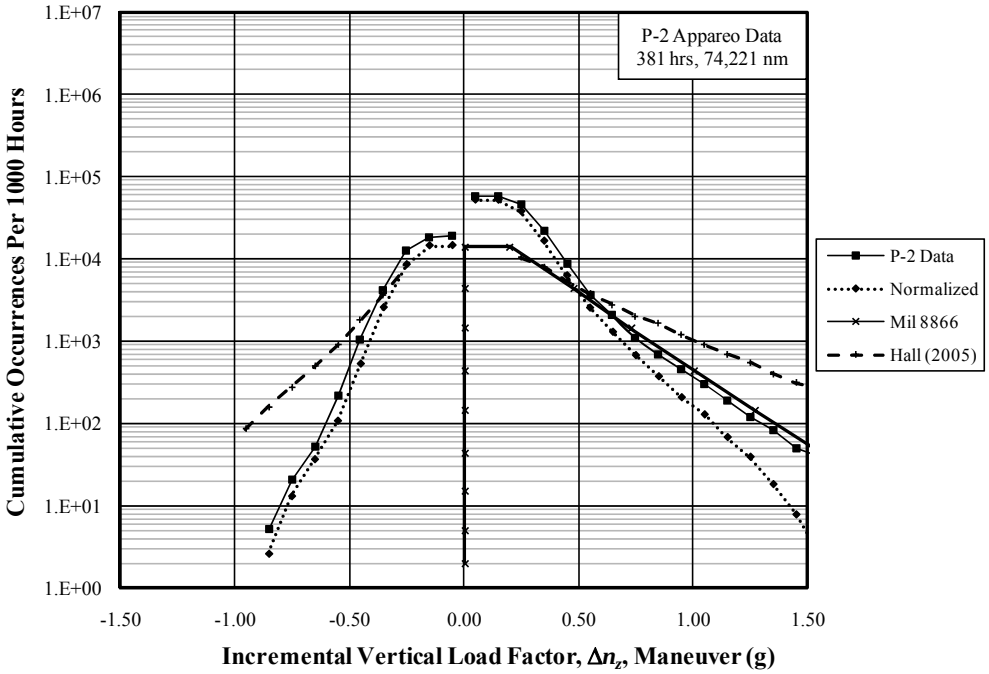

(a) P2V—Appareo System

Figure A-39. Effect of Weight on Cumulative Occurrences of Incremental Vertical Maneuver Load Factor, all Altitudes, all Phases

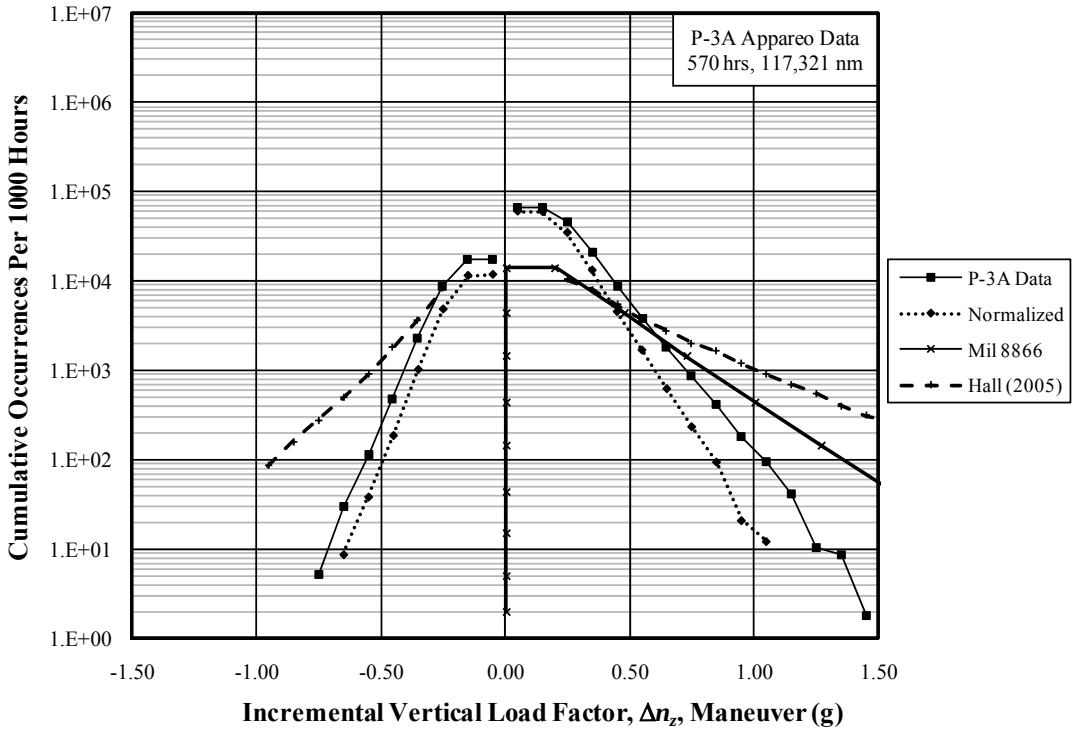

(b) P3A—Appareo System

Figure A-39. Effect of Weight on Cumulative Occurrences of Incremental Vertical Maneuver Load Factor, all Altitudes, all Phases (Continued)